THE ROLE OF CRAC CHANNELS IN LYMPHATIC ENDOTHELIAL CELLS RESPONDING TO FLUID SHEAR STRESS AND HISTAMINE

A Dissertation

by

HONGJIANG SI

Submitted to the Office of Graduate and Professional Studies of
Texas A&M University
in partial fulfillment of the requirements for the degree of

DOCTOR OF PHILOSOPHY

Chair of Committee,	Shenyuan L. Zhang
Co-Chair of Committee,	Xu Peng
Committee Members,	David C. Zawieja
	Cynthia J. Meininger
	Travis W. Hein
Head of Department,	Warren E. Zimmer

May 2019

Major Subject: Medical Sciences

ABSTRACT

The lymphatic system maintains body fluid homeostasis, lipid absorption, and immune surveillance by transporting fluid, macromolecules, and cells back to the circulatory system. Disrupted lymphatic integrity or pumping causes numerous severe diseases, including lymphedema and inflammatory disorders. Calcium (Ca^{2+}) release-activated Ca^{2+} (CRAC) channels mediate the ubiquitous store-operated Ca^{2+} entry (SOCE) and are essential for various cellular processes (e.g., T cell activation, mast cell degranulation, and endothelial cell proliferation). However, the role of CRAC channels in the lymphatic system remains unclear. In this dissertation we addressed the function of CRAC channels in cultured lymphatic endothelial cells (LECs) responding to fluid shear stress (FSS) and histamine. In the model of FSS stimulation, we described the Ca^{2+} dynamics triggered by FSS in LECs and determined the necessity of CRAC channels, formed by Orai1 and STIM1 proteins, in the Ca^{2+} signaling utilizing pharmacological blockers and RNA interference (RNAi). By using confocal imaging and RNA-sequencing (RNA-Seq), we further found that the activation of nuclear factor of activated T-cells (NFAT) and transcriptional reprogramming downstream of FSS were also dependent on CRAC channels. Our quantitative PCR (qPCR) and enzyme-linked immunosorbent assay (ELISA) data also showed that blocking CRAC channels abolished the regulation of interleukin-8 (IL-8) secretion by FSS, indicating that CRAC channels are required in FSS-induced cytokine modulation. In addition, we studied the Ca^{2+} signaling in LECs upon histamine stimulation using single-cell Ca^{2+} imaging and

discovered that histamine evoked the intracellular Ca^{2+} store release through H_1 receptors (H_1R) and phospholipase C (PLC). The subsequent sustained Ca^{2+} entry from the extracellular solution triggered by histamine was mediated by CRAC channels. We also examined the lymphatic endothelial barrier function after histamine stimulation and found that the hyperpermeability and VE-cadherin disruption caused by histamine was attenuated by CRAC channel blockers. Moreover, the knockdown of CRAC channels diminished the inflammatory cytokine expression after histamine stimulation in LECs. In summary, this study demonstrated the essential role of CRAC channels in both mechanotransduction and histamine-elicited inflammatory responses in LECs.

DEDICATION

This dissertation is dedicated to my fiancée and my parents who have been supporting me and making me a better person in my life.

ACKNOWLEDGEMENTS

I would like to thank my committee chair and mentor, Dr. Shenyuan L. Zhang, my committee co-chair, Dr. Xu Peng, and my committee members, Dr. David C. Zawieja, Dr. Cynthia Meininger, and Dr. Travis W. Hein, for their guidance and support throughout the course of this research.

I would also like to thank Dr. Harris J. Granger, Dr. Lih Kuo, Dr. Anatoliy A. Gashev, Dr. Warren Zimmer, Dr. Mariappan Muthuchamy, Dr. Carl W. Tong, and Dr. Binu Tharakan for their support and advice.

Thanks also go to my wonderful colleagues who helped and encouraged me during my study: Dr. Hongying Zheng and Dr. Meng-Hua Zhou for their technical instructions, Dr. Olga Y. Gasheva, Dr. Wei Wang, and Dr. Walter E. Cromer for their effort in teaching me to isolate lymphatic vessels; Dr. Yang Liu for her instructions in molecular biology; Dr. Andreea Trache, Anna Webb, and Dr. Irina T. Nizamutdinova for their help in confocal imaging.

I would also like to thank the office staff, Tina R. Mendoza, Starla K. Clover, Stephanie A. Hilliard, Marquita M. Adrian, Amelia Rodriguez, and Laura Daniel, for all their patient help and hard work.

Finally, thanks to my fellow students and other people in Department of Medical Physiology who made this department a warm home.

CONTRIBUTORS AND FUNDING SOURCES

Contributors

This work was supervised by a dissertation committee consisting of Dr. Shenyuan L. Zhang [advisor, Department of Medical Physiology], Dr. Xu Peng [co-chair of committee, Department of Medical Physiology], Dr. David C. Zawieja [committee member, Department Head, Department of Medical Physiology], Dr. Cynthia Meininger [committee member, Department of Medical Physiology], and Dr. Travis W. Hein [committee member, Department of Medical Physiology].

Dr. Shenyuan L. Zhang contributed to the experimental design, data collection, data analysis, and writing in all manuscripts. Dr. David C Zawieja, Dr. Cynthia Meininger, and Dr. Travis W. Hein contributed to the experimental design of the shear stress treatment on lymphatic endothelial cells in Chapter 2. Dr. David C Zawieja also helped write and edit the manuscript in Chapter 2. Dr. Xu Peng helped edit both manuscripts in Chapter 2 and 3. Ms. Anna Webb provided technical support for the confocal imaging in Chapter 2.

All other work conducted for the dissertation was completed by the student independently.

Funding Sources

This work was supported by the American Heart Association and Texas A&M University Health Science Center startup funds.

TABLE OF CONTENTS

Page

LIST OF FIGURES

Page

LIST OF TABLES

Page

1. INTRODUCTION

1.1. The lymphatic system

The lymphatic system is composed of lymphatic organs, lymphatic vessels, and the lymph transported in the vessels (1). The major functions of the lymphatic system include body fluid homeostasis, immune surveillance, and dietary lipid absorption (2). The lymph is formed in the initial lymphatics that are blind-ended lymphatic capillaries constructed of one layer of partially overlapping LECs usually without a continuous basement membrane or lymphatic muscle coverage (3). Compared to post-capillary venules, the initial lymphatics have a higher permeability to the body fluid containing macromolecules and cells due to the loose “button-like” junctional structures (4). This unique endothelial alignment in the initial lymphatics allows temporary openings between two adjacent LECs, forming “primary lymphatic valves” in the vessel wall to allow fluid entrance while preventing fluid exit (5, 6). Therefore, the initial lymphatics can take up the excess fluid accumulated in the interstitial space when the interstitial pressure is higher than the pressure inside the vessel, and transport the lymph to the collecting lymphatic vessels (2, 7). Similarly, the initial lymphatics in the small intestine, also known as lacteals, collect dietary lipid contained in the chylomicrons via the primary lymphatic valves and move them to the bloodstream (8).

The collecting lymphatic vessels, compared to the initial lymphatics, have tighter endothelial junctions, luminal lymphatic valves, and a significant amount of lymphatic muscle cells on the outside of lymphatic endothelium (1, 9). These lymphatic muscle

cells, with the contractile properties of both cardiac muscle and vascular smooth muscle cells, provide the intrinsic force to drive the lymph forward with spontaneous and rhythmical contractions (5, 10-12). The lymphatic valves, formed by LECs and extracellular matrix, divide collecting lymphatic vessels into many segments, termed lymphangions, and minimize lymph backflow between the lymphangion contractions (13). With this phasic pumping of collecting lymphatic vessels, the lymph is transported to the lymphatic trunk through a series of lymph nodes (5).

The transport of antigens and immune cells from the peripheral tissues to the lymph nodes is critical to initiate adaptive immune responses and maintain immune surveillance (2). Most pathogens (e.g., soluble factors, bacteria and viruses) are collected by the initial lymphatics through the primary lymphatic valves when the intercellular gaps are opened (6). The soluble antigens are transported quickly to the draining lymph node conduit system and processed by resident dendritic cells (DCs) in the lymph node (14). The larger pathogens are captured by the lymph node sinus macrophages and presented to the B cells (15, 16). Meanwhile, DCs carrying antigens and some T cells migrate from the interstitial spaces to the lymphatics via a chemotactic response to CCL21, an important chemokine produced by LECs that interacts with the CCR7 on the surface of migrating immune cells (17-19). These immune cells are carried by lymph flow to the lymph node B cell or T cell areas for immune surveillance and leave the lymph node for further immune responses (20, 21). After exiting the last set of lymph nodes, the lymph is collected by the lymphatic trunks, drained into lymphatic ducts, and finally returned to the blood circulation (1).

1.2. The lymphatics in lymphedema and inflammation

The lymphatic system plays a critical role in many human diseases, including lymphedema, metabolic syndrome, inflammation, and cancer metastasis, corresponding to its major functions in maintaining fluid homeostasis, lipid uptake, and immune surveillance (2, 22). Lymphedema is characterized as a set of chronic and debilitating pathological conditions with regional swelling of the extremities caused by the accumulation of protein-rich fluid in the interstitial area (23). Primary lymphedema is caused by hereditary genetic defects while secondary lymphedema results predominantly from compromised lymph drainage following infection, surgery, or radiotherapy (24). For example, surgery or radiotherapy to treat breast cancer is a common cause of secondary lymphedema in the arm on the treated side of the body due to the lymph node dissection and lymphatic vessel disruption during the treatments (25, 26). Although several techniques (e.g., lymphoscintigraphy and optical frequency domain imaging) have been developed to image lymph transport *in vivo*, curable treatments for lymphedema are still lacking (27, 28). In animal models, some studies have shown the possibility of improving lymphangiogenesis by applying vascular endothelial growth factor C or D (VEGF-C or D) to promote the proliferation of LECs (29-33). However, considering the effects of VEGFs, whether this approach could rebuild the lymphatic network and restore lymphatic pumping without aggravating the vessel leakage or leukocyte infiltration in human patients is still unknown.

As an essential part of immune surveillance, the lymphatic system is involved in various inflammatory conditions as well as cancer metastasis, but the exact functions and mechanisms are still under debate (2). Inflammation is a self-defensive process during infection, injury, and other insults, involving the accumulation of leukocytes and cytokines in the damaged tissues (34). In acute inflammations, such as in infections or wounds, VEGF-A and -C are highly expressed by several cell types (e.g., activated macrophages and DCs) in the injured tissue, promoting lymphangiogenesis to facilitate fluid removal and leukocyte migration (35, 36). On the other hand, the lymphatic dysfunction is also associated with pathological conditions accompanying chronic inflammation. For example, lymphatic obstruction or dysfunction is closely linked to the pathogenesis of inflammatory bowel disease (IBD) (37). It has been suggested that failure to clear the lipid, leukocytes, and inflammatory mediators out of the gut by the lymphatic system contributes to the intestinal inflammation and immune disturbance in IBD (11, 38, 39).

1.3. The role of LECs in regulating lymphatic pumping

Lymphatic pumping, including both extrinsic and intrinsic pumping, is essential to propel lymph against the pressure gradient and gravity back to the bloodstream in the human body (11). The extrinsic pumping exists mostly in the tissues or organs with self-compression activities (e.g., heart and skeletal muscle) where the tissue/organ compression and expansion drives lymph forward; on the other hand, intrinsic pumping refers to the spontaneous and phasic contraction of lymphatic muscle cells, generating

force to drive the lymph flow in most tissues (5). The lymphatic pumping frequency and amplitude is dynamically regulated by multiple factors, including neural stimuli and mechanical forces (12, 40, 41). One major mechanical force modulating lymphatic contractile function is fluid shear stress (FSS), which is extremely variable and bidirectional in most regions of the lymphatic system (42). Both frequency and amplitude of lymphatic pumping are inhibited when a high flow is imposed on an isolated rat lymphatic vessel, which is mostly abolished by removing LECs or blocking nitric oxide (NO) production, indicating a critical role of LECs in this process (43).

Lymphatic endothelium, a fundamental layer of the lymphatic vessels, is subjected to lymph flow directly and provides the necessary signals to modulate lymphatic pumping (44). The endothelium-derived NO is synthesized from L-arginine by the endothelial nitric oxide synthase (eNOS), a Ca^{2+}/calmodulin-dependent enzyme (45, 46). In blood vessels, NO is regarded as a vasodilator that also inhibits smooth muscle proliferation, platelet aggregation, and leukocyte activation (47-51). In the lymphatics, NO has a similar function in endothelium-dependent vessel relaxation (52). More importantly, lymphatic contractions upregulate the production of NO in a frequency-dependent manner, while the NO, in return, slows down the contractions to reduce lymph flow (43, 52-55). Although the detailed mechanism of this LEC-dependent regulation of lymphatic pumping is still unclear, FSS is considered one of the most predominant factors triggering this process (56). In addition, histamine is also reported to alter lymphatic contractions and a recent study showed the involvement of LEC-

derived histamine in flow-mediated lymphatic relaxation, suggesting more potential signaling pathways contributing to the control of lymphatic pumping (57, 58).

1.4. Vascular and endothelial responses to histamine

Histamine is an inflammatory mediator commonly used to study cellular or tissue responses to inflammation in cultured cells or in animals (59). Histamine binds four subtypes of G protein-coupled receptors (GPCRs), H_1R – H_4R, after being produced predominantly by mast cells and basophils in humans (60). Histamine is known to alter the contraction and permeability of both blood vessels and lymphatic vessels, thereby causing vasodilation, enhanced lymphatic phasic contractility and edema in inflammatory regions (57, 59, 61). Meanwhile, histamine is also involved in FSS-dependent lymphatic vessel relaxation, indicating its unique function in the lymphatics (58). It is well established that histamine enhances intracellular Ca^{2+} concentration ($[Ca^{2+}]_i$), modulates the cell skeleton, and increases permeability in blood endothelial cells (BECs) (62). The hyperpermeability is largely caused by the disruption of intercellular junctions, including adherens and tight junctions (61, 63-65). One well-accepted mechanism behind these junctional gaps is that histamine triggers Ca^{2+}-dependent retraction of BECs via the interaction between F-actin and myosin, thereby breaking adherens and tight junctions temporarily (62, 66, 67). In this process, the Rho family of GTPases (especially RhoA) is considered to be involved in the formation of stress fibers and cell retraction (67-69). In addition, histamine also stimulates the production of NO in a Ca^{2+}-dependent manner, possibly explaining the effects of

histamine in vasodilation and relaxation (70). Furthermore, histamine increases the expression of inflammatory cytokines, interleukin (IL)-6 and IL-8, in BECs as a relatively chronic effect (> 4 hours after stimulation), suggesting its involvement in the late stages of inflammatory reactions (71, 72).

As discussed above, Ca^{2+} signaling is essential for many histamine responses (e.g., cell retraction and NO production) in BECs. Histamine activates the PLC family through the Gq subunit of H_1R and hydrolyzes the phospholipid phosphatidylinositol 4,5-bisphosphate (PIP2) to generate inositol 1,4,5-trisphosphate (IP_3) and diacyl glycerol (DAG) (60, 73). IP_3 functions as a second messenger to release the endoplasmic reticulum (ER) Ca^{2+} store after binding to its receptor (IP_3R) on the ER membrane, and elicits downstream Ca^{2+} signaling in BECs (60, 73).

1.5. Ca^{2+} release-activated Ca^{2+} (CRAC) channel

Ca^{2+} is one of the most ubiquitous second messengers transducing the stimuli from the cell surface receptors to downstream cellular functions (74). The Ca^{2+} signaling profile, both spatial and temporal, is critical for many fundamental cellular processes, for example, heart contraction, immune cell activation, and neural transmission (75). There are two major sources to elevate $[Ca^{2+}]_i$ rapidly and activate downstream Ca^{2+} responsive proteins: the intracellular Ca^{2+} store and the extracellular environment (76). Since the intracellular Ca^{2+} store release is normally transient and needs to be refilled after each opening, the Ca^{2+} entry from the extracellular environment via Ca^{2+} permeable channels is necessary to maintain proper Ca^{2+} homeostasis (77). SOCE is a widespread

Ca^{2+} signal refilling the ER Ca^{2+} store after its depletion by introducing Ca^{2+} influx across the plasma membrane (78). One extensively studied channel mediating SOCE is the CRAC channel, a highly Ca^{2+}-selective channel with low single-channel conductance (79, 80).

The CRAC channel is typically activated by the IP_3R-elicited ER Ca^{2+} depletion following GPCR activation and PLC-catalyzed IP_3 production (79). The electrophysiological properties of the CRAC current (I_{CRAC}) have been studied in multiple cell types (78). It has a signature inwardly rectifying current–voltage relationship with an extremely high selectivity of Ca^{2+} over monovalent cations (about 1000:1); on the other hand, the CRAC channel shows a very low single-channel conductance (< 1 pS) and is regulated by both fast (milliseconds) and slow (seconds to tens of seconds) Ca^{2+}-dependent inactivation (81, 82). The CRAC channel has little voltage-dependent gating and is not responsive to most voltage-gated/L-type Ca^{2+} channel blockers, indicating its distinction from the L-type Ca^{2+} channels (83).

The molecular identity of the CRAC channel was discovered by several groups in 2005 and 2006: stromal interaction molecule (STIM) proteins on the ER membrane and Orai proteins on the plasma membrane (PM) (84-92). Orai1 has two paralogues, Orai2 and Orai3, while STIM1 has one paralogue, STIM2, in humans (83).

Human Orai1, with 301 amino acids and four transmembrane (TM) domains, forms the CRAC channel on the PM (79). The TM1 domain of Orai1 was shown to form the channel pore with a glutamate residue (E106) serving as the Ca^{2+} binding site (87-89, 91). Recent crystal structure of *Drosophila* Orai1 revealed that six Orai1 subunits form

one Ca^{2+}-selective pore, and further functional analysis *in vitro* confirmed this finding, suggesting that the Orai1 channel functions as a hexamer (93-96).

Human STIM1 is a single-pass TM protein containing 685 amino acids, primarily located on the ER membrane with its N-terminus inside the ER lumen and the C-terminus facing the cytosol, sensing the Ca^{2+} inside the ER via its low-affinity EF hand calcium-binding motif (97). It also contains a sterile alpha motif (SAM) at the N-terminus, which can be unfolded when the Ca^{2+} is dissociated from the EF hand motif upon ER Ca^{2+} depletion (98). This unfolding process comes with the oligomerization and translocation of STIM1 to the ER-PM junctions where STIM1 proteins cluster into large puncta (99, 100). The C-terminus of STIM1 consists of three coiled-coil domains (CC1, CC2, and CC3), an inhibitory domain, serine/proline and lysine rich regions, and a TRIP domain (77). STIM1 interacts with Orai1 through a CRAC activation domain (CAD) within the coiled-coil domains and gate Orai1 channels to allow influx of extracellular Ca^{2+} into the puncta area (101, 102).

The Orai2 and Orai3 proteins also have four TM domains like Orai1 and elicit store-operated Ca^{2+} currents like I_{CRAC} when overexpressed with STIM1 (103). However, their kinetics of channel activation and inactivation, as well as their ion selectivity and pharmacological sensitivity are different from Orai1 channels (104, 105). Moreover, the expression patterns of Orai1, 2, and 3 are not identical. Orai1 and Orai3 are found in most examined human and murine tissues, while Orai2 is limited to some species-dependent specific tissues (lung and spleen in both human and mouse, kidney in only human, and brain in only mouse) (103, 106). Although the Ca^{2+} currents through

Orai2 and Orai3 channels are defined when overexpressed *in vitro*, the functional study of endogenous Orai2 and Orai3 is still limited (77); hence, their functional necessity and distinctions from Orai1 channels remain to be explored.

STIM2 is widely and robustly expressed in most human and murine tissues and cells with STIM1 (97). STIM2 can form heteropolymers with STIM1 and its homopolymers can also activate Orai1 channels in both a store-dependent and store-independent manner *in vitro*, possibly because it does not require complete ER depletion to gate CRAC channels (107). Furthermore, STIM2 knockout in T cells showed intriguing results indicating that the initial I_{CRAC} was preserved with weakened long-term Ca^{2+} signaling and downstream nuclear factor activation (108). Until now, the specific role of STIM2 and its functional relationship with STIM1 are still under debate.

1.6. Pharmacological inhibition and activation of the CRAC channels

With the discovery of the CRAC channel and its functions, many pharmacological tools have been developed to modulate its activities. Inhibitors of CRAC channels were applied to study SOCE much earlier than the identification of Orai1 and STIM1 proteins, in which Gd^{3+} and La^{3+} are the most widely used ones (109). These trivalent lanthanides, Gd^{3+} and La^{3+}, block the CRAC channels pore completely at the sub-micromolar levels (110). In comparation, other Ca^{2+} channels require higher concentrations for total blockage; for example, TRPC channels need 100 µM of Gd^{3+} for complete blockage (76). Another famous inhibitor of CRAC channels is 2-aminoethyldiphenyl borinate (2-APB), which has been shown to activate Orai1 and

Orai2 channels transiently and then block their functions at high concentrations (25-100 μM) (104, 111, 112). The mechanism is partially explained by the prevention of STIM1 puncta formation at the ER-PM junctions (113). There is another CRAC channel inhibitor, ML-9, sharing a similar mechanism with 2-APB by impairing STIM1 movement. ML-9 was discovered as a myosin light chain kinase (MLCK) inhibitor, but its inhibition of CRAC channels is not MLCK dependent (114, 115). Many other compounds or drugs have been developed in several labs and by pharmaceutical companies to block CRAC channels, including BTP1-3, analogs of APB, Nocodazole, Synta66, SKF-96365, NPPB, and so on (116). All of these compounds showed high CRAC channel blocking potency, but their specificity and side effects on other Ca^{2+} channels need more attention and research.

Unlike the variety of CRAC channel inhibitors, the knowledge regarding the activators of CRAC channels is still very limited. Since the CRAC channel is store-operated, any drug, that releases ER Ca^{2+} or prevents ER refilling, can activate the CRAC channels indirectly through intracellular store depletion (76). However, 2-APB is the only small-molecule compound with well-defined characteristics of direct CRAC channel gating so far (76). As described above, although 2-APB is a CRAC channel inhibitor at high concentrations (>25 μM); it promotes Orai1 channel activity in several cell types and gates Orai3 channels strongly and consistently at lower concentrations (<20 μM) (113). Interestingly, the 2-APB-induced Orai3 current is not identical to the native store-operated Orai3 current with regard to Ca^{2+} selectivity (117, 118). Meanwhile, Orai2 channels do not respond to low-concentration of 2-APB, indicating a

unique pharmacological mechanism underlying 2-APB-induced CRAC channel activity (113). After the intense study of Orai1 and STIM1 proteins in the last decade, a few macromolecular factors have been reported to gate CRAC channels directly. Especially, a peptide shown to be the Orai1-interactive region of STIM1 can gate Orai1 channels regardless of store depletion (119-122).

Overall, many groups and companies are studying drugs that modulate CRAC channel activities and functions. Although the mechanisms and pharmacological properties of many drugs have not been elucidated *in vivo* yet, studies of their actions have provided insight for the development of other potential drugs to treat CRAC-related diseases in humans.

1.7. The functions of CRAC channels in diseases

Disrupted CRAC channel functions due to loss-of-function (LOF) Orai1 mutations have been found to cause severe combined immunodeficiency (SCID) in several families. The first family identified with a loss of SOCE in their T cells, B cells, and fibroblasts had a missense mutation (asparagine 91 to tryptophan, R91W) at a preserved site located in the first TM domain of Orai1 protein (123, 124). The R91W mutation does not alter the Orai1 expression or localization on the PM but leads to the absence of SOCE and I_{CRAC} through Orai1 channels (90). The T cells from these patients are normally developed; however, cell activation is markedly compromised and cytokine production is deficient (123, 124). Further analysis revealed that the abolished Orai1 channel conductance results in the failure of required Ca^{2+} signaling for T cell activation

and NFAT translocation into the nucleus (123, 125). Another family with similar syndromes was diagnosed to carry a frame-shift mutation of Orai1 (Orai1-A88EfsX25) at the A88 position causing a premature termination of protein transcription and translation (126). The patients carrying the Orai1-A88EfsX25 mutation lack complete and functional Orai1 proteins in their cells, and therefore, lose the normal activation and function of T cells (127). One more patient suffering from immunodeficiency was reported with Orai1 protein absent on the cell membrane and the SOCE severely diminished in multiple cell types, including T cells and B cells (128). In this patient, two missense mutations were identified in Orai1, A103E and L194P, at the TM1 and TM3 regions, respectively (126). These two mutations destabilize the endogenous Orai1 protein expression, weaken the normal activation of immune cells, and lead to immunodeficiency in the patient (126).

On the other hand, LOF mutations in STIM1 are also associated with immune dysfunctions. One family suffering from immune disorders had significantly decreased expression of STIM1 protein and was diagnosed to have an insertion in the STIM1 gene (STIM1-E128RfsX9) that causes premature termination of protein transcription and translation (129). In this case, the endogenous STIM2 is not able to rescue the SOCE or I_{CRAC} in the patients; nevertheless, ectopic expression of STIM1 or STIM2 can successfully rescue the absent *in vitro* SOCE in cells extracted from these patients (129). These STIM1-deficient patients have lymphoproliferative autoimmune diseases in addition to immunodeficiency, while only one Orai1-deficient patient has a similar

condition, suggesting a critical role of STIM1 in maintaining immune tolerance in humans.

Besides immune disorders, patients with compromised CRAC channel function also suffer from non-immune-related diseases, including but not limited to myopathy and anhydrotic ectodermal dysplasia (EDA). The muscular hypotonia is observed in most Orai1- or STIM1-deficient patients, and is characterized as muscle fatigue, respiratory muscle weakness, reduced walking distance, and impaired head control (126, 127, 129). The muscle biopsy of an Orai1-deficient patient reveals significantly unbalanced type I and type II fibers in the skeletal muscle cells, indicating the necessity of Orai1 function in muscle fiber differentiation (126). However, the muscle biopsy of STIM1-deficient patients does not show similar results (129). Moreover, STIM1-deficient patients and two surviving Orai1-deficient patients display notable EDA, characterized as defects in dental enamel and sweat gland development (126, 129).

Recently, gain-of-function (GOF) mutations in STIM1 and Orai1 have been found to cause tubular aggregate myopathy (TAM), Stormorken syndrome, and York platelet syndrome in human patients (130-133). Most of the mutations in TAM patients (STIM1-H72Q, N80T, G81D, D84E, D84G, S88G, L96V, F108I, F108L, H109 N, H109R, I115F) are observed in the STIM1 luminal EF-hand region, with two more mutations (STIM1-R304W and R304Q) discovered in the CC2 domain of STIM1 (134-139). These GOF STIM1 mutations cause oligomerization of STIM1 proteins regardless of endoplasmic/sarcoplasmic reticulum (ER/SR) Ca^{2+} depletion and, thereby, recruit and gate CRAC channels constantly (130). The mutations in the EF-hand region possibly

share a similar mechanism of disrupting Ca^{2+} binding or destabilizing interaction with the SAM domain (130, 137). The R304W/Q mutation in the CC2 domain is believed to elongate the C-terminus of STIM1 and expose the CAD to activate the CRAC channel continuously (140). Moreover, six missense mutations (Orai1- S97C, G98S, V107M, L138F, T184M, and P245L) have been found at the TM domains of Orai1 in these patients, all causing high resting cytosolic Ca^{2+} levels (133, 141-143). G98S and V107M have been shown to conduct spontaneous Ca^{2+} influx independent of STIM1, while T184M and P245L display excessive Ca^{2+} influx with STIM1 (144).

In order to better understand the function of CRAC channels *in vivo*, several lines of mice lacking Orai1 or STIM1/STIM2 genes have been generated in the last decade. Most mice lacking Orai1 or STIM1 show perinatal death due to complicated pathological conditions including poor skeletal muscle development and respiratory failure (79). However, partial survival can be achieved by intercrossing the Orai1/STIM1 knockout mice (C57Bl/6) with outbred ICR mice, or by using mice with mixed genetic backgrounds, or by performing conditional knockout to delete Orai1/STIM1 only in specific cell types (108, 145-147). Consistent with human patients, most of these surviving mice have significantly diminished CRAC channel function in CD^{4+} and CD^{8+} T cells, B cells, mast cells, macrophages, and fibroblasts (108, 145-147). As a result, the expression of cytokines (e.g., IL-2, IL-4, IL-6, and interferon-γ) by T cells and mast cells are remarkably downregulated, while the proliferation of B cells is inhibited as well (108, 146). In STIM1 knockout and STIM1/2 double knockout mice, lymphoproliferative phenotypes, reduced regulatory T cell populations, and autoimmune

conditions are also observed (108, 148). Regarding skeletal muscle composition, STIM1 knockout mice displayed large muscle loss and mitochondriopathy, causing perinatal lethality (149). In addition, the Orai1 or STIM1/2 knockout mice display some other phenotypes, including notably smaller size and hair loss, which are partially related to the symptoms in human patients (79).

Taken together, proper activation of the CRAC channels is critical for function of the immune system, skeletal muscles, and other tissues (e.g., teeth and sweat glands) in humans and mice. While both LOF and GOF, defects of the CRAC channels cause significant impairment of cell/tissue development and function, complete loss of CRAC channel activity leads to lethal pathological conditions in human patients and knockout mouse models.

1.8. CRAC channels in the vascular system

In the blood vascular system, the expression of Orai and STIM proteins has been discovered in both vascular smooth muscle cells (VSMCs) and BECs (150-153). In the VSMC, Ca^{2+} signaling is mediated by many different Ca^{2+} permeable channels (e.g., voltage-gated L-type Ca^{2+} channels, CRAC channels, receptor-operated channels, stretch-activated channels, and transient receptor potential channels), so the role of the CRAC channels in cellular function is complicated (154). Although CRAC channel blockage by either anti-Orai1 antibody or RNAi against Orai1 inhibits the contractile responses in mouse aorta VSMCs *in vivo* and *ex vivo*, CRAC channel blockers have little impact in this process unless the SR store is strongly depleted (155-157). These results

suggest that the Ca^{2+} signaling regulating the contractile profile of the VSMC requires CRAC channels when the SR is depleted but is relatively independent of CRAC channels in maintaining its tone when the SR Ca^{2+} store is not significantly altered (158). On the other hand, the expression and activity of the CRAC channels are enhanced during VSMC proliferation and migration, and suppressing CRAC channels by siRNAs targeting of either Orai1 or STIM1 impairs the proliferation and migration of aortic VSMCs *in vitro*, indicating the essential role of the CRAC channels in the VSMC remodeling processes (151, 155, 157, 159, 160). A possible explanation is that CRAC channel function is required for platelet-derived growth factor (PDGF) signaling, the major signaling pathway controlling the recruitment of VSMCs in angiogenesis (157).

Intriguingly, the CRAC channel is also critical for the VEGF signaling, proliferation, and migration of human umbilical vein endothelial cells (HUVECs) *in vitro* (161). Blocking CRAC channels with blockers or protein knockdown results in remarkable defects in cell growth and tube formation that mimics angiogenesis *in vitro* (141, 161). Consistently, knockout of Orai1 or STIM1 in mice inhibits the formation and remodeling of the carotid artery *in vivo*, indicating the essential role of the CRAC channels in the blood vessel formation and remodeling processes (159, 162, 163). Moreover, I_{CRAC} is important for the Ca^{2+} mobilization upon histamine stimulation, downstream NFAT translocation, and IL-8 expression in HUVECs, suggesting that the CRAC channel participates in the inflammatory responses in the vasculature (164).

Compared with the findings in the blood vessels, the knowledge of the CRAC channels in the lymphatic system is still very limited. FSS has been shown to induce

magnitude-dependent Ca^{2+} dynamics in cultured human dermal LECs (HDLECs) and a CRAC channel blocker, Synta66, can inhibit this Ca^{2+} response, indicating a possible involvement of the CRAC channels in FSS-elicited Ca^{2+} dynamics in LECs (165). Recently, Orai1 was found to be important for laminar flow-induced LEC proliferation and lymphatic growth through a complex formed by Krüppel-like factors (KLF) and PROX1 (166, 167). However, the detailed characterization and molecular basis of the CRAC channels in the Ca^{2+} mobilization following FSS or other stimuli in the lymphatic system remains to be elucidated. Furthermore, how the CRAC channel participates in the regulation of lymphatic function in physiological and pathological conditions is still largely unknown.

1.9. Specific aims of this dissertation

The first aim of this dissertation was to determine the role of the CRAC channels in the mechanotransduction of FSS and the downstream signaling pathways in LECs. We first examined the involvement of the CRAC channels in the Ca^{2+} dynamics upon FSS application on HDLECs utilizing single-cell calcium imaging, pharmacological drugs, and molecular biological tools. We further studied the necessity of CRAC channels in NFAT translocation and following transcriptional reprograming after FSS stimulation.

The second aim of this dissertation was to demonstrate the function of the CRAC channels in the histamine responses in LECs. We examined the role of the CRAC channels in the Ca^{2+} signaling evoked by histamine in HDLECs using pharmacological

blockers and RNA interference. Additionally, we tested the possible histamine receptor and the downstream enzyme that releases the ER Ca^{2+} store to activate the CRAC channels. We also studied the function of the CRAC channels in the hyperpermeability and inflammatory cytokine expression after histamine stimulation in HDLECs.

2. THE CRAC CHANNELS ARE RESPONSIBLE FOR THE FLUID SHEAR STRESS-INDUCED INTRACELLULAR CALCIUM MOBILIZATION IN LYMPHATIC ENDOTHELIAL CELLS

2.1. Overview

Background: LECs are responsible for regulating the strength and the contraction frequency of lymphatic pumping in response to the dynamic changes of lymph flow/FSS under physiological and pathophysiological conditions. Previously, we reported that the flow-evoked calcium mobilization involves both intracellular Ca^{2+} store release and extracellular calcium entry, in a manner that is sensitive to the magnitude of FSS in LECs. However, the precise ion channel molecule(s) involved in this process are unknown. CRAC channels are critical for many essential cellular processes and functions, including cell activation, proliferation, apoptosis, migration, contraction, and secretion. Nevertheless, the role of CRAC channels in mechanotransduction in LECs remains elusive.

Methods: The $[Ca^{2+}]_i$ was measured using a calcium imaging technique in cultured HDLECs subjected to constant FSS. An application of channel blockers, RNAi, and overexpression of dominant-negative (DN) channel subunits were utilized to unveil the channel molecule(s) involved in the mechanotransduction in HDLECs. Additionally, mRNA sequencing (RNA-Seq) was employed to show the transcriptional reprogramming of the signaling pathways following the FSS-induced $[Ca^{2+}]_i$ mobilization.

Results: Pharmacological blockade of CRAC channels and DN-Orail1 overexpression abolished the FSS-induced Ca^{2+} entry as well as the Ca^{2+}-dependent nuclear translocation of NFAT for the regulation of downstream gene expression. Consistently, knocking down the endogenous Orai1 or STIM1 by siRNA transfection in HDLECs suppressed $[Ca^{2+}]_i$ mobilization and its downstream signaling. RNA-seq in HDLECs revealed significant transcriptional regulation by FSS, including the downregulation of proinflammatory cytokines and chemokines, that was partially reversed by CRAC channel blockage. Moreover, our data demonstrated that purinoceptors (P2X/2Y), but not Piezo1/2 or TRPV4, were involved in the FSS-induced $[Ca^{2+}]_i$ mobilization in our model.

Conclusions: Here we show that CRAC channels, formed by Orai1 and STIM1 proteins, are responsible for mediating both thapsigargin- and FSS-evoked Ca^{2+} entry in HDLECs. Our results indicate that CRAC channels serve as a signal transducer in the lymphatic vessels to convert physical stimulations (FSS) into intracellular Ca^{2+} signals and the downstream regulation of gene expression. The FSS-induced Ca^{2+} signaling has been proposed to regulate nitric oxide (NO) production, lymphatic remodeling, and lymph transportation; thus, our research is expected to have a potentially strong impact on understanding FSS-regulated lymphatic functions under both physiological and pathological conditions.

2.2. Introduction

The blood and lymphatic endothelium constantly sense the fluid shear stress (FSS) for the proper modulation of vessel functions and remodeling (168). The vessel tone and permeability are dynamically regulated by FSS in both blood and lymphatic vessels, while the pumping activity is also modulated by FSS in collecting lymphatic vessels (43, 169). Some molecular mechanisms of these regulations have been characterized in BECs. Laminar FSS evokes an acute increase in $[Ca^{2+}]_i$ in these ECs, promotes endothelial nitric oxide synthase (eNOS) activity through both calmodulin-dependent and -independent mechanisms to enhance the production of nitric oxide (NO), and thereby relaxes vascular smooth muscle cells and reduces vessel tone (170). On the other hand, oscillatory FSS not only stimulates an acute increase of NO, but also promotes a sustained production of reactive oxygen species (ROS) through nicotinamide adenine dinucleotide phosphate hydrogen (NADPH) oxidase and, therefore, potentially causes endothelial inflammatory responses (171). In rat lymphatic vessels, physiologically-high FSS significantly decreases the vessel tone, pumping frequency, and pumping amplitude (43). This modulation is partially caused by eNOS-NO signaling but may also involve histamine synthesis and production (172). Additionally, FSS has a critical impact on EC alignment, cellular skeleton arrangement, and vascular remodeling (173). Disrupted FSS patterns are major causes of inappropriate cellular responses and vascular diseases, including atherosclerosis and inflammation, highlighting the importance of understanding and regulating the cellular processes involved in the mechanosensing to prevent these pathological responses (168, 174).

The lymphatic vasculature starts as a blind-ended conduit transporting body fluid, macromolecules, lymphocytes, and lipids from the interstitial space back to the blood circulation (1, 2, 165). The lymphatic system has a vital role of immune surveillance by transporting antigens and antigen-presenting cells to the lymph nodes and then transporting activated immune cells and secreted cytokines to the blood (25, 175, 176). The lymph flow has a much smaller velocity and varying oscillations compared with blood flow in arteries or veins, but still shows a notable regulatory effect on the vessel tone and contractions, and hence controls the rate of lymph transportation (1, 177, 178). Due to the large differences between the flows applied to ECs and LECs in the blood and lymphatic circulation, LECs are considered to present unique sensitivity and responses to the FSS (5, 177).

Intracellular Ca^{2+}, as a ubiquitous key second messenger, modulates various cell processes and functions in vascular ECs (179). Chronic Ca^{2+} signaling is required for the EC proliferation and tube formation in responding to VEGF that is critical for angiogenesis and vascular remodeling (161, 180). An acute increase of $[Ca^{2+}]_i$ is responsible for the NO production via phosphorylated eNOS and cytoskeleton reorganization through activated myosin light chain kinase (MLCK), which regulates vessel tone and permeability (181-184). FSS is known to trigger a significant increase of $[Ca^{2+}]_i$ in ECs and LECs; however, the detailed Ca^{2+} conducting channels, downstream signaling pathways, and mechanotransduction mechanisms remain unclear (165, 185).

The SOCE, mediated by Ca^{2+} release-activated Ca^{2+} (CRAC) channels, is a fundamental mechanism of Ca^{2+} intrusion to take up Ca^{2+} from the extracellular

environment after the depletion of the ER/SR Ca^{2+} store (78, 84-87, 89-91, 186). Sustained Ca^{2+} entry through CRAC channels is vital for various cell functions (e.g., T cell activation and EC proliferation) but has not been elucidated in the mechanotransduction in ECs or LECs (187-189).

In recent studies, we measured the FSS-mediated $[Ca^{2+}]_i$ dynamics in HDLEC and showed that the calcium level was dependent on the magnitude of FSS and came from both the intracellular Ca^{2+} stores and the extracellular environment (165). We further identified the sensitivity of $[Ca^{2+}]_i$ dynamics to the pharmacological blockage of CRAC channels using Synta66 (165). Another recent study also discovered that Orai1-mediated Ca^{2+} influx is necessary for formation of the KLF2/PROX1 complex and flow-induced lymphatic sprouting (166, 167). In this study, we investigated the Ca^{2+} channel molecules and Ca^{2+} signaling involved in the mechanotransduction and downstream transcriptional regulation in LECs. Our data indicate that Orai1 and STIM1 mediates the $[Ca^{2+}]_i$ dynamics upon FSS stimulation in LECs, resulting in NFAT nuclear translocation and global regulation in gene transcription.

2.3. Materials and methods

2.3.1. Cell culture

HDLECs derived from juvenile human foreskin were obtained from PromoCell and cultured in the microvascular endothelial growth medium 2 (MV2), also from PromoCell. HDLECs were maintained following the manufacturer's protocol and transfected using the Lonza Nucleofector. Cells with passages less than ten were used

for all the experiments. For $[Ca^{2+}]_i$ imaging or confocal imaging, cells were seeded onto glass coverslips pretreated with 2% gelatin.

2.3.2. Shear stress apparatus

The shear stress applied to the HDLECs was generated by a mechanical stirrer consisting of a precision controller and a rotating whip (Instech Laboratories, Inc.) or an orbital shaker (Lab-line Instruments, Inc.). The fluid flow velocity was measured using fluorescent microspheres with a spinning disk confocal microscopy technique. Fluorescent microspheres (d = 0.5 μm) were obtained from Fisher Scientific and the movement traces of the microspheres were measured right above the cytoplasmic membrane using a spinning disk confocal microscope (Leica) with an exposure time of 30 msec. The cells were visualized by loading them with the Celltracker Green CMFDA dye (Thermo-Fisher Scientific) 30 min before experiments. The distance of movement within 30 msec was measured with the ImageJ software and the velocity was calculated using the equation Velocity = Distance / Exposure time. The fluid shear stress was calculated using $\tau = \mu \frac{du}{dy}$, where τ is the fluid shear stress, μ is the dynamic viscosity of the fluid, u is the velocity of the fluid along the boundary, and y is the height above the boundary.

2.3.3. Chemicals and solutions for Ca^{2+} imaging

Thapsigargin and BTP2 were purchased from EMD. ATP was obtained from Fisher Scientific. Suramin sodium salt was obtained from VWR. Gelatin solution (2 %), $GdCl_3$, and other chemicals in the solutions were purchased from Sigma. The salt solution composition is summarized in Table 1. The measured osmolality was 319

mOsm ± 2%. The pH was 7.35 and was adjusted with the appropriate amount of sodium hydroxide.

2.3.4. Single-cell Ca^{2+} imaging

Ca^{2+} imaging was performed on an IX-81 (Olympus) microscope-based system, as described previously (190). HDLECs were incubated with 2 µM Fura-2 AM in the culture medium at 37°C for 40 minutes. Transfected cells were identified by the presence of fused eGFP; Semrock filters (BrightLine single-band multi-exciter filter set, optimized for Fura-2) were used to minimize contamination of Fura-2 fluorescence by bleed-through of eGFP fluorescence. Data were analyzed with the Metafluor software (Universal Imaging) and the OriginPro 8 software (OriginLab) and are expressed as means ± standard error of mean (SEM).

2.3.5. RNA interference

For knockdown of Orai1, Orai2, Orai3, STIM1, STIM2, Piezo-1, and Piezo-2, a mixture of four siRNAs was purchased from Dharmacon. HDLECs were transfected with siRNAs using the Lipofectamine RNAiMAX Transfection Reagent (Life Technologies) according to the manufacturer's instructions.

2.3.6. Molecular cloning and transfection

The generation of eGFP-tagged wild-type (WT) hOrai1, hOrai1-E106A mutant, and recombinant adenoviruses carrying eGFP-NFATc1 was described previously (164). HDLECs were transfected (Amaxa Nucleofector Kits, Lonza) with plasmid clones and used for experiments 48 h after transfection.

2.3.7. RNA isolation and reverse transcription polymerase chain reaction (RT-PCR)

Total RNA was isolated from HDLECs using the RNeasy Mini Kits (Qiagen), following the manufacturer's protocol. The first-strand cDNA was generated using the SuperScript IV First-Strand Synthesis System (Thermo-Fisher Scientific) and RT-PCR was conducted as described before (164, 191). The quantitative reverse transcription polymerase chain reactions (qRT-PCRs) were performed using RT2 SYBR Green ROX qPCR Mastermix (Qiagen).

2.3.8. mRNA sequencing and analysis

The HDLECs were cultured to form a monolayer and treated with orbital FSS on an orbital shaker placed in the incubator for 2 hours. The total RNA was extracted from HDLECs using RNeasy Mini Kits (Qiagen) following the manufacturer's protocol with all additional washes and on-column DNase I treatment. RNA concentration and integrity were determined using a Nanodrop and Agilent 2100 Bioanalyzer, respectively. Samples with the RNA integrity number (RIN) larger than 7.1 were utilized for library construction using the NEBNext mRNA Library Prep Reagent Set for Illumina (NEB inc.). Purified libraries were sequenced on an Illumina NovaSeq 6000 sequencer at paired-end 150 bp coverage depth and 20 million raw reads per sample. The output reads were first trimmed out to remove adaptors and then mapped to the human genome (GRCh38.p10) using a combined pipeline of TopHat2 (192) and bowtie2 (193). The mapped reads were counted and summarized using featureCounts (194). Differential gene expression analysis was performed using R/Bioconductor package edgeR (195).

Gene ontology and pathway enrichment analysis were performed using DAVID Bioinformatics Resources 6.8 (196, 197).

2.3.9. Western blots

Whole cell extracts were resolved by SDS-PAGE and transferred to nitrocellulose membranes using a transfer apparatus, according to the manufacturer's protocols (Bio-Rad). Samples were then analyzed by standard western blotting. Immunoblots were incubated with the primary antibodies as indicated, including rabbit anti-STIM1 (1:1000), rabbit anti-STIM2 (1:500, Alomone Labs), mouse anti-GAPDH (1:10,000, Fitzgerald clone 6C5), rabbit anti-Orai1 (1:500, Aviva Systems Biology), and mouse anti-GFP-HRP (1:1000, Miltenyi Biotec).

2.3.10. Enzyme-linked immunosorbent assay (ELISA)

The ELISA targeting interleukin 8 was performed utilizing the Human CXCL8/IL-8 Quantikine ELISA Kit (R&D Systems), following the manufacturer's protocol.

2.3.11. Confocal imaging

HDLECs were seeded on 35-mm glass bottom dishes (MatTek) coated with 2% gelatin. HDLECs were fixed by 4% PFA after shear stress treatments for 1 hour at room temperature. Fixed cells were washed with PBS and viewed under a confocal laser-scanning microscope (FV300; Olympus) equipped with the FluoView software. Confocal microscopy was performed at the Integrated Microscopy and Imaging Laboratory in the Department of Medical Physiology, Texas A&M University Health Science Center, Temple, Texas.

2.3.12. Statistical analysis

All data collected were from at least three independent experiments and are expressed as mean ± SEM. Statistical significance was evaluated using SAS software (University Edition) and assessed by one-way ANOVA and Tukey post-hoc test or unpaired t-test. Statistically significant differences were assumed at P-value ≤ 0.05.

2.4. Results

2.4.1. CRAC channel blockers can inhibit FSS-induced Ca^{2+} influx

Based on the fact that FSS-induced $[Ca^{2+}]_i$ mobilization in HDLECs (1) has two typical components of CRAC channel-mediated $[Ca^{2+}]_i$ mobilization (i.e., release of the intracellular Ca^{2+} store and the extracellular Ca^{2+} entry) and (2) is sensitive to Synta66, a CRAC channel blocker, we tested the hypothesis that CRAC channels are involved in mediating this mechanotransduction event. We started with measuring store-operated Ca^{2+} entry in HDLECs in a traditional way via the application of thapsigargin (TG), a sarco/endoplasmic reticulum Ca^{2+}-ATPase (SERCA) pump inhibitor, in the absence of extracellular Ca^{2+} (the Ca0 solution, see Table 1), which passively depletes Ca^{2+} from the store in conjunction with evoking SOCE (Figure 1A). A peak (746 ± 38 nM) of the $[Ca^{2+}]_i$ signal was observed characteristically within two minutes after the addition of a physiological saline solution containing 2 mM Ca^{2+} (Ca2, see Table 1), followed by a plateau stage lasting for tens of minutes (600 ± 34 nM at the time point of 5 minutes following the Ca2 addition, Figure 1D). As expected, this Ca^{2+} influx was highly sensitive to both classic CRAC channel blockers tested in this study, Gd^{3+} and

Table 1 Saline solution composition (all concentrations in mM)

Solution	**Ca2**	**Ca0**
NaCl	155	153
KCl	4.5	4.5
CaCl2	2	0
MgCl2	1	3
EGTA	0	1
HEPES	5	5
D-glucose	10	10

BTP2 (Figure 1B-D), indicating that CRAC channels are likely the main channel molecules conducting SOCE in HDLECs.

For the next step, we set up a system with a mechanical stirrer consisting of a precision controller and a rotating whip on top of the cultured cells as our main method to apply FSS to HDLECs for $[Ca^{2+}]_i$ monitoring. Significant $[Ca^{2+}]_i$ mobilization was observed as anticipated and the signal increased when the FSS rose (Figure 2A). Under a setting with an estimated 4 dyne/cm^2 FSS, a constant/stable, saturated $[Ca^{2+}]_i$ signal was recorded with a peak (747 ± 16 nM) and a gradually decreased plateau (662 ± 18 nM, measured 20 minutes after the initiation of the FSS (Figure 2). Removing the extracellular Ca^{2+} from the bath solution dramatically diminished but did not completely abolish the $[Ca^{2+}]_i$ signal, with a remaining, transient peak (108 ± 7 nM, Figure 2). This observation confirms that FSS-induced $[Ca^{2+}]_i$ mobilization has two components as mentioned above, which was further validated in our complementary experiments using Mag-Fluo4, a low affinity Ca^{2+} binding dye and ER Ca^{2+} indicator, to detect a significant drop in the $[Ca^{2+}]_{ER}$ of HDLECs upon FSS stimulations (Figure 2B). Interestingly, the FSS-induced Ca^{2+} influx can also be effectively inhibited by both Gd^{3+} and BTP2 (Figure 3A-D), suggesting a potential major contribution of CRAC channels in mediating this Ca^{2+} influx, and as a key step in the loop of mechanosensation in the lymphatic endothelium.

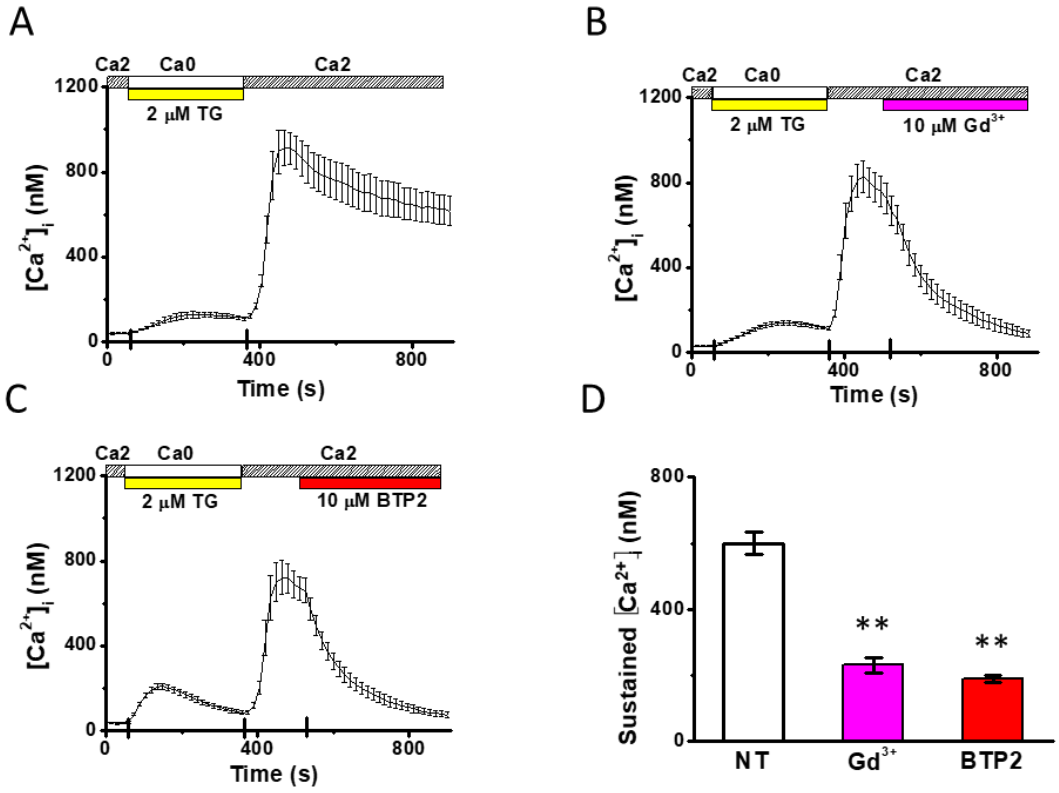

Figure 1. TG-triggered (store-operated) Ca^{2+} entry is strongly suppressed by CRAC channel blockers in HDLECs.

A. Representative $[Ca^{2+}]_i$ (mean ± SEM) measurements show TG (2 μM)-evoked, store-operated Ca^{2+} entries in HDLECs (n = 12 cells). The top bars indicate the type of extracellular solutions (Table 1) applied to the cells, and the vertical lines on the x-axis indicate the time of solution change. **B and C.** Representative $[Ca^{2+}]_i$ recordings show TG-evoked Ca^{2+} entries with low doses of CRAC channel blockers, Gd^{3+} (10 μM, n = 11 cells, **B**) and BTP2 (10 μM, n = 8 cells, **C**). **D.** Statistical analyses of averaged, sustained $[Ca^{2+}]_i$ values coupled to the TG-dependent Ca^{2+} influx, obtained at 10 minutes after the application of TG, for the three groups of cells (n = 85, 32, and 30 cells, respectively). NT: non-treated, the control group. **: $p < 0.01$ compared with the control.

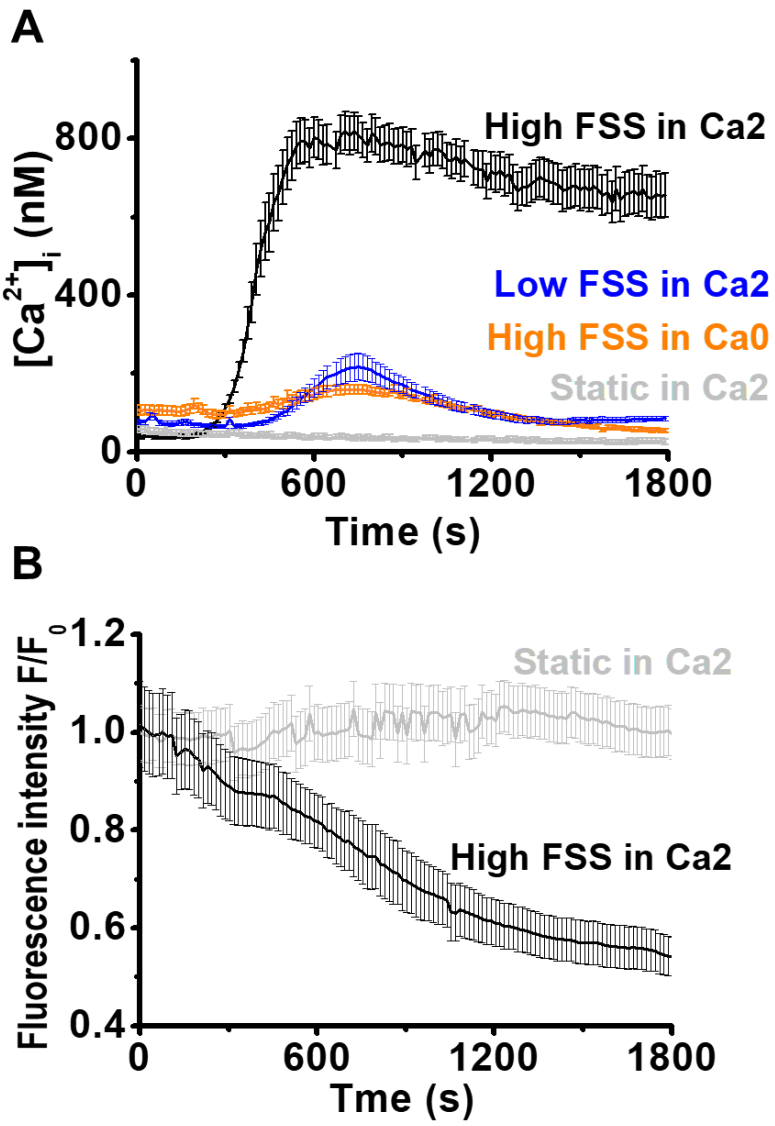

Figure 2. FSS-induced intracellular Ca^{2+} dynamics in HDLECs.
A. Representative $[Ca^{2+}]_i$ traces show the cytosolic Ca^{2+} dynamics in HDLECs at the static condition in Ca2 solution (grey), subjected to low FSS in Ca2 solution (blue), or subjected to high FSS in Ca2 (black) or Ca0 (orange) solutions. **B.** Representative fluorescence intensity traces show the Ca^{2+} levels in the ER at static condition (grey) or subjected to high FSS (black) in HDLECs incubated with Ca2 solution.

2.4.2. FSS-induced Ca^{2+} entry can be suppressed by a DN Orai1 mutant (Orai1-E106A) or RNAi against Orai1 or STIM1

We next worked to dissect the molecular mechanism underlying this FSS-triggered $[Ca^{2+}]_i$ mobilization in LECs via more specific molecular biology tools. To identify the specific channel molecule(s) that mediates the Ca^{2+} entry following FSS-evoked store release, we employed Orai1-E106A, a well-established dominant-negative Orai1 mutant to suppress the activity of endogenous Orai channels, the best-characterized store-operated channels so far (87). The point mutation, E106A, is located on the channel selectivity filter and upsets channel function by altering/eliminating the channels' permeability to Ca^{2+}. The eGFP alone (the negative control) and the eGFP-fused Orai1-E106A cDNA constructs were delivered into HDLECs via nucleofection. While the cells expressing eGFP responded normally to the TG stimulation (Figure 4A and 4C) and the FSS stimuli (Figure 4D and 4F), the cells expressing eGFP-Orai1-E106A displayed diminished store-operated Ca^{2+} entries in response to TG (Figure 4B and 4C) as well as FSS (Figure 4E and 4F), emphasizing a central role of Orai channels in FSS-evoked Ca^{2+} influx.

There are three genes (*hOrai1*, *hOrai2*, and *hOrai3*) in the human genome that code for the Orai channel pore-forming subunits (Orai1, Orai2, and Orai3, respectively) with similar Ca^{2+}/CRAC channel functions at the molecular level; yet it seems that Orai1 is much more dominant in controlling CRAC channel physiological functions in most cellular systems tested so far. To evaluate their potential, functional roles in mediating SOCE in lymphatic endothelial cells, we applied the RNAi approach. HDLECs were

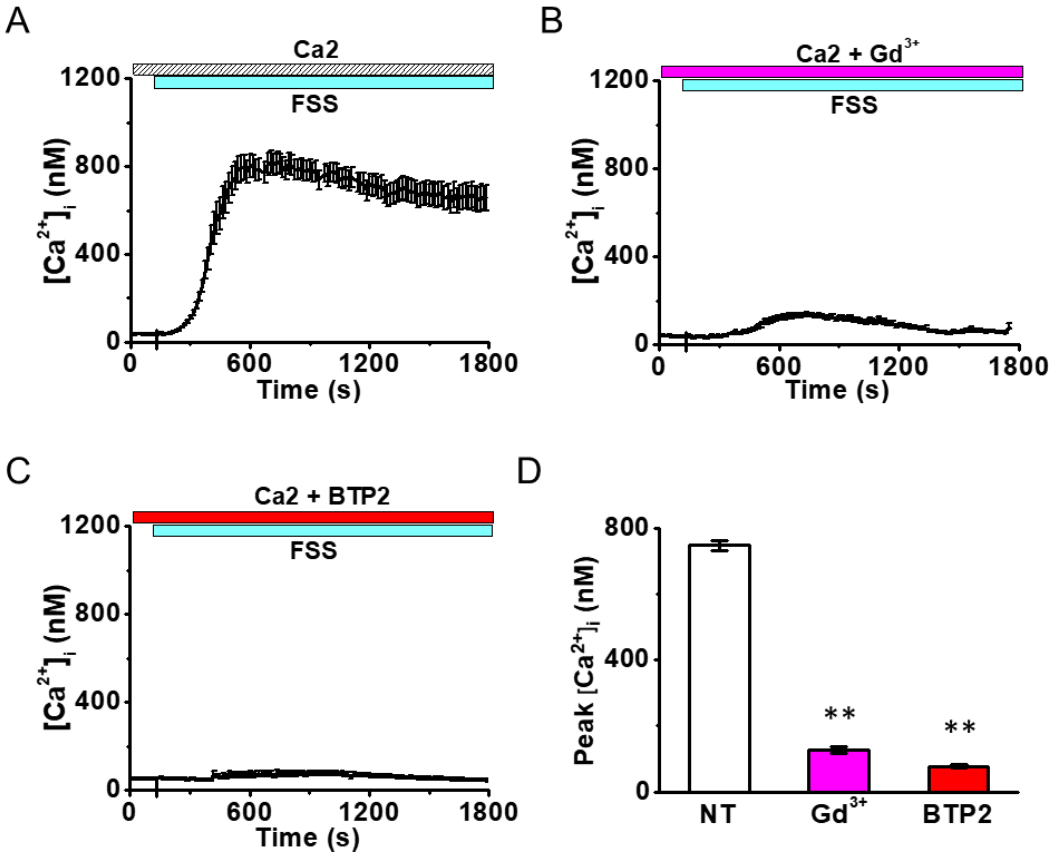

Figure 3. FSS-induced Ca^{2+} entry is sensitive to CRAC channel blockers in HDLECs.

A. A representative, averaged $[Ca^{2+}]_i$ trace shows FSS-evoked Ca^{2+} entries in HDLECs (n = 17 cells). **B and C.** Representative $[Ca^{2+}]_i$ measurements show FSS-evoked Ca^{2+} entries in HDLECs are suppressed by both CRAC channel blockers, Gd^{3+} (n = 16 cells, **B**) and BTP2 (n = 19 cells, **C**). **D.** Statistical analyses of the averaged, peak $[Ca^{2+}]_i$ values coupled to the FSS-dependent Ca^{2+} influx for the three groups of cells (n = 201, 85, and 46 cells, respectively) confirmed significant decrease of FSS-induced Ca^{2+} mobilization by classic CRAC channel blockers in HDLECs. **: $p < 0.01$ compared with the control.

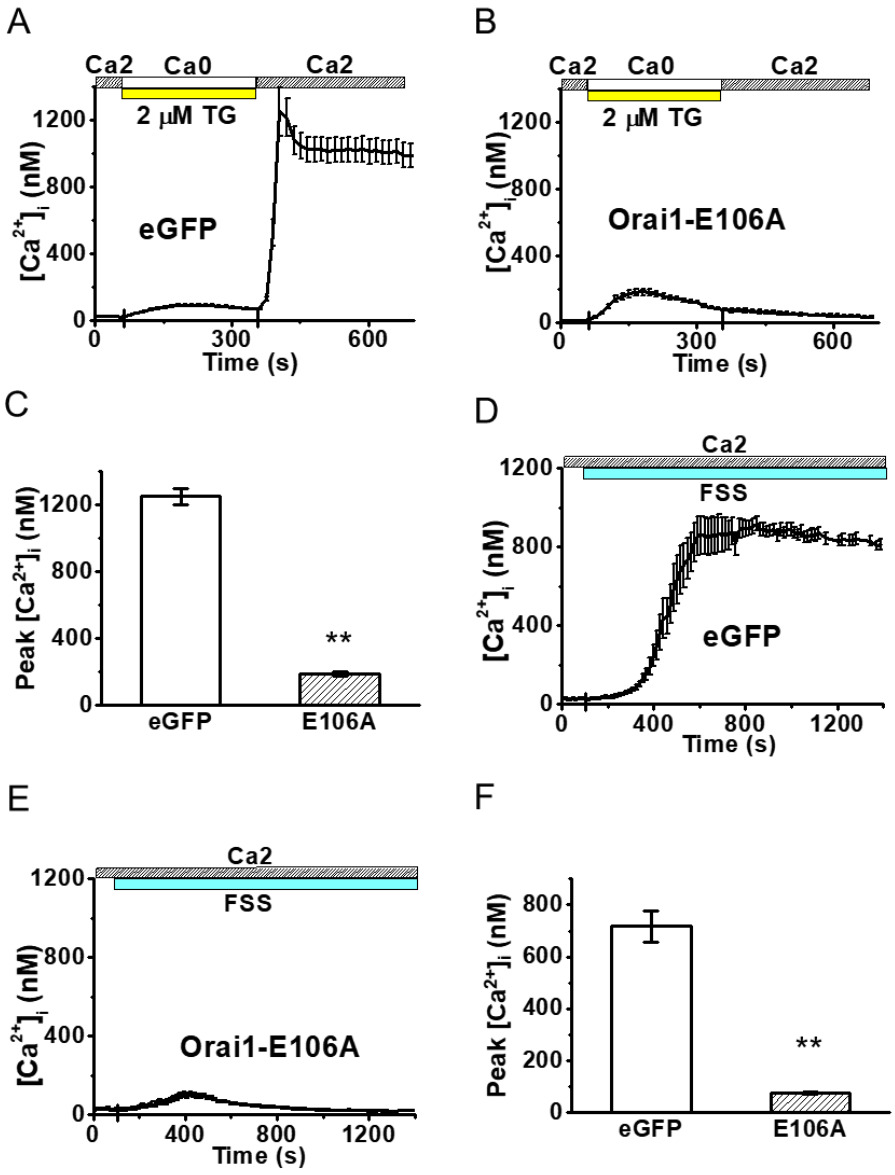

Figure 4. SOCE and FSS-induced Ca^{2+} mobilizations are both abolished by Orai1-E106A, a dominant-negative Orai1 mutant.

A and B. Representative $[Ca^{2+}]_i$ responses show TG-evoked Ca^{2+} mobilizations in HDLECs transfected with eGFP (*n* = 4 cells, **A**) or the eGFP-Orai1-E106A mutant (*n* = 5 cells, **B**). **D and E.** Representative $[Ca^{2+}]_i$ measurements show FSS-evoked Ca^{2+} mobilizations in HDLECs transfected with eGFP (*n* = 8 cells, **D**) or eGFP-Orai1-E106A (*n* = 4 cells, **E**). **C and F.** Statistical analyses of averaged peak $[Ca^{2+}]_i$ values coupled to stimulations/treatments (TG, *n* = 37 and 15 cells, **C** or FSS, *n* = 30 and 25 cells, **F**) compared with the control (eGFP) group. **: $p < 0.01$ compared with the control.

transfected with siRNAs against individual Orai genes separately to disrupt the endogenous expression of the corresponding channel subunits. Cells that were not treated (non-transfected, NT) were tested in parallel. While Orai2-siRNAs or Orai3-siRNAs did not significantly alter TG-evoked Ca^{2+} influx, compared with untreated cells (Figure 5A, 5C, 5D, and 5E), Orai1-siRNAs treated cells showed very little SOCE overall upon TG stimulation (Figure 5B and 5E), indicating that Orai1 is the main CRAC/Orai channel subunit functioning in LECs to conduct SOCE. Consistently, RNAi against Orai1, but not Orai2 or Orai3, also prevented HDLECs from responding to the FSS stimuli for intracellular Ca^{2+} mobilization (Figure 6A–6E). The effects of RNAi on the expression of Orai genes, especially *hOrai1*, was confirmed by both RT-PCR (Figure 5F) and western blot (Figure 6F).

Orai channels are nowadays known to be activated by physical interactions with the STIM molecules located on the ER membrane, which oligomerize upon Ca^{2+} release from the ER and migrate toward the ER-PM junctions. Therefore, we also examined the involvement of *hSTIM1* and *hSTIM2*, the two human STIM genes, in mediating both SOCE and mechanotransduction of the FSS in HDLECs via RNAi. In cells transfected with siRNAs specifically targeting STIM1, TG and FSS failed to stimulate Ca^{2+} influx (Figure 7A, 7B, 7D, 7E, 7G, and 7H). In contrast, gene silencing of STIM2 did not considerably reduce Ca^{2+} influx in response to TG or FSS (Figure 7C, 7F, 7G, and 7H). The specificity and efficacy of all the STIM siRNA species on HDLECs were verified by western blot (Figure 7I).

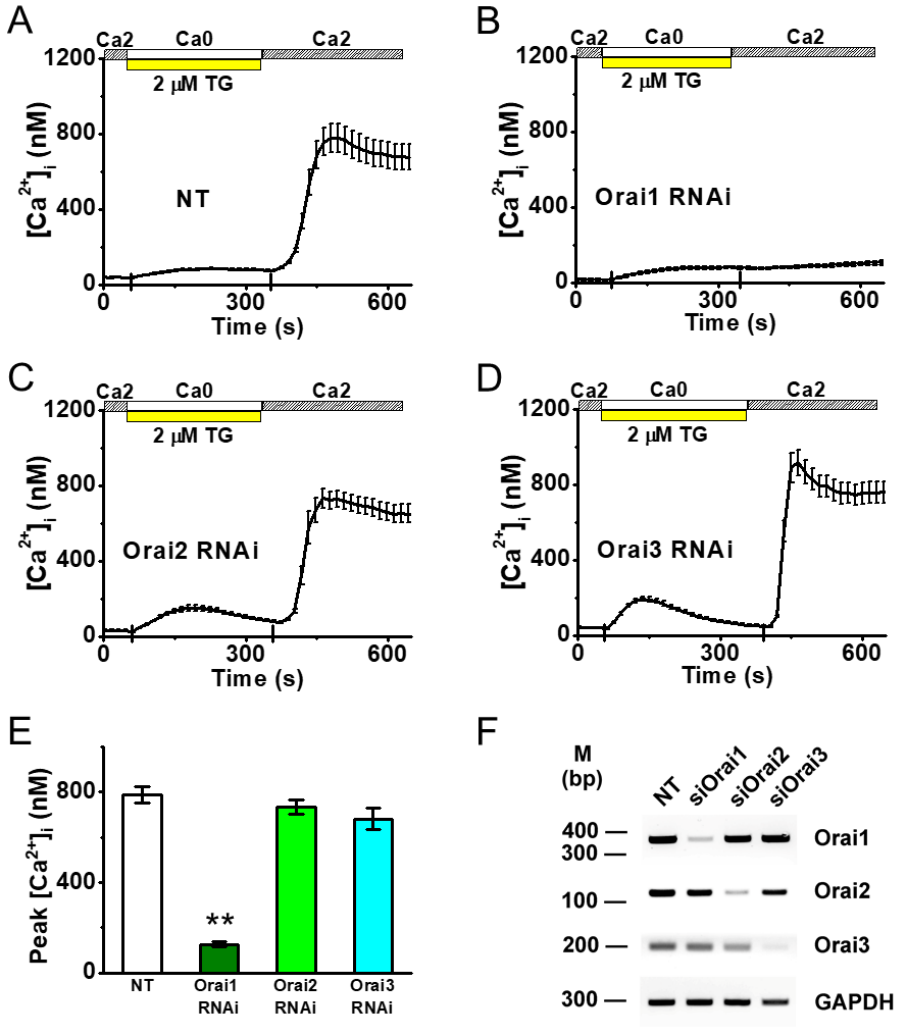

Figure 5. SOCE is mediated by Orai1, but not Orai2 or Orai3, in HDLECs. **A-D.** Representative $[Ca^{2+}]_i$ traces from HDLECs show TG-evoked Ca^{2+} entries with no extra treatment (NT, *n* = 13 cells, **A**) or treated with siRNAs targeting Orai1 (*n* = 16 cells, **B**), Orai2 (*n* = 13 cells, **C**) or Orai3 (*n* = 23 cells, **D**) for three days. **E.** Statistical analyses of averaged, peak $[Ca^{2+}]_i$ values coupled to TG-dependent Ca^{2+} influx show a significant decrease of SOCE, compared to cells treated with no treatment, by RNAi against Orai1, but not Orai2 or Orai3 (*n* = 85, 45, 31, and 49 cells, respectively). **: $p < 0.01$ compared with the control (NT). **F.** Representative RT-PCR results confirm siRNA-mediated gene silencing of Orai1, Orai2, or Orai3 in HDLECs. The mRNA levels of GAPDH from individual samples were examined to verify the application of equal amount of total RNAs for the RT-PCR assays. M: DNA markers; NT: non-treated.

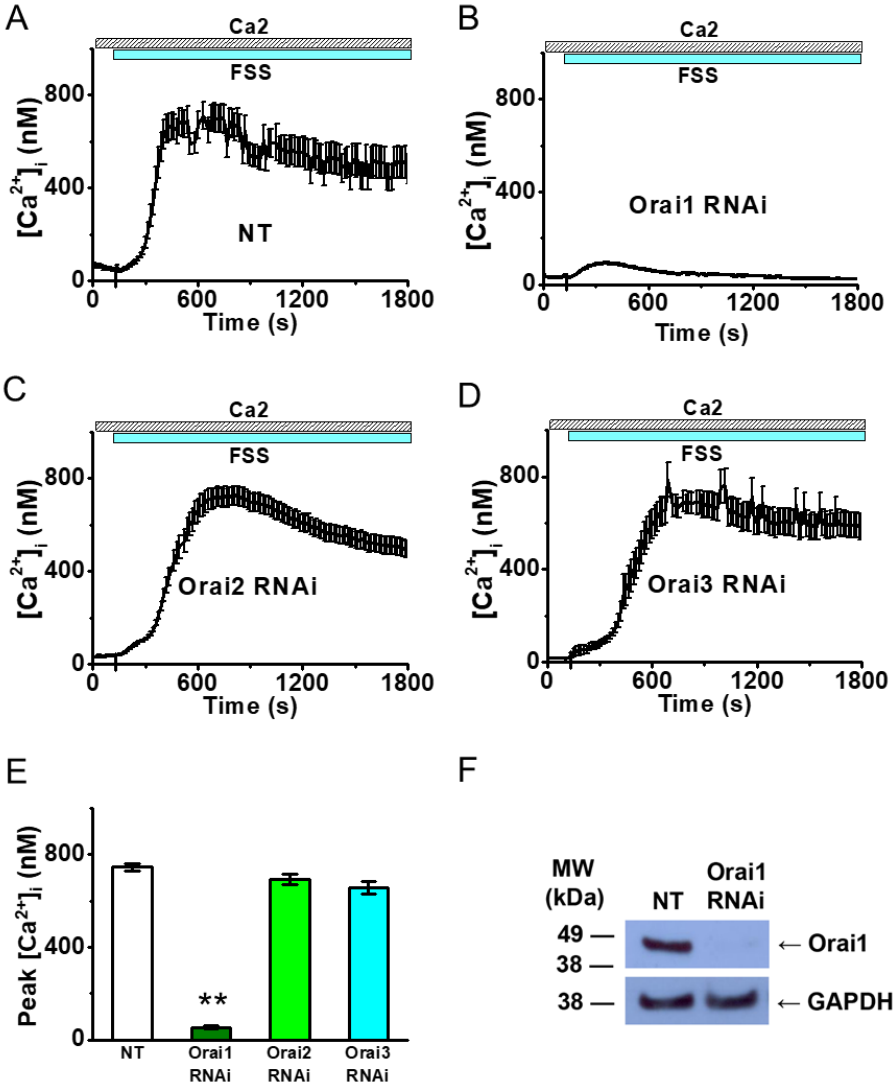

Figure 6. FSS-induced Ca^{2+} entry is mediated by Orai1, but not Orai2 or Orai3, in HDLECs.

A-D. Representative $[Ca^{2+}]_i$ measurements show FSS-evoked Ca^{2+} entries in HDLECs with no treatment (*n* = 17 cells, **A**) or treated with siRNAs against Orai1 (*n* = 25 cells, **B**), Orai2 (*n* = 34 cells, **C**) or Orai3 (*n* = 9 cells, **D**). **E.** Statistical analyses of averaged, peak $[Ca^{2+}]_i$ values coupled to FSS-dependent Ca^{2+} mobilizations confirm a significant decrease, compared to cells with no treatment, by Orai1 RNAi, but not Orai2 or Orai3 RNAi (*n* = 201, 109, 90, and 76 cells, respectively). **F.** Western blot validation of siRNA-mediated gene silencing of Orai1 in HDLECs is shown. The protein levels of GAPDH from individual samples were examined to verify the application of equal amount of total cell lysates for Western blot assays. MW: molecular weight.

These results point out that Orai1 and STIM1 together, the pore-forming and activating subunits, respectively, comprise the main type of lymphatic endothelial CRAC channel, downstream of the release of the ER Ca^{2+} store, mediating SOCE as well as $[Ca^{2+}]_i$ mobilization upon FSS stimuli.

2.4.3. While Piezo1/2 are not the likely FSS sensor for the observed $[Ca^{2+}]_i$ mobilization, P2X/2Y receptors may partially contribute to this mechanotransduction process

After the identification of CRAC channels and Orai1/STIM1 proteins as the dominant type of Ca^{2+} channels and their chief underlying molecular components, respectively, in LECs to mediate FSS-induced $[Ca^{2+}]_i$ mobilization in our settings, our next goal is to characterize the upstream signaling pathway and other indispensable molecules that directly relay the mechanical force (FSS) to store release/depletion for the activation of CRAC channels. For this purpose, we aimed to address the long-sought, shear mechanosensor in the lymphatic endothelium. We started with testing a potential role of Piezo channels (Piezo1 and Piezo2), a recently recognized two-member family of mechanosensitive ion channels. Piezo1 was proposed to act as a shear sensor in embryonic BECs for vascular development and structure maintenance, and is able to conduct Ca^{2+} influx under relatively strong FSS stimuli ($\geq$ 5 dym/cm^2). It is possible that its activation is either upstream or downstream of the activation of CRAC channels during all mechanotransduction events. Surprisingly, inhibiting the expression of Piezo1 or Piezo2 alone by RNAi did not significantly influence the peak amplitude of FSS-

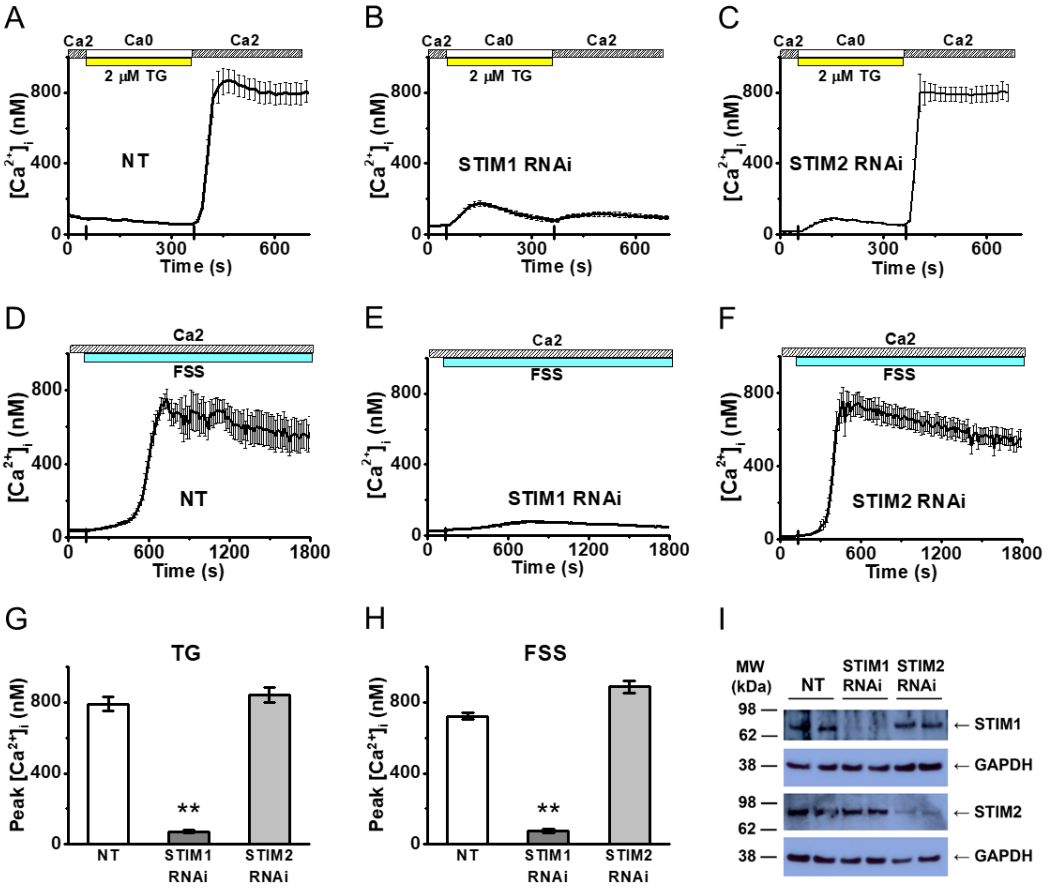

Figure 7. SOCE and FSS-induced Ca^{2+} entry are mediated by STIM1 in HDLECs. **A-C.** Representative $[Ca^{2+}]_i$ recordings show TG-evoked Ca^{2+} entries in HDLECs with no treatment (*n* = 20 cells, **A**) or treated with siRNAs silencing STIM1 (*n* = 6 cells, **B**) or STIM2 (*n* = 14 cells, **C**). **D-F.** Representative averaged cytosolic Ca^{2+} concentrations were obtained from FSS-stimulated HDLECs with no treatment (*n* = 6 cells, **D**) or treated with siRNAs specific to STIM1 (*n* = 14 cells, **E**) or STIM2 (*n* = 18 cells, **F**). **G and H.** Statistical analyses of averaged, peak $[Ca^{2+}]_i$ values following the stimulations (TG, *n* = 85, 65, and 59 cells, **G**, or FSS, *n* = 201, 49, and 71 cells, **H**) show a significant decrease of Ca^{2+} mobilizations upon both types of stimulations by STIM1 RNAi, but not STIM2 RNAi. **: $p < 0.01$ compared with the control (NT). **I.** Representative Western blot results show the specific reduction of the STIM1 and STIM2 proteins in HDLECs treated with the corresponding siRNAs.

induced $[Ca^{2+}]_i$ mobilization in HDLECs (Figure 8A-8C and 8E). Several anti-Piezo1 and anti-Piezo2 antibodies were tested, but none of them could clearly detect the expression of the corresponding endogenous proteins in HDLECs. On the other hand, at the mRNA level, the expression and effective silencing by RNAi of both molecules were validated via RT-PCR (Figure 8F). Since Piezo1 and Piezo2 could possibly function redundantly at the molecular level or form hetero-trimers as functional channels, we tested the effects of silencing both genes at the same time. However, this treatment also did not significantly affect the peak amplitude of FSS-induced $[Ca^{2+}]_i$ mobilization in HDLEC (Figure 8D and 8E).

After ruling out a possible contribution of Piezo channels in the process of mediating $[Ca^{2+}]_i$ mobilization in our current settings (relatively low FSS onto cultured juvenile LECs), we moved onto the ATP-gated P2X receptors, a family of cation channels that has been suggested to be downstream of FSS conducting Ca^{2+} entry. Together with P2Y receptors, another family of GPCRs, these purinergic receptors were proposed to be activated by shear-induced release of ATP. In order to validate their functional existence in LECs, we stimulated HDLECs with two different concentrations of ATP (1 and 10 μM) and simultaneously monitored $[Ca^{2+}]_i$ mobilization. Within a 10-minute recording, we constantly observed a sharp but relatively transient peak (300 ± 25 nM with 1 μM ATP and 627 ± 52 nM with 10 μM ATP, respectively; Figure 9A-9C) evoked within a minute after the application of ATP; consistent with the typical purinergic receptor-mediated $[Ca^{2+}]_i$ mobilization reported/described before. To further

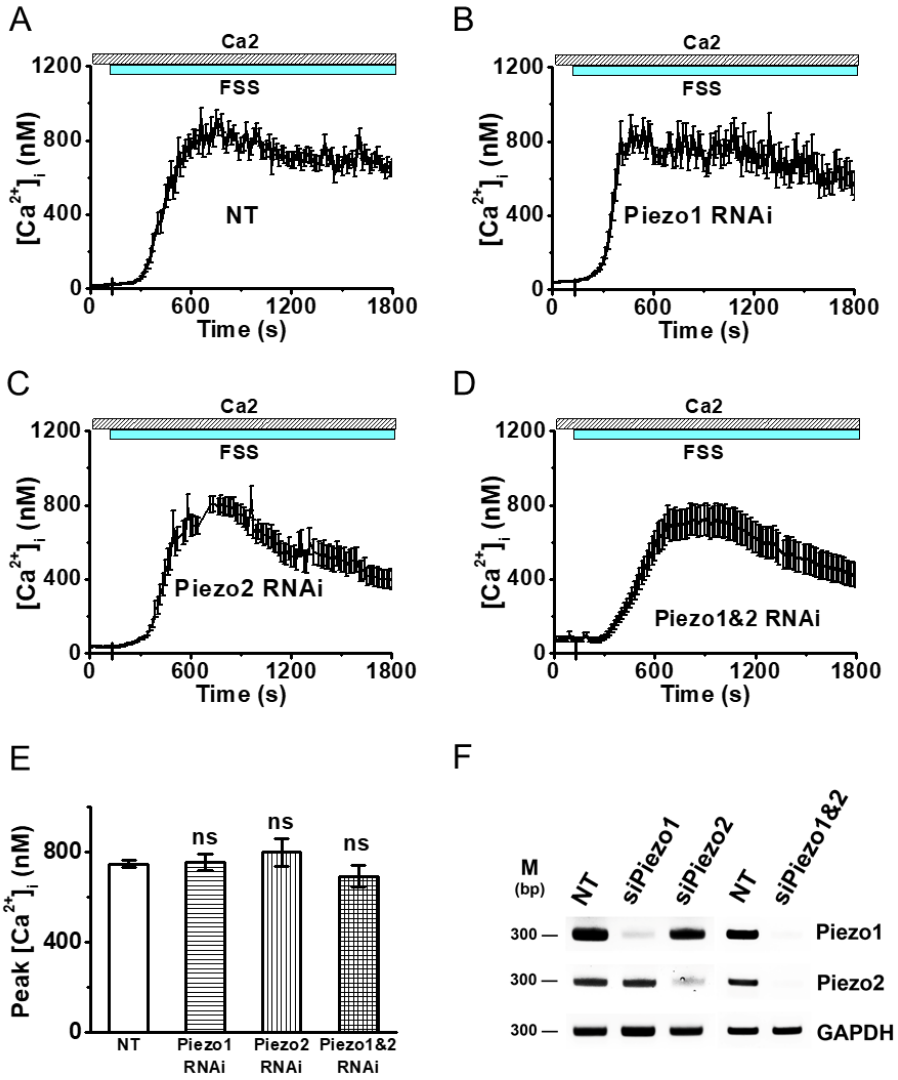

Figure 8. Piezo proteins do not contribute to the FSS-induced Ca2+ mobilization. **A-D.** Representative $[Ca^{2+}]_i$ recordings illustrate FSS-triggered Ca^{2+} mobilization in HDLECs with no treatment (NT, *n* = 25 cells, **A**) or transfected with siRNAs silencing Piezo1 (*n* = 11 cells, **B**), or Piezo2 (*n* = 18 cells, **C**), or both Piezo1 and Piezo2 (n = 13 cells, **D**). **E.** Peak $[Ca^{2+}]_i$ values were averaged for comparison (*n* = 201, 86, 49, and 40 cells, respectively). **F.** RT-PCR validation of siRNA-mediated gene silencing of Piezo1 or Piezo2 in HDLECs is shown. The mRNA levels of GAPDH from individual samples were examined to verify the equal loading of samples. M: DNA markers.

evaluate the source/molecular mechanism behind this observed, ATP-dependent $[Ca^{2+}]_i$ phenomenon in HDLECs, we applied suramin, a universal antagonist to both P2X and P2Y receptors, which nearly completely abolished the ATP-induced $[Ca^{2+}]_i$ peaks after a 10-minute pre-incubation with the cells (Figure 9A-9C). Strikingly, suramin also slightly reduced FSS-induced $[Ca^{2+}]_i$ mobilization (a 16% decrease, Figure 9D-9F), indicating that P2X/2Y signaling contributes partially to the mechanotransduction of FSS stimulations in our settings.

Next, we studied a third Ca^{2+}-permeable cation channel, TRPV4, for its potential role in our observed FSS-induced $[Ca^{2+}]_i$ mobilization. TRPV4 is another channel candidate previously proposed to be downstream of FSS for shear mechanosensing. Our experimental data showed that with the application/pre-incubation of a TRV4 specific antagonist, GSK2193874, the FSS-induced $[Ca^{2+}]_i$ mobilization was not influenced in our current settings (Figure 9G-9I).

2.4.4. RNA-Seq revealed a global regulation of transcription and inhibition of inflammatory genes triggered by FSS, which is partially dependent on CRAC channels

Following the $[Ca^{2+}]_i$ mobilization studies, we investigated the downstream regulation of FSS on gene expression. We first tested the possible activation of the NFAT, a family of highly Ca^{2+}/calmodulin dependent transcriptional factors. In most cell types, NFAT rests in the cytosol until increased $[Ca^{2+}]_i$ activates calmodulin and thereby dephosphorylates NFAT to induce its nuclear translocation and transcriptional regulations. We observed the subcellular locations of NFATc1 in HDLECs transfected

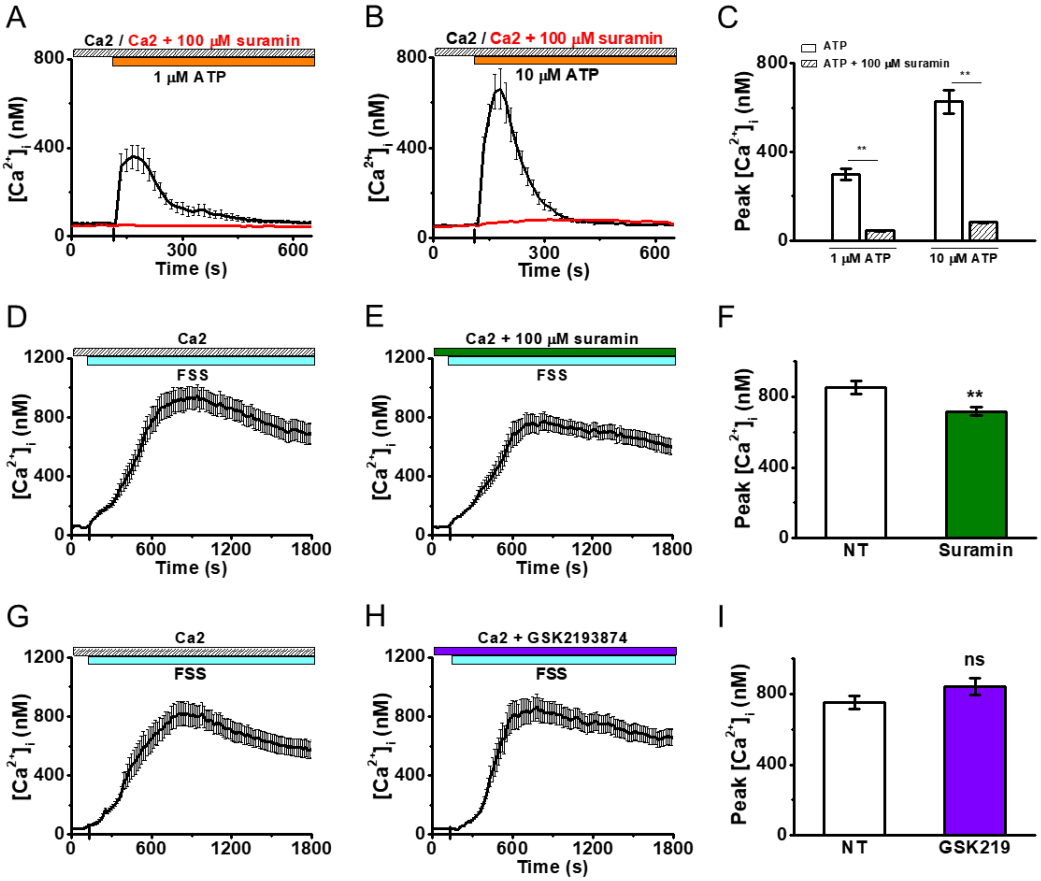

Figure 9. FSS-induced Ca^{2+} entry is partially repressed by a P2X and P2Y receptor antagonist but is not influenced by a TRPV4 channel blocker.
A and B. Representative, averaged $[Ca^{2+}]_i$ dynamics were traced from HDLECs stimulated by 1 μM (*n* = 23 and 18 cells, **A**) or 10 μM (*n* = 29 and 23 cells, **B**) ATP, with or without the pre-incubation with 100 μM suramin. **C.** Statistical analyses of averaged peak $[Ca^{2+}]_i$ values following the ATP treatment confirm the suppressive effects from suramin (*n* = 71, 55, 57, and 74 cells, respectively). **D and E.** Mobilization of cytosolic Ca^{2+} in response to FSS was also recorded from cells treated with (*n* = 32 cells, **D**) or without (*n* = 24 cells, **E**) 100 μM suramin. **F.** Averaged peak $[Ca^{2+}]_i$ values from cells stimulated with FSS alone (*n* = 135 cells) or in the presence of 100 μM suramin (*n* = 245 cells) are shown. **G and H.** Mobilization of cytosolic Ca^{2+} in response to FSS was also recorded from cells treated with (*n* = 17 cells, **H**) or without (*n* = 18 cells, **G**) 100 nM GSK2193874. **I.** Averaged peak $[Ca^{2+}]_i$ values from cells stimulated with FSS alone (*n* = 55 cells) or in the presence of 100 nM GSK2193874 (*n* = 56 cells) are shown. **: $p < 0.01$ compared with the control.

with eGFP-tagged NFATc1. The eGFP-NFATc1 molecules were mostly distributed in the cytoplasm in static HDLECs (Figure 10A and 10F), while they accumulated in the nuclei in HDLECs treated with either TG or FSS for 30 minutes (Figure 10B, 10C, and 10F). This nuclear translocation was blocked by the knockdown of either Orai1 or STIM1 (Figure 10D-10F), supporting our hypothesis that FSS stimulates the nuclear translocation of NFAT through CRAC-mediated Ca^{2+} entry.

To determine the gene expression profile and transcriptional regulation occurring after FSS treatment, HDLECs with normal CRAC channel function or blocked CRAC channel function (by Gd^{3+} or Orai1 knockdown) were treated with FSS via orbital shaker for 2 hours in the incubator and the gene expression profile was obtained using RNA-Seq. The control (static) group and FSS-treated group presented 19252 expressed transcripts (detected in at least half of the samples), in which 2364 genes were significantly up-regulated after FSS treatment while 2075 were significantly down-regulated (False Discovery Rate/FDR < 0.05, Figure 11A). We performed gene ontology (GO) enrichment analysis on the significantly differentially expressed genes and found that they were enriched for the genes involved in cell proliferation, migration, cytoskeleton reorganization, angiogenesis, and leukocyte migration (Figure 11B-11C).

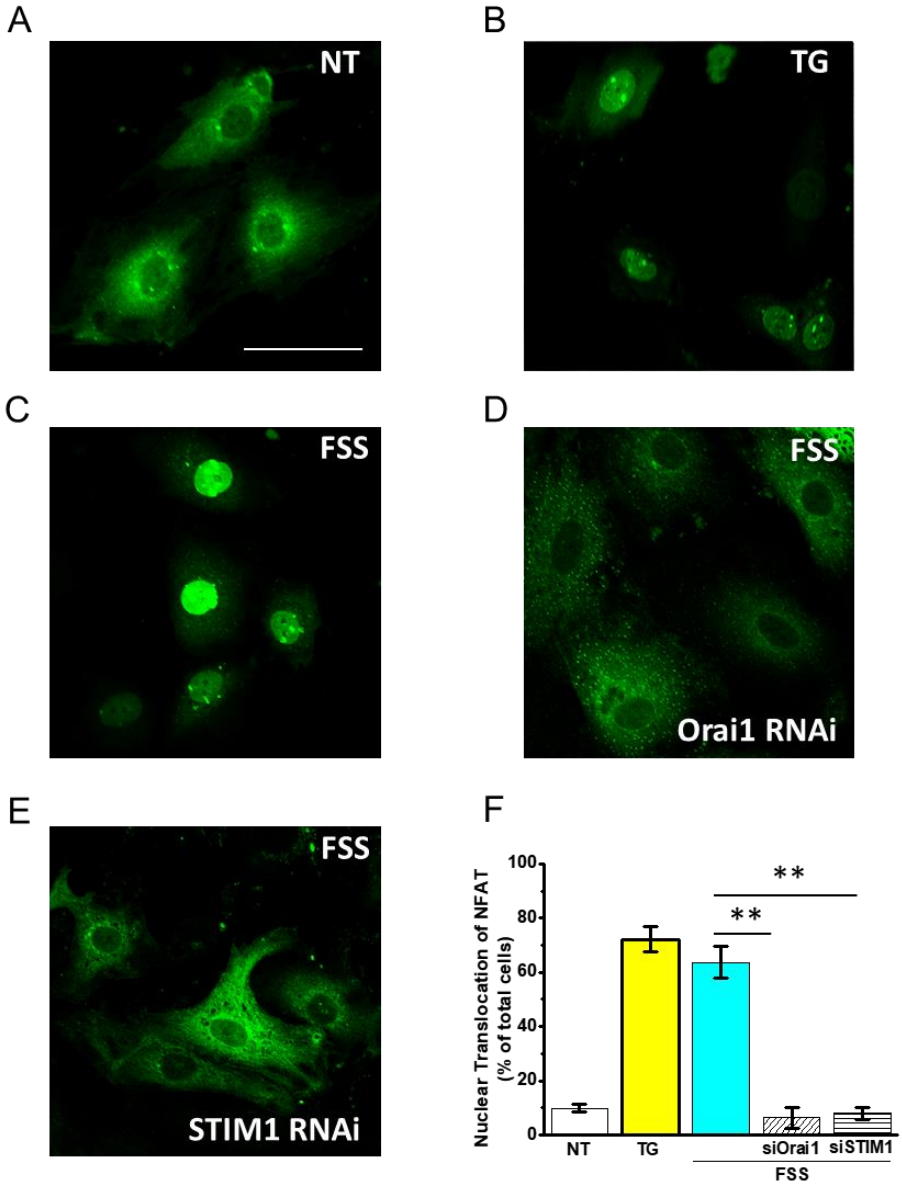

Figure 10. CRAC channel-mediated calcium entry is essential for NFAT nuclear translocation in HDLECs upon FSS stimulation.

A-E. Representative confocal images show the subcellular distributions of over-expressed eGFP-NFAT (green) in HDLECs without treatment (**A**), pretreated with TG (**B**), FSS (**C**) or treated with siRNAs against Orai1 (**D**) or STIM1 (**E**) before FSS stimulations. Scale bars, 20 μm. **F.** Quantitative results on NFAT nuclear translocation from 153 to 434 cells for each set of experiments are shown (n = 341, 359, 434, 153, and 184 cells, respectively). NT: non-treated, the control group. FSS: the fluid shear stress stimulated group. **: $p < 0.01$ compared with the third column (FSS alone).

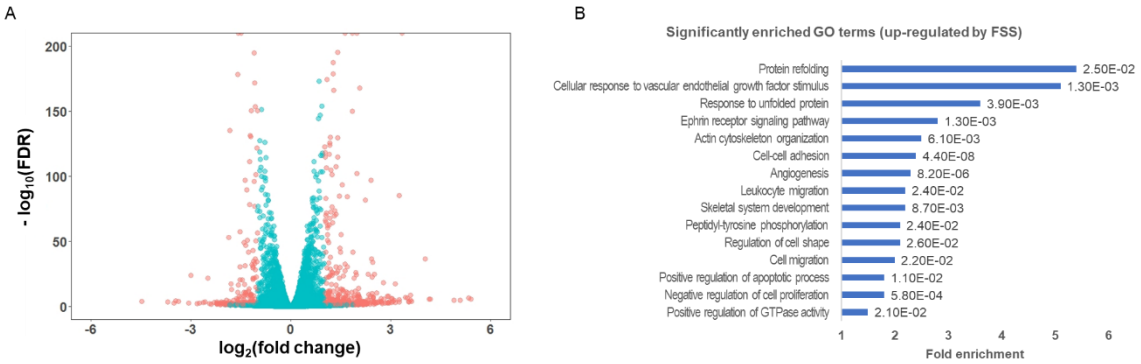

Figure 11. FSS changes the transcriptional expression patterns in HDLECs, which is partially reversed by CRAC channel inhibition.

A. Volcano plot of differentially expressed genes identified in the static HDLECs versus in the HDLEC treated with FSS for 2 hours. The y-axis corresponds to the $\log_{10}$ [false discovery rate (FDR)], and the x-axis displays the $\log_2$ [fold change (FC) value]. The red dots represent the significantly differentially expressed transcripts (FDR < 0.05 and FC > 1); the blue dots represent the transcripts whose expression levels do not reach statistical significance ($p > 0.05$ or FC < 1). **B-C.** Gene ontology (GO) term enrichment analysis for biological processes of (**B**) up- and (**C**) down-regulated genes by FSS treatment. For each GO term, the fold enrichment is displayed in the x-axis and the false discovery rate (FDR) is shown at the end of the bar. **D.** Heatmap and hierarchical clustering of differentially expressed transcripts in HDLECs treated with FSS, or FSS and 10 μM Gd^{3+}, or FSS and siRNAs targeting Orai1. The heatmap displays all transcripts that are differently expressed in the FSS-treated group compared to the static group; the blue-to-yellow colors shows the log2(FC) compared to the transcripts in static HDLECs. The red lines show where the cluster tree is cut to determine cluster membership and the red arrows indicate the clusters where most transcripts are reversed by both CRAC inhibitory approaches. **E.** GO term enrichment analysis for biological processes of the genes reversed by both CRAC channel inhibitory methods. **F.** Quantitative RT-PCR showed the relative mRNA expression levels of IL-8 in untreated HDLECs, FSS-treated HDLECs, and FSS-treated HDLECs with Gd^{3+} or Orai1 knockdown. GAPDH was used as the reference gene in the quantitative RT-PCR and the results were normalized to the IL-8 levels in untreated cells. **G.** The secreted IL-8 concentrations in the culture medium were measured by ELISA for untreated HDLECs, FSS-treated HDLECs, and FSS-treated HDLECs with Gd^{3+} or Orai1 knockdown. The IL-8 concentrations were normalized to the cell number of each well. The significant differences are marked by different letters from a to b.

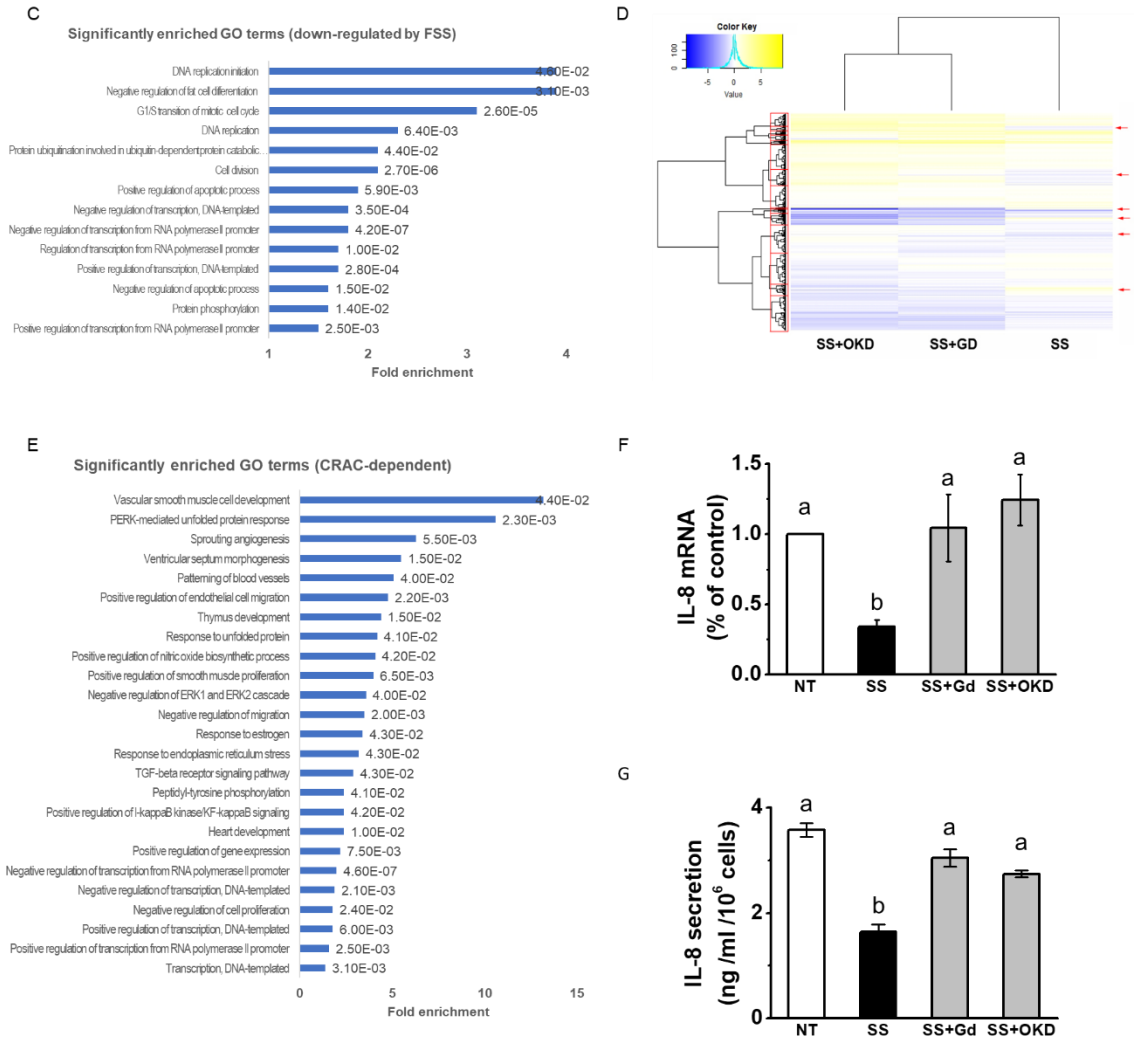

Figure 11 Continued.

When further reviewing the top 20 most significantly up-/down-regulated genes (Table 2 and Table 3), we noticed the enhanced expression of three members of the Krüppel-Like Factor (KLF) family (KLF2, KLF4, and KLF10), together with the reduced expression of three endothelial inflammation-related genes (EDN1, IL1R and BMP4). After examining all expressed KLF family members (Fragments Per Kilobase of transcript per Million mapped reads/FPKM > 0.1), we found a significant increase in KLF2, 3, 4, 7, 10, 11, and 13 and a significant decrease in KLF5, 6, and 15 (Figure 12A). Given that KLF2 and KLF4 are well characterized to be flow sensitive, anti-inflammatory and atheroprotective in vascular ECs, and while KLF6 is linked to post-injury responses, we hypothesized an anti-inflammatory effect in HDLEC responding to our flow settings. Indeed, we discovered down-regulation of multiple pro-inflammatory cytokines and chemokines (e.g., IL-7, CXCL8, IL-16, IL-34, CSF2, CXCL1, and CX3CL1); additionally, IL-11 with anti-inflammatory functions was significantly enhanced (Figure 12B and C).

Based on the previously elucidated essential role of CRAC channels in transducing FSS to intracellular $[Ca^{2+}]_i$ signals, we hypothesized that these transcriptional regulations may partially depend on functional CRAC channels. To test this hypothesis, we conducted hierarchical clustering on all significantly differentially expressed genes in the FSS-treated group compared to the control group (Figure 11D). According to the differential expression patterns, genes were divided into 15 branches. Six out of the 15 clusters indicated by red arrows contained genes with altered

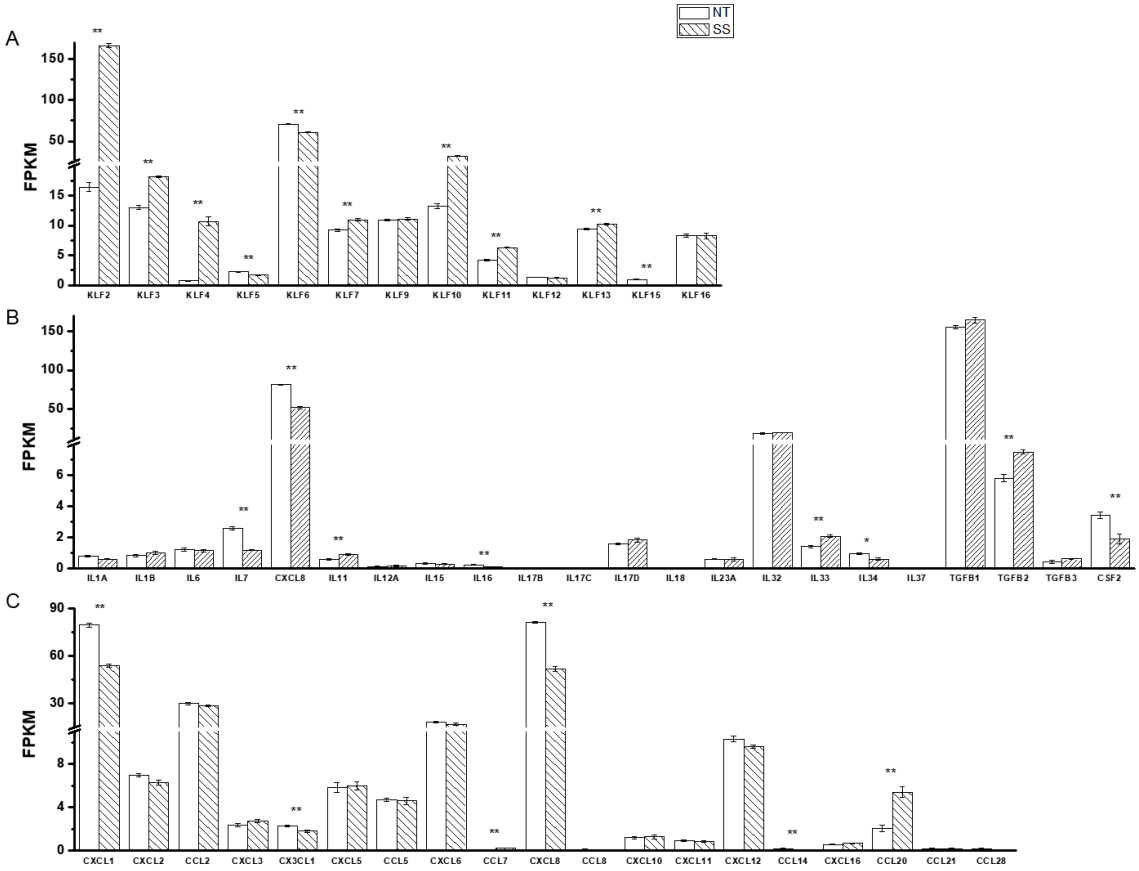

Figure 12. FSS changes the transcription of KLF proteins, cytokines, and chemokines in HDLECs.

A-C. The expression levels are summarized in the bar graphs showing fragments per kilobase of transcript per million mapped reads (FPKM) of KLF family proteins (**A**), cytokines (**B**), and chemokines (**C**). **: $p < 0.01$ compared with the control (NT).

Table 2 The top 20 most significantly up-regulated genes after FSS treatment in HDLEC revealed by RNA-Seq.

Ensembl ID	Gene Symbol	log_2FC	log_2CPM	FDR
ENSG00000127528	KLF2	3.340593	7.5214	0
ENSG00000154734	ADAMTS1	1.852677	6.047111	0
ENSG00000157514	TSC22D3	1.982984	5.713949	0
ENSG00000161940	BCL6B	1.623965	6.863269	0
ENSG00000168209	DDIT4	2.347908	5.761071	6.80E-291
ENSG00000171246	NPTX1	2.393685	5.476566	3.07E-277
ENSG00000111057	KRT18	1.7674	5.572662	2.34E-254
ENSG00000159388	BTG2	1.403718	6.060101	1.17E-245
ENSG00000158859	ADAMTS4	1.595409	5.916264	1.49E-240
ENSG00000065054	SLC9A3R2	1.219064	7.756011	5.45E-221
ENSG00000178726	THBD	1.080693	7.068044	4.96E-216
ENSG00000130300	PLVAP	1.157293	7.165574	1.17E-210
ENSG00000136826	KLF4	3.86256	4.35514	2.33E-210
ENSG00000124019	FAM124B	1.647365	5.636945	2.20E-205
ENSG00000138166	DUSP5	1.406011	5.739041	6.14E-193
ENSG00000136237	RAPGEF5	1.270256	6.09258	3.16E-185
ENSG00000155090	KLF10	1.266579	6.493032	2.23E-176
ENSG00000099875	MKNK2	1.078537	7.081555	4.16E-172
ENSG00000118900	UBN1	0.854547	7.439096	7.19E-171

Table 3 The top 20 most significantly down-regulated genes after FSS treatment in HDLEC revealed by RNA-Seq.

Ensembl ID	Gene	log_2FC	log_2CPM	FDR
ENSG00000078401	EDN1	-1.49098	8.5773	0
ENSG00000091879	ANGPT2	-1.58439	8.050441	0
ENSG00000198355	PIM3	-1.83446	6.875175	1.30E-243
ENSG00000168874	ATOH8	-1.6146	6.290829	3.70E-226
ENSG00000142871	CYR61	-1.12881	9.866753	4.85E-225
ENSG00000115594	IL1R1	-1.61786	6.079865	7.66E-201
ENSG00000118515	SGK1	-1.10974	7.558955	2.04E-192
ENSG00000102760	RGCC	-1.60481	5.738586	4.86E-176
ENSG00000100311	PDGFB	-1.09028	8.611032	8.79E-170
ENSG00000184588	PDE4B	-1.0683	6.861541	2.50E-151
ENSG00000164442	CITED2	-0.89073	6.765355	2.38E-149
ENSG00000125378	BMP4	-1.18575	6.535266	1.75E-148
ENSG00000134508	CABLES1	-1.00396	6.123824	2.58E-148
ENSG00000115738	ID2	-1.8272	4.098779	4.99E-133
ENSG00000156049	GNA14	-1.21516	5.714715	3.68E-129
ENSG00000099860	GADD45B	-1.21406	6.265636	1.71E-128
ENSG00000138449	SLC40A1	-0.92876	7.000056	1.89E-125
ENSG00000253276	CCDC71L	-0.78179	7.290359	6.37E-124
ENSG00000214944	ARHGEF28	-1.02544	6.416631	6.29E-120

expression by FSS that were reversed by CRAC channel blockage. Specifically, 723 of 2364 up-regulated genes in the FSS group were significantly reduced in both groups with blocked CRAC channels. In contrast, 623 of 2075 transcripts down-regulated by FSS were significantly enhanced by CRAC channels inhibition in both groups. These 1346 genes represent CRAC-dependent transcriptional regulations by FSS. To determine the cellular processes linked to these genes, GO enrichment analysis was performed and the results showed significant enrichment in genes for vascular smooth muscle cell development, angiogenesis, NO synthesis, TGF-β signaling, and NFκB signaling (Figure 11E). To confirm the role of CRAC channels in the FSS-induced cytokine expression change in HDLECs, we performed quantitative RT-PCR and ELISA to study the mRNA levels and secreted protein levels of interleukin 8 (IL-8/CXCL8), respectively. FSS treatment for two hours was able to reduce the mRNA level of IL-8 by approximately 65% in HDLECs compared to the untreated cells; however, this effect was completely inhibited by CRAC channel blockage with 10 μM Gd^{3+} or Orai1 knockdown (Figure 11F). Consistently, treating HDLEC with FSS for 16 hours markedly decreased the IL-8 concentration in the culture medium by approximately 55% and blocking CRAC channels using the same approaches significantly attenuated this alteration (Figure 11G). These data suggest that FSS-induced transcriptional reprogramming is partially dependent on CRAC channel activity and blocking CRAC channels obstructs some inflammatory responses to FSS (e.g., interleukin expression and secretion).

2.5. Discussion

The lymphatic system transports various lymphocytes and antigens, in addition to body fluid, macromolecules, and lipids, to the lymph nodes and exports activated lymphocytes and immune factors to the blood circulation, thereby maintaining optimal immune surveillance and responses (25). Orai1 proteins, CRAC channel forming units, were abundantly expressed in multiple primary and secondary lymphoid tissues, including thymus, spleens, tonsils, lymph nodes, and lymphocytes, in humans (126, 146). The patients with defects in CRAC channel molecules suffer from critical immune diseases (e.g., Severe Combined Immune Deficiency/SCID and autoimmune diseases) caused in part by abnormal lymphocyte functions (90, 126, 129). Consistent with the observations in humans, Orai1 or STIM1/2 knockout mice display multiple defects in the lymphatic system and the immune system, including splenomegaly, lymphadenopathy, and decreased cytokine production by lymphocytes (108, 146). Despite the importance of CRAC channels in the lymphatic tissues and immune responses, the channel activities and functions are still unclear in the lymphatic vasculature. In the present study, we elucidated the expression of CRAC channel components, Orai1 and STIM1, at both mRNA and protein levels in HDLECs; we also unveiled a dominant function of CRAC channels in mediating the FSS-induced $[Ca^{2+}]_i$ dynamics, downstream NFAT nuclear translocation, and global transcriptional regulation in HDLECs. These results clearly demonstrate the vital role of CRAC channels in the electrophysical transduction of mechanical forces and downstream genetic reprograming in LECs.

Our previous studies specifically showed the FSS-induced $[Ca^{2+}]_i$ mobilization in LECs from both intracellular and extracellular Ca^{2+} sources (165), but the identity of the channel molecules mediating this Ca^{2+} signal remained elusive. In this study, we revealed that constant FSS stimulation released ER Ca^{2+} stores and induced a significant $[Ca^{2+}]_i$ entry via CRAC channels in HDLEC. Application of classic CRAC channel blockers and overexpression of DN-Orai1 proteins all robustly reduced the FSS-induced Ca2+ mobilization into the cells; moreover, knocking down either endogenous Orai1 or STIM1 proteins by siRNAs remarkably diminished the $[Ca^{2+}]_i$ peak and abolished the plateau, indicating that CRAC channels, formed by Orai1 and STIM1 molecules, are predominantly responsible for the Ca^{2+} entry from the extracellular spaces upon FSS stimulation in HDLECs. Orai2/3 and STIM2 were also proposed to mediate Ca^{2+} entry in previous studies but knocking down Orai2/3 or STIM2 did not demonstrate significant inhibition of the FSS-induced Ca^{2+} mobilization in our model, confirming our result that Orai1 and STIM1 are the fundamental molecules in this process.

One of the most intriguing topics in the field of vascular physiology is the meticulous mechanism of shear stress sensing and the "sensor" molecules involved. Many molecules/complexes have been proposed to sense mechanical forces in different flow conditions and various cell types (173, 198-201). Since the commonly observed $[Ca^{2+}]_i$ dynamics following FSS stimulation in both ECs and LECs suggests the involvement of Ca^{2+} signaling in converting physical forces into intracellular electrochemical signals (165, 202), we examined several proposed sensor molecules using Ca^{2+} responses as our readouts. Piezo1 and Piezo2 proteins form non-selective

cation channels that are activated by physical stimuli on the PM and convert extracellular mechanical signals into cation influx in multiple cell types (203). Piezo1 is required for the alignment of BECs responding to blood flow and the development of blood vasculature in mice; while Piezo2 is involved in the touch sensation in mice (204-207). Importantly, loss of Piezo1 function was recently shown to cause congenital lymphoedema in human patients carrying mutations in PIEZO1 gene, as well as defects in lymphatic valve formation in EC- or LEC-specific PIEZO1 knockout mice (205, 208). Together, these *in vivo* observations suggest an essential role of Piezo proteins in vascular development and possibly in LEC mechanotransduction. TRPV4 is another channel reported to mediate FSS-induced Ca^{2+} influx and important in FSS-induced blood vasodilation (209, 210). Similarly, the purinoceptors, P2X/2Y, are also extensively studied in the mechanotransduction and found to be important in FSS-induced Ca^{2+} influx, BEC alignment, and vasodilation in blood vessels (199, 211-213). Our data in this study rejected a principal function for Piezo1/2 proteins or TRPV4 channels in the FSS-induced Ca^{2+} responses using molecular and pharmacological tools. Notwithstanding, P2X/P2Y displayed a marginal role in the FSS-induced $[Ca^{2+}]_i$ mobilization in our experimental setting, implying the potential involvement of ATP in FSS processes in LECs. Our results suggest a promising approach to identify shear sensing units using Ca^{2+} responses as convenient readouts. Together with our mRNA-Seq data showing the transcriptional levels of all highly expressed membrane proteins in LECs (predicted by The Human Protein Atlas, https://www.proteinatlas.org, Table 4),

our study paves the way for further characterization of the direct sensor(s) that convert the changes of membrane tension into biochemical signals and release the ER Ca^{2+} store.

Besides the shear sensing mechanisms, downstream functional responses in ECs are also sophisticated when subjected to distinct flow patterns (168). Specifically, disturbed flow (e.g., blood flow in the carotid artery sinus and other branching positions) induces inflammatory and atheroprone responses, while high steady flow inhibits these responses and is atheroprotective (168, 174). Nevertheless, unlike the relatively steady nature of blood flow, lymph flow is extremely dynamic, disturbed at the valve sites and branch points and commonly oscillatory in collecting lymphatic vessels at physiological conditions, yet show no signs of atherogenesis (1, 5, 177). So the LECs have unique responses to various flow patterns. In the present study, our RNA-Seq data showed reduced transcription levels of some major pro-inflammatory cytokines and enhanced levels of anti-inflammatory cytokines in HDLECs under orbital FSS estimated to be 4 $dyns/cm^2$. Consistently, we also observed increased expressions of KLF2 and KLF4 that were reported to be anti-inflammatory and atheroprotective in atherosclerosis models. These findings indicate a potential protective role of orbital FSS in HDLEC, suggesting disparate flow responses in LECs compared with BECs.

In conclusion, we present comprehensive evidence in this study to characterize FSS-induced $[Ca^{2+}]_i$ signaling and to understand the specific channels and fundamental molecules mediating FSS-induced $[Ca^{2+}]_i$ dynamics and downstream transcriptome regulations in LECs. Our findings should provide insight into the molecular mechanisms

of mechanotransduction in LECs and the vascular regulation brought about by flow in the lymphatic system.

Table 4 The top 100 most abundantly expressed predicted membrane protein genes in HDLEC.

Ensembl ID	Gene Symbol	FPKM
ENSG00000198804	GK	4262.565
ENSG00000198712	GLMP	3827.362
ENSG00000198899	L1CAM	3152.669
ENSG00000198886	MT-ND1	2263.712
ENSG00000198938	MFAP3L	2088.205
ENSG00000212907	KIR3DL2	1688.662
ENSG00000198695	MT-CO2	1540.381
ENSG00000198727	LRRTM3	1285.865
ENSG00000198888	SHISA4	1283.146
ENSG00000198786	TMEM184B	1194.872
ENSG00000198840	SELENOT	922.6772
ENSG00000198763	APCDD1L	851.108
ENSG00000126709	IFI6	794.7977
ENSG00000106991	ENG	617.5708
ENSG00000228253	C19orf24	462.943
ENSG00000142089	IFITM3	426.2275
ENSG00000084234	APLP2	418.6642
ENSG00000105974	CAV1	393.9038
ENSG00000142192	APP	366.9639
ENSG00000088832	FKBP1A	311.6461
ENSG00000261371	TMEM249	269.1223
ENSG00000150938	CRIM1	268.9733
ENSG00000169100	SLC25A6	264.0027
ENSG00000161638	ITGA5	263.3546
ENSG00000179776	CDH5	259.2923
ENSG00000150093	ITGB1	253.7635
ENSG00000163513	TGFBR2	236.0307
ENSG00000134294	SLC38A2	221.8109
ENSG00000085063	CD59	219.0095
ENSG00000128567	PODXL	210.1234
ENSG00000204592	DISP3	209.8835
ENSG00000234745	SHISA8	195.8041
ENSG00000129562	DAD1	192.1531
ENSG00000152661	GJA1	186.4857
ENSG00000152558	TMEM123	186.2306
ENSG00000135404	CD63	180.3649
ENSG00000068697	LAPTM4A	168.9131

Table 4 Continued

Ensembl ID	Gene Symbol	FPKM
ENSG00000183255	PTTG1IP	165.8474
ENSG00000002586	CD99	165.6159
ENSG00000066056	TIE1	162.0884
ENSG00000010278	CD9	159.4076
ENSG00000005022	SLC25A5	158.7829
ENSG00000176435	CLEC14A	156.0934
ENSG00000117298	ECE1	153.0533
ENSG00000004399	PLXND1	152.153
ENSG00000197747	LHFPL5	148.921
ENSG00000134352	IL6ST	141.9589
ENSG00000168899	VAMP5	138.8527
ENSG00000148175	STOM	136.659
ENSG00000125810	CD93	132.4288
ENSG00000127022	CANX	132.2754
ENSG00000135318	NT5E	131.3201
ENSG00000100300	TSPO	130.1026
ENSG00000169908	TM4SF1	120.6594
ENSG00000170989	S1PR1	120.4933
ENSG00000228474	LINC01125	120.1467
ENSG00000204525	MUC21	119.6251
ENSG00000187513	ATP13A5	118.6901
ENSG00000118705	RPN2	116.8466
ENSG00000185201	MC2R	115.5946
ENSG00000172270	BSG	113.7177
ENSG00000149925	ALDOA	112.7447
ENSG00000140564	FURIN	112.6937
ENSG00000148248	SURF4	108.9876
ENSG00000058262	SEC61A1	106.1474
ENSG00000162618	ADGRL4	105.6132
ENSG00000069849	ATP1B3	105.0178
ENSG00000157227	MMP14	104.7785
ENSG00000115310	RTN4	104.5998
ENSG00000196411	NPIPB15	99.85414
ENSG00000099282	TSPAN15	98.77917
ENSG00000198856	LTN1	98.42202
ENSG00000139644	TMBIM6	97.77429
ENSG00000136156	ITM2B	97.44957
ENSG00000206503	HACD2	96.73154

Table 4 Continued

Ensembl ID	Gene Symbol	FPKM
ENSG00000185896	FFAR3	95.78088
ENSG00000181104	F2R	95.15766
ENSG00000177697	CD151	95.145
ENSG00000184840	DRD1	92.73211
ENSG00000143870	PDIA6	91.26543
ENSG00000110108	TMEM109	91.01703
ENSG00000154133	ROBO4	90.34233
ENSG00000076706	MCAM	89.77205
ENSG00000073008	PVR	89.46667
ENSG00000162493	PDPN	88.76727
ENSG00000113732	ATP6V0E1	87.60019
ENSG00000137409	MTCH1	87.40874
ENSG00000138448	ITGAV	86.20617
ENSG00000163399	ATP1A1	85.67757
ENSG00000114698	PLSCR4	85.50376
ENSG00000165678	GHITM	85.40497
ENSG00000111897	SERINC1	83.77665
ENSG00000136026	CKAP4	83.68886
ENSG00000120279	MYCT1	83.44524
ENSG00000101384	JAG1	83.19346
ENSG00000010327	STAB1	82.79328
ENSG00000170540	ARL6IP1	82.79269
ENSG00000198053	43164	81.88087
ENSG00000112697	TMEM30A	81.59537
ENSG00000106803	SEC61B	81.24746

3. THE CRAC CHANNELS ARE RESPONSIBLE FOR HISTAMINE-INDUCED CALCIUM ENTRY, HYPERPERMEABILITY, AND INTERLEUKIN SYNTHESIS IN LYMPHATIC ENDOTHELIAL CELLS

3.1. Overview

The lymphatic functions needed to maintain lymph transport and immune surveillance can be impaired by infection and inflammation, thereby causing debilitating disorders such as lymphedema and inflammatory bowel disease. Histamine is a key inflammatory mediator known to trigger vasodilation and vessel hyperpermeability upon binding to its receptors and evoking $[Ca^{2+}]_i$ dynamics for the downstream signal transduction. However, the exact molecular mechanisms behind the $[Ca^{2+}]_i$ dynamics and the downstream cellular effects have not been elucidated in the lymphatic system. Here, we show that CRAC channels, formed by Orai1 and STIM1 proteins, are required for the histamine-elicited Ca^{2+} signaling in LECs. Blockers or antagonists against CRAC channels, phospholipase C, and H_1R receptors all significantly diminished the histamine-evoked $[Ca^{2+}]_i$ dynamics in LECs. Knockdown of endogenous Orai1 or STIM1 by siRNAs also abolished the Ca^{2+} entry upon histamine stimulation in LECs. Furthermore, the histamine-triggered endothelial hyperpermeability and VE-cadherin disruption were remarkably attenuated by CRAC channel blockers. Additionally, the upregulated expression of inflammatory cytokines, interleukin-6 and -8, after histamine stimulation was abolished by silencing Orai1 or STIM1 with RNAi in LECs. Taken together, our data demonstrate the essential role of CRAC channels in mediating the $[Ca^{2+}]_i$ signaling

and downstream endothelial barrier and inflammatory functions induced by histamine in LECs.

3.2. Introduction

The lymphatic system provides essential pathways to transport the accumulated fluid, proteins, and cells from the interstitial spaces back to the circulatory system, thereby maintaining the body fluid homeostasis and immune surveillance (1, 2). Compromised lymphatic functions or integrity leads to many severe diseases, including lymphedema and inflammation (25). In the past two decades, several studies have discovered the critical roles of lymphatic vessels in immune responses and inflammatory diseases (e.g., inflammatory bowel disease / IBD and renal inflammations) (22, 37, 175, 214, 215). LECs line the lumen of lymphatic vessels and are exposed directly to the lymph (216-218). LECs remodel their cytoskeleton structures and intercellular junctions upon inflammatory stimuli in pathological conditions; they also synthesize cytokines to attract leukocytes and mediate leukocyte entry into the lymphatic system to aid in immune responses (9, 219, 220). However, the cellular and molecular mechanisms underlying the lymphatic responses to inflammatory stimuli are still at early stages of understanding.

Histamine is an important inflammatory mediator released predominantly by mast cells and basophils, causing vasodilation, vascular hyperpermeability, smooth muscle contraction, arrhythmias and altering lymphatic vessel contractile and pumping activities (59, 60). Histamine binds to four GPCRs, H_1R – H_4R, on the PM and triggers

$[Ca^{2+}]_i$ elevation, F-actin remodeling, intercellular junction reassembly, and cytokine production in BECs (62, 66, 71-73). Histamine has been shown to activate the PLC family through its receptors and generates IP_3 and diacylglycerol as second messengers to release the ER Ca^{2+} stores and trigger downstream Ca^{2+} signaling in BECs (62, 164, 221).

The CRAC channel, formed by Orai and STIM proteins, is a key route for sustained Ca^{2+} influx following intracellular Ca^{2+} store release in various cell types (78, 84-92, 222). Proper CRAC channel function is essential for the Ca^{2+} signaling to support the activation of T lymphocytes, development of B lymphocytes, and release of cytokines from mast cells (186, 187). Previously, we showed that CRAC channels mediate Ca^{2+} entry upon histamine stimulation and are necessary for the NFAT translocation and IL-8 production in HUVECs (164). However, the role of CRAC channels in the lymphatic responses to histamine, especially the permeability alteration and inflammatory responses, remains elusive.

In this study, we show that histamine-evoked $[Ca^{2+}]_i$ increase includes a Ca^{2+} store release through H_1R and a sustained Ca^{2+} influx via CRAC channels in HDLECs. This CRAC channel-mediated Ca^{2+} signaling is required for both increased permeability and enhanced interleukin (IL) -6 and -8 expressions after histamine stimulation in HDLECs.

3.3. Materials and methods

3.3.1. Chemicals

Physiological saline solutions (Table 1) were prepared using chemicals of reagent grade purchased from Sigma-Aldrich. The measured osmolality was 319 mOsm ± 2% and the pH was adjusted with sodium hydroxide to 7.35. Histamine, gelatin solution (2%), diphenhydramine hydrochloride, fexofenadine hydrochloride, and $GdCl_3$ were also purchased from Sigma-Aldrich. Fura-2 AM, thapsigargin, BTP2, SKF-96365, and U-73122 were purchased from Thermo-Fisher Scientific.

3.3.2. Human dermal lymphatic endothelial cell culture

HDLECs derived from juvenile human foreskin and microvascular endothelial growth medium 2 (MV2) were purchased from PromoCell. HDLECs were maintained following the manufacturer's protocol and passaged with trypsin-EDTA (0.05%) at confluence. Cells with passages less than ten were used for all experiments. For $[Ca^{2+}]_i$ imaging or confocal imaging, cells were seeded onto glass coverslips pretreated with 2% gelatin.

3.3.3. Single-cell $[Ca^{2+}]_i$ imaging

Single-cell $[Ca^{2+}]_i$ imaging was conducted using an IX-81 (Olympus) microscope-based system, as described previously (223). HDLECs were loaded with 2 μM Fura-2 AM in the culture medium in the incubator (37 °C and 5% CO_2) for 40 minutes. Loaded cells were briefly washed using Ca2 solution after loading and then bathed in saline solutions used in each $[Ca^{2+}]_i$ imaging experiment. The fluorescence

density and ratio data were analyzed with the Metafluor software (Universal Imaging) and the OriginPro 8 software (OriginLab) and expressed as mean ± SEM.

3.3.4. RNA interference

For knockdown of Orai1 and STIM1, a mixture of four siRNAs targeting each gene was purchased from Dharmacon. HDLECs were cultured to 75% confluency and transfected with siRNAs using the Lipofectamine RNAiMAX Transfection Reagent (Life technologies) according to the manufacturer's instructions. Cells were used in experiments within 60-72 hours post transfection.

3.3.5. RNA isolation and quantitative RT-PCR

Total RNA was isolated from HDLECs using the RNeasy Mini Kit (Qiagen) following the manufacturer’s protocol. The first-strand cDNA generation was achieved with the SuperScript IV First-Strand Synthesis System (Thermo-Fisher Scientific). The qRT-PCRs were performed using RT2 SYBR Green ROX qPCR Mastermix (Qiagen). GAPDH was used as the reference gene and the primers used in this study are summarized in Table 5.

3.3.6. Western blots

Whole cell lysates were separated by SDS-PAGE and transferred to nitrocellulose membranes using a transfer apparatus according to the manufacturer’s protocols (Bio-Rad). Samples were then analyzed by standard western blotting. Immunoblots were probed with the primary antibodies including rabbit anti-STIM1 (1:2500) (85), rabbit anti-Orai1 (1:500, Aviva Systems Biology) and mouse anti-GAPDH (1:1000, Santa Cruz).

3.3.7. Immunofluorescence and confocal imaging

HDLECs were cultured on glass coverslips pretreated with 2% gelatin to form monolayers and treated with 20 μM histamine, 20 μM histamine with 10 μM BTP2, or 20 μM histamine with 10 μM Gd^{3+} for 30 minutes in the incubator (37 °C and 5% CO_2). Cells with or without treatment were then fixed in 4% paraformaldehyde in PBS. VE-cadherin was recognized with primary anti-VE-cadherin antibody (1:100, Santa Cruz) and Alexa Fluor® 594-conjugated secondary antibody (1:200, Thermo-Fisher Scientific). Cells were mounted using ProLong™ Gold Antifade Mountant with DAPI (Thermo-Fisher Scientific) and finally visualized utilizing a confocal laser-scanning microscope (FV300; Olympus) equipped with the FluoView software. Confocal microscopy was performed at the Integrated Microscopy and Imaging Laboratory in the Department of Medical Physiology, Texas A&M University Health Science Center, Temple, Texas.

3.3.8. Permeability assays

HDLEC (4 x 10^4 cells/well) were seeded in 6.5 mm Transwell® filter inserts with 0.4 μM pores (polyester membrane, Corning-Costar) and cultured to confluence for 48 hours. For the Transwell® assay, fluorescein isothiocyanate (FITC)-dextran (40 kDa, 1 mg/ml; Sigma-Aldrich) was added to the upper compartment of the Transwell® inserts with or without 20 μM histamine, 10 μM BTP2, or 10 μM Gd^{3+} for 30 minutes in the

Table 5 Primers used in qRT-PCR analysis (sequence 5’ → 3’)

Gene	**Forward**	**Reverse**
IL-6	GGTACATCCTCGACGGCATCT	GTGCCTCTTTGCTGCTTTCAC
IL-8	AGCACTCCATAAGGCACAAA	ACACACAGTGAGATGGTTCC
SCF	CCAGAACCCAGGCTCTTTAC	GATTTTTGGCCTTCCCTTTCTC
GAPDH	TATAAATTGAGCCCGCAGCC	TTCCCGTTCTCAGCCTTGAC

incubator (37 °C and 5% CO_2). Medium samples (300 µl) were taken from each lower compartment and added to three microplate wells (100 µl / well), and fluorescence (485 nm / 510 nm) of the samples was measured with a fluorescence plate reader (Bio-Rad). The mean fluorescence recorded from the sample obtained from untreated cells was set as 1. Fluorescence from other groups was expressed as a relative value compared to the control level. For the transendothelial electrical resistance (TEER) assay, the Transwell® insert with a confluent HDLEC monolayer was installed in an EndOhm Cell Culture Cup Chamber (6 mm, World Precision Instruments) with 1 ml of fresh medium. The apparatus was placed on a heating pad at 37 °C and TEER was measured by an Epithelial Volt/Ohm Meter (EVOM2) together with an STX2 electrode. An empty insert with culture medium but no cells was used as the blank for each day's experiment. For each insert with an HDLEC monolayer, a TEER baseline was measured with 180 µl medium, and then TEER was further measured after 20 µM histamine, 10 µM BTP2, or 10 µM Gd^{3+} was added to the medium. The blank TEER was subtracted from all TEER readings and the TEER baseline was set as 1 for each experiment.

3.3.9. Statistical analysis

All data were collected from at least three independent experiments and presented as mean ± SEM. Statistical significance was evaluated using SAS software (University Edition) and assessed by one-way ANOVA and Tukey post-hoc test (among multiple groups) or Student's t-test (between two groups). Statistically significant difference was determined by P-value $\leqslant 0.05$.

3.4. Results

3.4.1. Histamine evokes sustained $[Ca^{2+}]_i$ dynamics in HDLECs in a dose-dependent manner

To study the $[Ca^{2+}]_i$ dynamics in living HDLECs, we loaded cells with 2 μM Fura-2-AM in culture medium for 40 minutes in the incubator and imaged cells in a saline solution containing 2 mM Ca^{2+} (Ca2, see Table 1) at room temperature. Different concentrations (10, 20, 50, and 100 μM) of histamine were applied to the cells respectively and elicited a dose-dependent increase of $[Ca^{2+}]_i$ that peaked within 60 seconds (Figure 13A - D). When 10 μM histamine was applied, $[Ca^{2+}]_i$ approached the peak (246 ± 15 nM) within 60 seconds and displayed a slowly descending plateau with a sustained $[Ca^{2+}]_i$ level of 101 ± 9 nM at 3 minutes after histamine application (Figure 13A, E, and F). The $[Ca^{2+}]_i$ levels returned to the resting state in approximately 6 minutes post histamine stimulation at 10 μM after a gradually descending plateau (Figure 13A). With 20 μM histamine, the $[Ca^{2+}]_i$ reached a peak of 338 ± 14 nM and maintained a higher plateau with a sustained $[Ca^{2+}]_i$ level of 180 ± 8 nM (Figure 13B, E, and F). The maximal $[Ca^{2+}]_i$ response was achieved at 50 μM histamine with a sharp peak of 415 ± 22 nM in 15 seconds and a sustained $[Ca^{2+}]_i$ level of 250 ± 10 nM at 3 minutes after histamine stimulation (Figure 13C, E, and F). Responses to 100 μM histamine did not show significant further enhancement of either peak (409 ± 18 nM) or sustained (285 ± 13 nM) $[Ca^{2+}]_i$ levels in HDLEC (Figure 13D, E, and F). With 50 or 100 μM histamine, the $[Ca^{2+}]_i$ levels were maintained higher than the resting level in our 500 seconds of recordings.

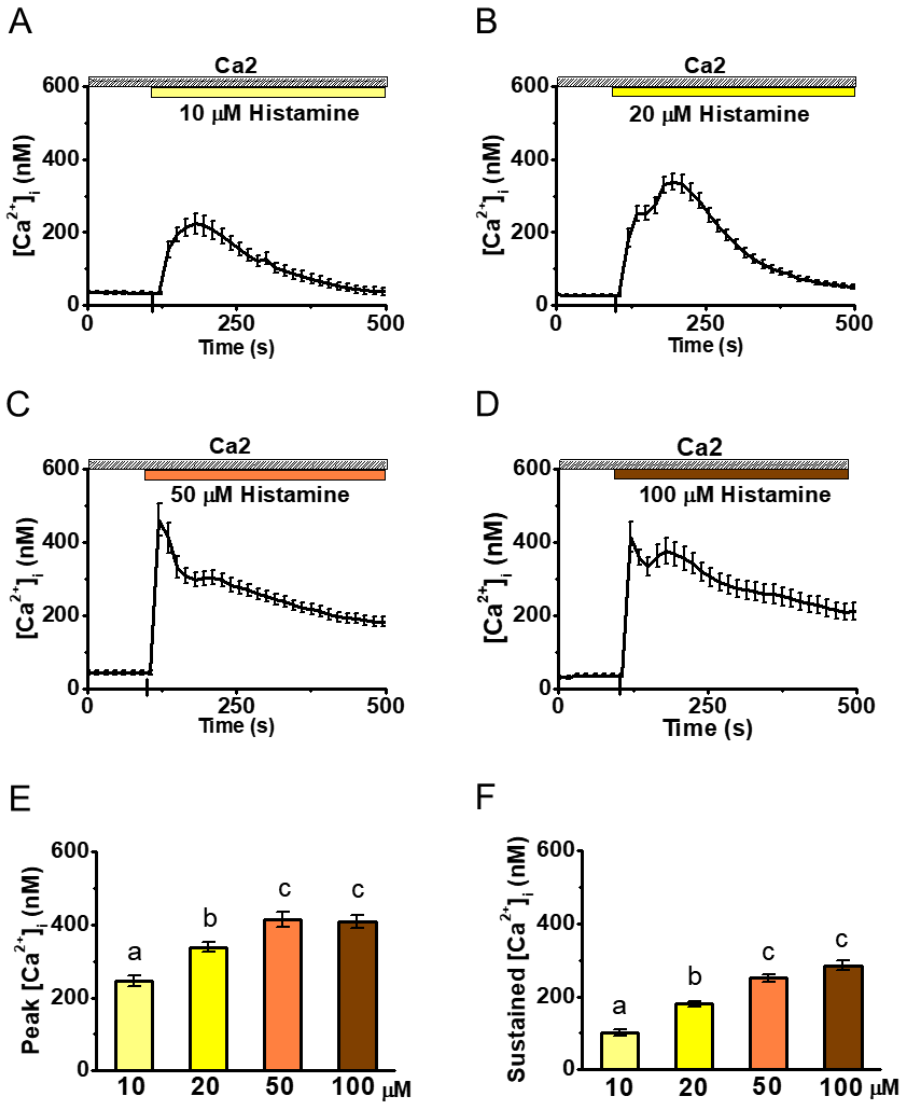

Figure 13. Histamine triggers Ca^{2+} dynamics in a concentration-dependent manner in HDLECs.

A – D. Representative $[Ca^{2+}]_i$ recordings show cytosolic Ca^{2+} concentrations upon histamine stimulations at 10 μM (**A**, n = 15 cells), 20 μM (**B**, n = 18 cells), 50 μM (**C**, n = 17 cells), and 100 μM (**D**, n = 26 cells). The top bars indicate the type of extracellular solutions (Table 1) applied to the cells and the vertical lines on the x-axis indicate the time of solution change. **E and F.** Statistical analysis of averaged, peak (**E**) and sustained (**F**) $[Ca^{2+}]_i$ levels coupled to histamine stimulations obtained at 3 minutes after the application of histamine, for the four different concentrations. Statistically significant differences are indicated by different letters from a to c.

3.4.2. The histamine-dependent $[Ca^{2+}]_i$ dynamics, containing both intracellular Ca^{2+} store release and extracellular Ca^{2+} entry, are mediated by H_1R and PLC in HDLECs

To identify the Ca^{2+} sources of histamine-triggered $[Ca^{2+}]_i$ dynamics in HDLECs, we changed the culture medium to a Ca^{2+}-free solution (Ca0, see Table 1) right after Fura-2-AM loading to avoid extracellular Ca^{2+} entry and recorded the $[Ca^{2+}]_i$ responses after histamine stimulation. Under this condition, the initial increase of $[Ca^{2+}]_i$ was still observed upon histamine addition without notable delays (Figure 14A and B). However, the peak $[Ca^{2+}]_i$ levels were lower than the control experiments in Ca2 solution and the sustained $[Ca^{2+}]_i$ plateau was eliminated in Ca0 solutions (Figure 14A, B, F, and G). These results indicate that histamine elicits the initial Ca^{2+} dynamics by releasing the intracellular Ca^{2+} store but the peak $[Ca^{2+}]_i$ and following plateau require Ca^{2+} import from extracellular environments.

Histamine binds to four subtypes of GPCRs in human cells (H_1R – H_4R) and H_1R was shown to mediate Ca^{2+} signaling in blood endothelium (62, 73). We utilized two classical H_1R antagonists, diphenhydramine (224) and fexofenadine (225), to evaluate the role of H_1R in histamine-evoked $[Ca^{2+}]_i$ dynamics in LECs. 30 μM diphenhydramine or 30 μM fexofenadine in the external Ca2 solution is sufficient to abolish $[Ca^{2+}]_i$ responses, including both the initial response that existed in Ca0 solution and the following plateau, indicating that the blockage of H_1R eliminated both intracellular Ca^{2+} store release and further Ca^{2+} entry from the extracellular solution (Figure 14C, D, F and G).

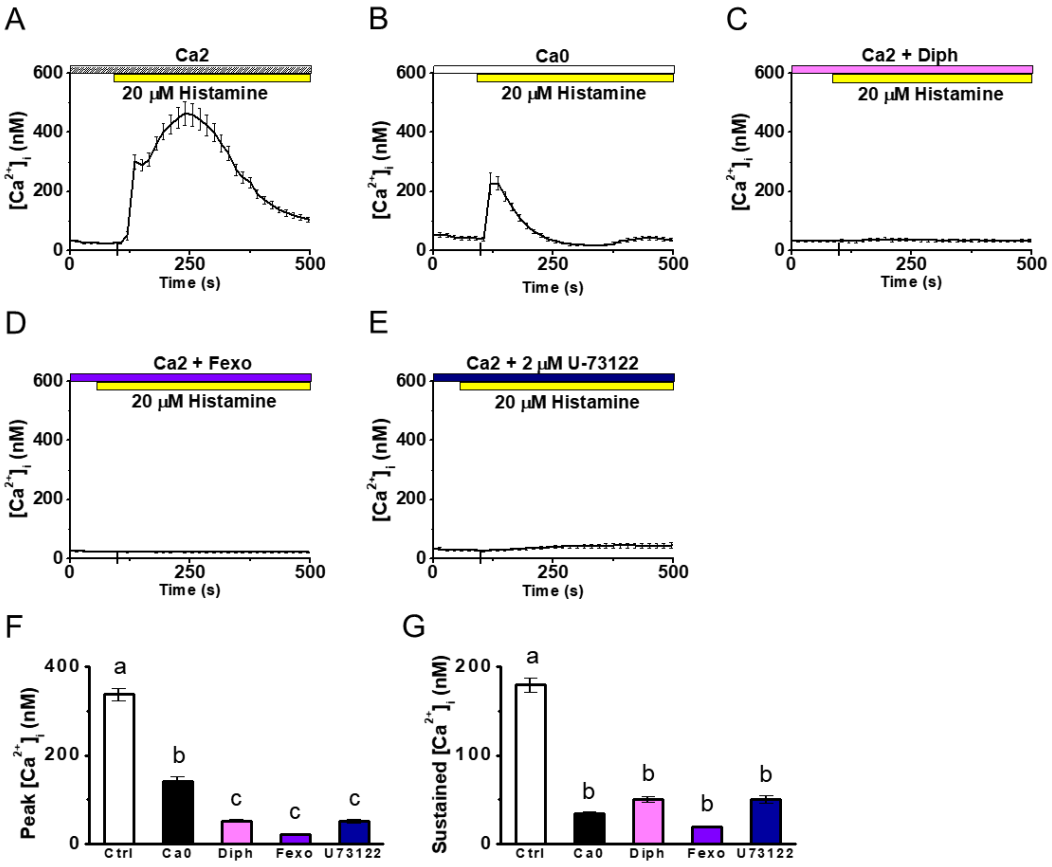

Figure 14. Antagonists targeting H_1R and PLC completely abolish the Ca^{2+} dynamics induced by histamine in HDLECs.

A – E. Representative $[Ca^{2+}]_i$ traces corresponding to 20 μM histamine in control Ca2 saline (**A**, n = 26 cells), Ca^{2+}-free (Ca0) saline (**B**, n = 17 cells), and Ca2 saline containing 30 μM diphenhydramine (**C**, n = 18 cells), 30 μM fexofenadine (**D**, n = 21 cells), or 2 μM U-73122 (**E**, n = 20 cells). **F and G.** Averaged peak (**F**) and sustained (**G**) $[Ca^{2+}]_i$ values are summarized and significant differences are denoted by different letters from a to c.

PLC is a major enzyme that connects GPCRs to ER Ca^{2+} store release by catalyzing the hydrolysis of PIP_2 to IP_3. The produced IP_3 then binds to the IP3 receptors on the ER membrane to release the ER Ca^{2+} store (226). To determine whether PLC is responsible for the histamine-dependent $[Ca^{2+}]_i$ responses in HDLECs, we applied a PLC inhibitor, U-73122 (227-231), before the histamine treatment. As expected, the histamine-triggered Ca^{2+} store release and Ca^{2+} entry were both diminished by 2 μM U-73122 (Figure 14E). Notably, the peak and sustained $[Ca^{2+}]_i$ levels treated with U-73122 and histamine are comparable to that with H_1R antagonists and histamine in HDLECs (Figure 14F and G), suggesting that PLC signaling is the dominant pathway linking H_1R to the ER Ca^{2+} store release upon histamine stimulation.

Taken together, our results suggest that histamine-triggered $[Ca^{2+}]_i$ dynamics in HDLECs is composed of a fast release of the intracellular ER Ca^{2+} store and a sustained Ca^{2+} influx from the external environment. Further, these two components of Ca^{2+} mobilization are most likely mediated by H_1R binding and downstream PLC activation.

3.4.3. The histamine-triggered $[Ca^{2+}]_i$ mobilization in HDLECs is inhibited by multiple CRAC channel blockers

CRAC channels have been shown to mediate SOCE after ER-store release in various cell types including endothelial cells (152, 232), therefore, we applied three different CRAC channel blockers, BTP2 (233), Gd^{3+} (86), and SKF-96365 (234), to determine whether CRAC channels mediate the sustained Ca^{2+} influx upon histamine stimulation. First, we validated the effect of three CRAC channel blockers, BTP2 (10 μM), Gd^{3+} (10 μM), and SKF-96356 (30 μM), in HDLECs in inhibiting SOCE evoked

by 2 μM TG. In the control experiments, TG inhibited the SERCA (235) and passively depleted the ER Ca^{2+} store in Ca0 solution; when Ca^{2+} was added back, a significant increase of $[Ca^{2+}]_i$ followed by a gradually descending plateau was observed as the SOCE refilled the ER Ca^{2+} store in HDLECs via CRAC channels (Figure 15A). As expected, the three CRAC channel blockers, independently applied to the external solution, effectively inhibited the Ca^{2+} influx through CRAC channels and thereby significantly diminished the sustained plateau $[Ca^{2+}]_i$ measured at 5 minutes after the application of blockers (Figure 15B – E). Interestingly, all three CRAC channel blockers were able to abolish the histamine-triggered Ca^{2+} influx into HDLECs (i.e., the sustained $[Ca^{2+}]_i$ plateau) but not the initial Ca^{2+} responses (Figure 16A – D). The histamine-evoked $[Ca^{2+}]_i$ dynamics in the cells treated with CRAC channel blockers are comparable to that in the Ca^{2+}-free solution (Figure 16E and F), suggesting that the CRAC channels are likely conducting the Ca^{2+} mobilization from the external solutions but have little impact on the intracellular Ca^{2+} store release upon histamine stimulation in HDLECs.

3.4.4. Genetic knockdown of Orai1 or STIM1 diminishes the histamine-dependent Ca^{2+} entry in HDLECs

The CRAC channels in BECs are predominantly formed by Orai1 proteins on the PM and STIM1 proteins on the ER membrane (236). To eliminate the possible off-target effect of CRAC channel blockers and to study the molecular basis of histamine-triggered $[Ca^{2+}]_i$ mobilization in HDLECs, we utilized the RNAi technique to genetically knockdown the expression of Orai1 or STIM1. HDLECs were transfected with siRNAs

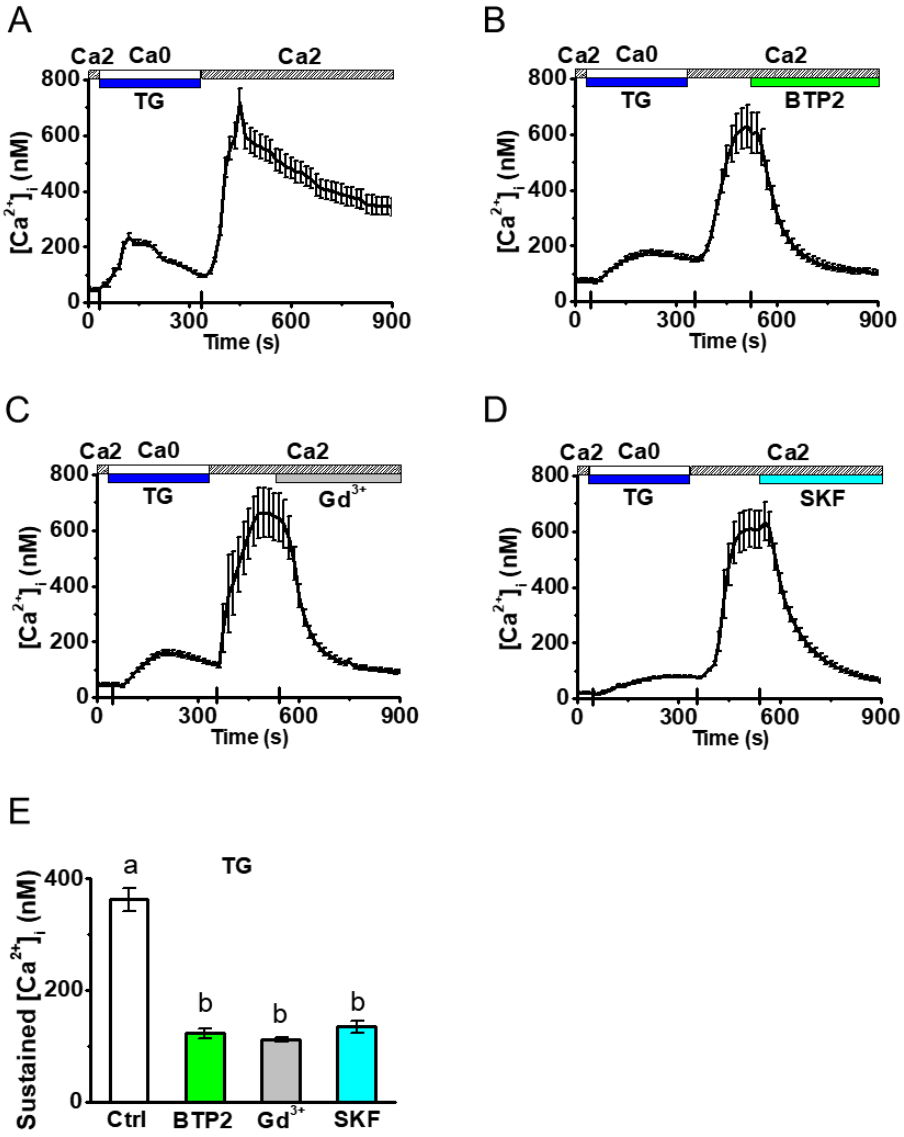

Figure 15. TG-induced SOCE is inhibited by CRAC channel blockers in HDLECs. **A – D.** Representative $[Ca^{2+}]_i$ measurements of SOCE evoked by 2 µM TG in HDLECs. Cells were bathed in Ca2 solution (**A**, n = 24 cells), or Ca2 solution containing 10 µM BTP2 (**B**, n = 23 cells), 10 µM Gd^{3+} (**C**, n = 18 cells), or 20 µM SKF-96365 (**D**, n = 22 cells). **E.** Statistical analysis of TG-evoked $[Ca^{2+}]_i$ levels at 5 minutes after the application of CRAC channel blockers in HDLECs. Significant differences are denoted by different letters.

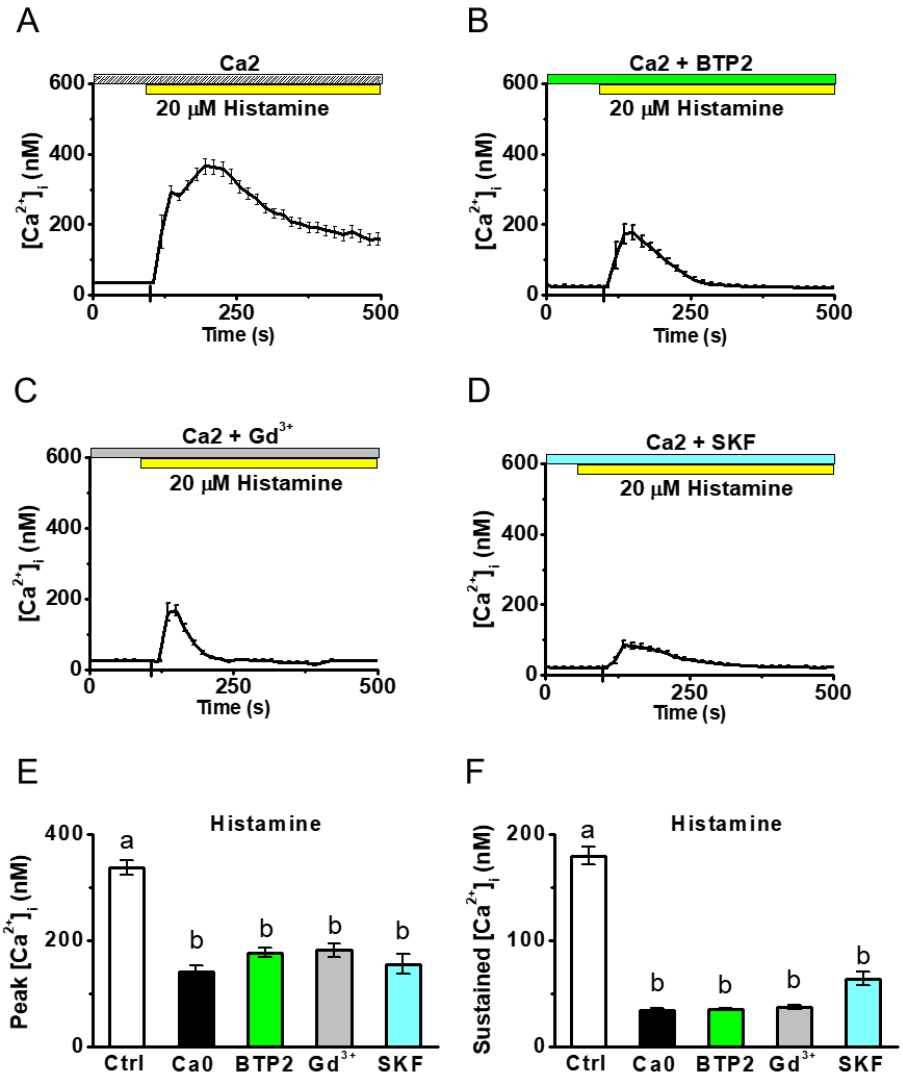

Figure 16. Histamine-induced Ca^{2+} entry is inhibited by CRAC channel blockers in HDLECs.

A – D. Representative $[Ca^{2+}]_i$ traces upon 20 μM histamine addition in Ca2 solution (**A**, n = 17 cells), or Ca2 solution with CRAC channel blockers, BTP2, Gd^{3+}, and SKF-96365 (**B – D**, n = 14, 24, and 21 cells, respectively). **E and F.** Statistical analysis of averaged peak (**E**) and sustained (**F**) $[Ca^{2+}]_i$ levels at 3 minutes after histamine treatment in HDLECs. Statistically significant differences are denoted by different letters.

targeting Orai1 or STIM1 to disrupt the endogenous expression of these two proteins, while non-targeting siRNAs were used as a negative control. We found that the non-targeting siRNAs-treated cells showed little effect on the TG-evoked and histamine-triggered Ca^{2+} dynamics in HDLECs compared to the untreated cells (Figure 17A and D). However, cells treated with siRNAs targeting either Orai1 or STIM1 lost the majority of their TG-evoked Ca^{2+} entry, indicating the necessary role of both Orai1 and STIM1 in maintaining functional CRAC channels (Figure 17B, C and G). Meanwhile, the cells with Orai1 or STIM1 knockdown also showed diminished Ca^{2+} responses upon histamine stimulations (Figure 17E, F and H), again indicating the essential role of CRAC channels, formed by Orai1 and STIM1, in mediating the histamine-triggered Ca^{2+} mobilization in HDLECs. The knockdown efficiency of siRNAs targeting Orai1 or STIM1 was confirmed by western blot (Figure 17I).

3.4.5. CRAC channel blockers attenuate histamine-induced VE-cadherin disruption and hyperpermeability in HDLECs

Given that histamine can induce blood vessel leakage by altering the endothelial cytoskeleton structures and disassembling cell-cell junctions in inflammatory responses (59, 61, 65, 66, 237), we sought to test whether histamine changed the lymphatic endothelial permeability and adherens junctions between LECs. The lymphatic endothelial permeability was measured by two different approaches, the traditional Transwell® assay with FITC - conjugated dextran (238, 239) and the TEER assay (240, 241). Both methods showed significant increase in lymphatic endothelial permeability after histamine stimulation: the fluorescent density increased by 80% and TEER dropped

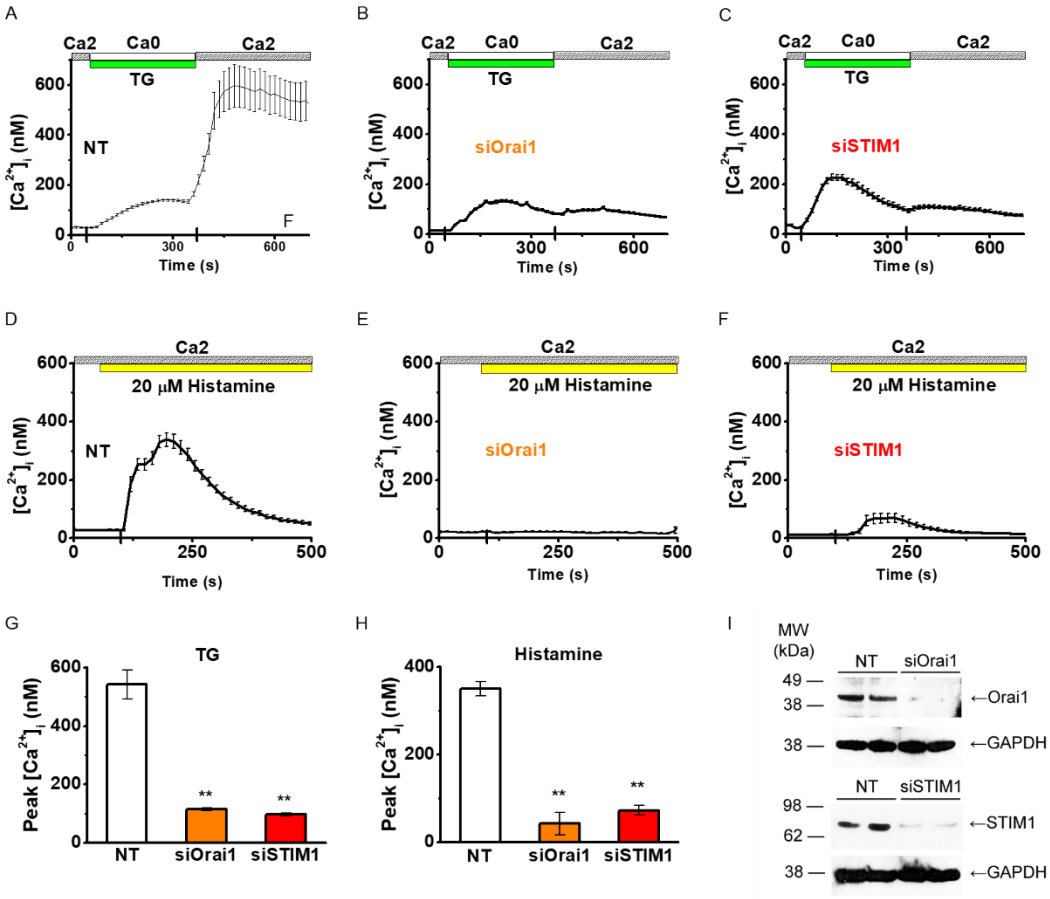

Figure 17. Histamine-induced Ca^{2+} dynamics require endogenous Orai1 and STIM1 in HDLECs.

A – C. Representative $[Ca^{2+}]_i$ measurements of cytosolic Ca^{2+} levels responding to TG-mediated stimulation in untreated HDLECs (**A**) or HDLECs treated with siRNAs targeting Orai1 (**B**) or STIM1 (**C**)**. D – F.** Representative $[Ca^{2+}]_i$ traces upon 20 μM histamine stimulation in untreated HDLECs (**D**) or HDLECs transfected with siRNAs against Orai1(**E**) or STIM1 (**F**)**. G and H.** Averaged peak $[Ca^{2+}]_i$ values corresponding to TG (**G**) or histamine (**H**) stimulation in the untreated control group, Orai1 knockdown group, and STIM1 knockdown group. **: $P < 0.01$ compared to the control group. **I.** Western blot of Orai1 and STIM1 proteins after the transfection of siRNAs. MW: molecular weight; NT: non-targeting siRNAs; siOrai1: siRNAs targeting Orai1; siSTIM1: siRNAs targeting STIM1.

by 40% in histamine-treated wells compared to the untreated control wells (Figure 18 A and B). Since we previously discovered that CRAC channel blockers could inhibit histamine-triggered $[Ca^{2+}]_i$ mobilization in HDLECs, we applied two blockers, BTP2 and Gd^{3+}, to study the functional role of CRAC channels in histamine-induced hyperpermeability in LECs. Intriguingly, the application of BTP2 or Gd^{3+} significantly diminished the histamine-induced leakage in the Transwell® assay and attenuated the drop in TEER (Figure 18 A and B), indicating a critical involvement of CRAC channel-mediated Ca^{2+} signaling in histamine-induced lymphatic endothelial leakage.

Because adherens junctions are critical for paracellular transportation and endothelial permeability (63), we examined the network structure of VE-cadherin, an EC-specific and Ca^{2+}-dependent adherens junction protein, by immunofluorescence. Consistent with our permeability data, the untreated confluent HDLEC monolayer displayed a strong, continuous, and intact network structure of VE-cadherins located at all intercellular contacts (Figure 18 C - E); however, 20 μM histamine treatment for 30 minutes significantly disrupted this structure and resulted in a weaker and intermittent VE-cadherin network with apparent gaps in the intercellular junctional areas (Figure 18 F - H). Again, the CRAC channel blockers, BTP2 or Gd^{3+}, independently inhibited histamine-induced VE-cadherin gaps and protected most intercellular spaces (Figure 18 I - N). Although a few gaps were still spotted in the HDLEC monolayers treated with histamine and BTP2 or Gd^{3+}, the major VE-cadherin network remained intact, and this protection of intercellular junctions could partially explain the effect of CRAC channel blockers in attenuating the hyperpermeability caused by histamine in LECs.

3.4.6. Orai1 or STIM1 knockdown prevent the enhanced expression of IL-6 and IL-8, but not SCF, mediated by histamine stimulation in HDLECs

Histamine, as an essential inflammatory mediator, is known to promote the expression of cytokines to attract immune cells in allergic inflammation (71, 72). Previously, we reported that histamine enhanced the expression and secretion of IL-8 in a CRAC-dependent manner in HUVECs (164). Here, we report that histamine was able to remarkably upregulate the mRNA levels of three critical cytokines expressed by LECs: IL-6, IL-8, and SCF. Treating HDLECs with 20 μM histamine for 2 hours caused 3.8-, 3.1-, and 7.9- fold increases of the mRNA levels for IL-6, IL-8, and SCF, respectively (Figure 19 A - C). Further treatment for 4 or 6 hours kept the mRNA levels significantly higher than those in untreated cells (Figure 19 A - C). Next, we knocked down the key components of CRAC channels, Orai1 and STIM1, by transfecting siRNAs targeting each gene in HDLECs. Surprisingly, while compromised CRAC channels averted the effect of histamine in elevating the expression of IL-6 and IL-8 (Figure 19 D and E), it led to little impact on the histamine-promoted expression of SCF in HDLECs (Figure 19 F). These findings indicate that in addition to CRAC-mediated Ca^{2+} signaling, the cytokine production upon histamine stimulation is dependent on other factors as well.

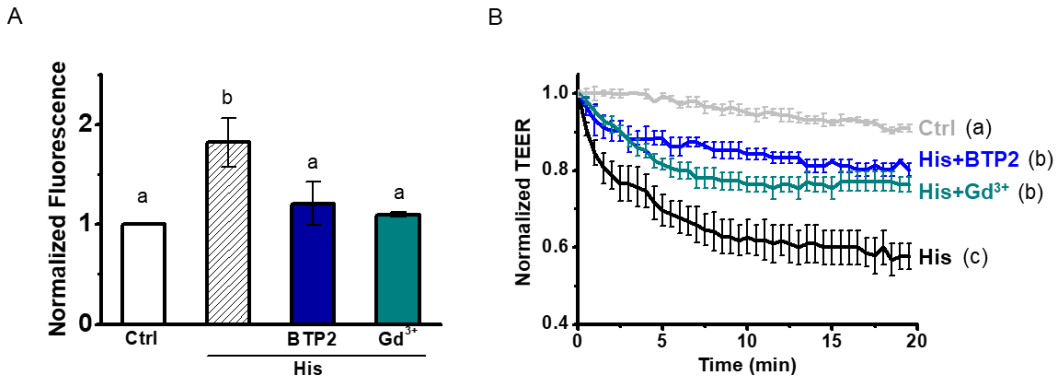

Figure 18. CRAC channel blockers attenuate histamine-induced hyperpermeability and VE-cadherin disruption in HDLECs.
A. The FITC-dextran fluorescence density in the lower chamber of each group was measured, normalized to that of the untreated control group, and summarized in the bar graph. **B.** TEER values of the HDLEC monolayer in each group were measured at indicated time points and normalized to the basal value at time 0. Values from at least three biological replicates were averaged for each group. **C – N**. Representative confocal immunofluorescence images showed VE-cadherin and DAPI staining in the HDLEC monolayer of each group. VE-cadherin and DAPI are displayed in red and blue, respectively, in the merged images on the right. The treatments are indicated on the left, VE-cadherin gaps are shown by yellow arrowheads, and the scale bar is 20 μm. Statistically significant differences are indicated by different letters from a to c. Ctrl: control; His: histamine.

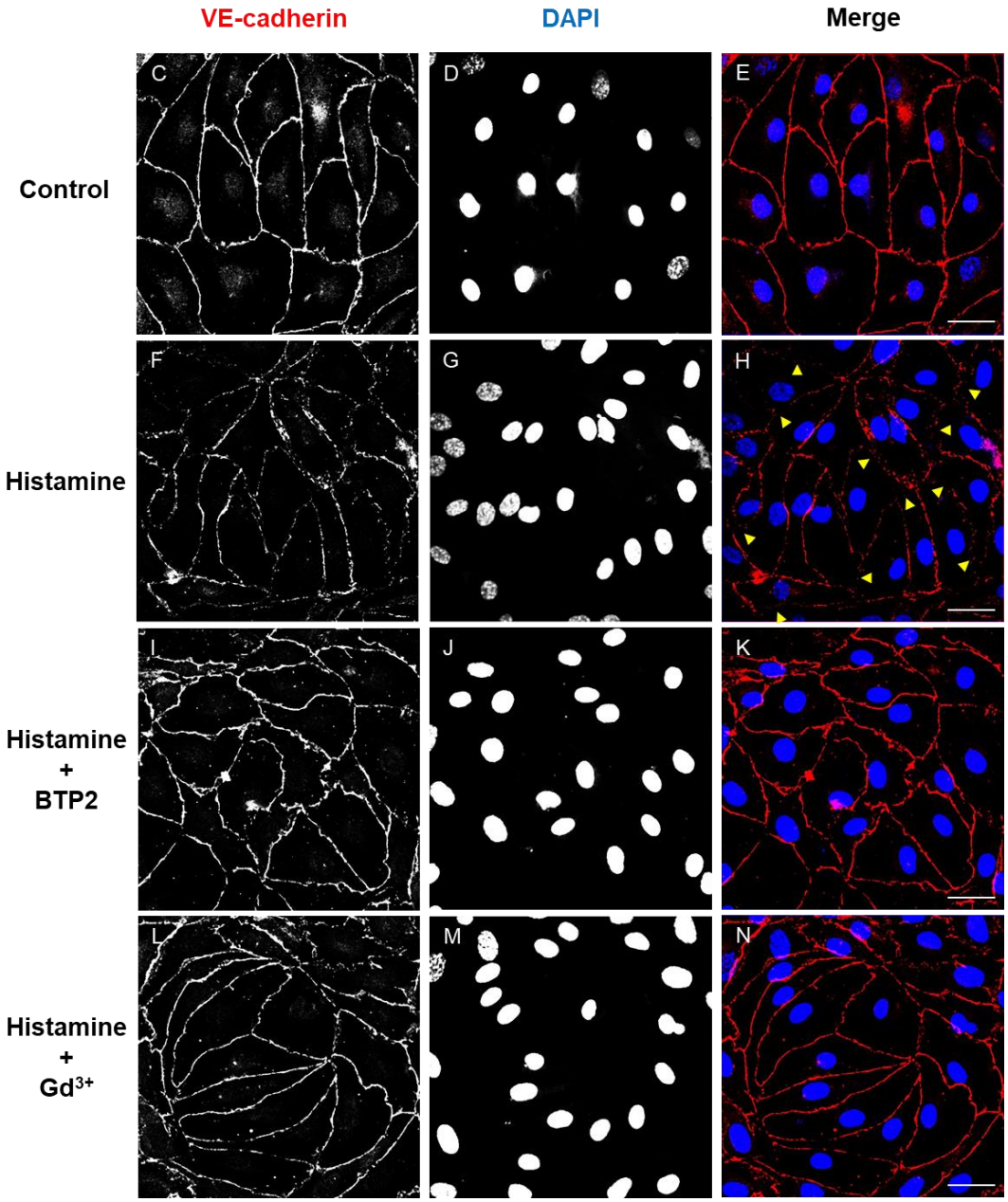

Figure 18 Continued.

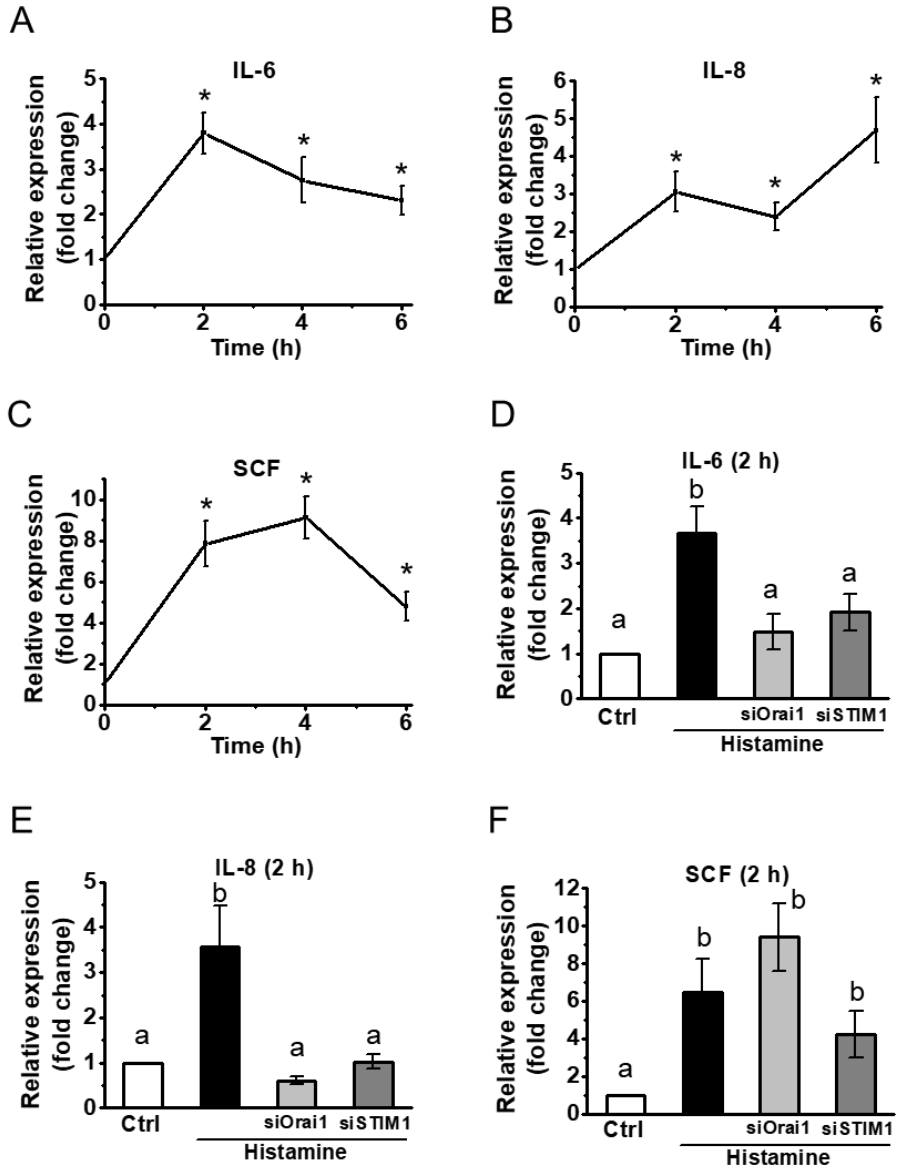

Figure 19. Orai1 or STIM1 knockdown prevents the histamine-induced upregulation of IL-6, IL-8, but not SCF, in HDLECs.

A – C. Quantitative RT-PCR analysis of mRNAs for IL-6 (**A**), IL-8 (**B**), and SCF (**C**) after histamine treatment for 2, 4, and 6 hours in HDLECs. GAPDH was used as the reference gene and all expressions are normalized to the basal expressions at time 0 (untreated control). **D – F.** Quantitative RT-PCR results of mRNAs for IL-6 (**D**) IL-8 (**E**), and SCF (**F**) two hours after histamine treatment in untreated control cells, Orai1-knockdown cells, and STIM1-knockdown cells. *: $P < 0.05$ compared to the untreated control in Student's t-tests. Statistical significance in Tukey's HSD test is indicated by different letters from a to b.

3.5. Discussion

The lymphatic system is a key pathway for the transport of antigens and lymphocytes from the tissue to the lymphatic nodes, and hence, regarded as a vital part of immune initiation and maintenance (2, 25, 175, 176, 242). Therefore, it is closely associated with numerous pathological conditions involving inflammation, including infection, allergy, IBD, rheumatoid arthritis, and wound healing (22, 37, 214, 215, 243-246). How the lymphatics regulates their vascular functions and immune responses in inflammatory conditions is now an emerging field of research (2, 22, 25, 37). Histamine is an inflammatory mediator widely used in the studies of *in vivo* and *in vitro* responses to inflammatory stimuli, and Ca^{2+} signaling is critical for histamine responses in various cell types (59, 60). However, the Ca^{2+} channels mediating this Ca^{2+} signaling and their functions in downstream cellular responses remain to be explored in the lymphatics. In this study, we showed that CRAC channels conduct the histamine-elicited Ca^{2+} entry and are necessary for the hyperpermeability as well as interleukin production following histamine stimulation in HDLECs. The essential role of CRAC channels in Ca^{2+} homeostasis and signaling has been shown in the immune cells and various other cell types or tissues (90, 125, 126, 187, 188, 247, 248). However, this is the first time that CRAC channels have been demonstrated to be required for the lymphatic endothelial response to histamine stimulation. Our findings suggest a critical contribution of CRAC channels in mediating inflammatory responses in the lymphatic endothelium and a potential function in immune reactions.

Utilizing pharmacological inhibitors, we demonstrated that histamine activates the PLC family after binding to the H_1R and triggers the intracellular Ca^{2+} store release followed by a sustained extracellular Ca^{2+} entry through CRAC channels in LECs. Our RNAi results provided further support that the endogenous CRAC channel components, Orai1 and STIM1, are indispensable for the Ca^{2+} influx into HDLECs upon histamine stimulation, indicating a unique function of CRAC channels in maintaining prolonged Ca^{2+} signaling in histamine-related inflammatory conditions. Notably, the ability for some intracellular Ca^{2+} store release remained after CRAC channel blockage. Thus, CRAC channels probably have a limited effect on those cellular functions only requiring a transient and relatively small Ca^{2+} signal to initiate. However, CRAC channels are vital for refilling the intracellular Ca^{2+} store, and hence, may be necessary for frequent or prolonged stimulation.

Histamine is well known to disrupt blood vascular barrier functions, especially in the microvasculature, during infection and allergy (59, 61, 237). A recent study showed that inflammatory mediators, histamine and thrombin, were also able to decrease the barrier function of cultured LECs, which is modulated by Rho kinase (ROCK) and cyclic adenosine monophosphate (cAMP) (219). Our present data provide the first link of the histamine-triggered endothelial hyperpermeability and adherens junction disruption to the Ca^{2+} signaling via CRAC channels, shedding light into the mechanism of how lymphatic vessels regulate the barrier functions upon inflammatory stimulations. VE-cadherin is a key component of adherens junctions connected to actin or actomyosin by p120, β-catenin and plakoglobin in ECs (9, 63). Several mechanisms have been

proposed to be responsible for compromised VE-cadherin stability and eventually enhanced vascular permeability, including but not limited to phosphorylation, internalization, enzymatic cleavage, and cellular retraction (239, 249). Ca^{2+} signaling is one of the most prominent intracellular pathways regulating VE-cadherin functions as shown by studies on VE-cadherin phosphorylation and actin-myosin contraction in BECs (65, 238, 249, 250). Here, we provide evidence for the function of CRAC-mediated Ca^{2+} signaling in LECs responding to histamine, indicating a novel potential target to treat pathological disorders involving increased lymphatic vascular permeability triggered by inflammatory mediators. Notably, because histamine-triggered lymphatic hyperpermeability could possibly weaken the lymphatic drainage of tissue fluid and worsen local swelling, anti-histamine medications may reduce lymph leakage and attenuate lymphedema caused by infection or inflammation.

The lymphatics recruit and transport leukocytes to the lymph nodes after they interact with antigens in infected or injured tissues, maintaining the proper immune surveillance (2, 25). This process is under dynamic control of cytokine/chemokine production and chemoattraction. LECs express various cytokines/chemokines, including IL-6, IL-8, and SCF, to recruit leukocytes and enhance EC-leukocyte interaction during inflammation (251-258). Our results demonstrated significant increases in the transcription of IL-6, IL-8, and SCF after histamine stimulation and showed that expression of IL-6 and IL-8 is dependent on CRAC channel function, suggesting a possible approach to regulate interleukin production and LEC-leukocyte interaction in inflammation. It is worth noting that the upregulated transcription of SCF was not

significantly affected by CRAC blockage, implying other intracellular signaling are also involved in modulating the transcriptional reprograming after histamine stimulation.

Overall, our data demonstrate the essential role of CRAC channels, formed by Orai1 and STIM1, in mediating histamine-evoked Ca^{2+} signaling and further alterations in barrier function and interleukin expression in LECs. These findings pave the way toward understanding lymphatic responses to inflammatory stimuli and developing potential therapeutic methods to treat inflammatory diseases.

4. CONCLUSIONS

4.1. Significance

The lymphatic system, compared with the blood circulation, is largely neglected in the research field, regardless of its fundamental role in maintaining body fluid homeostasis, immune surveillance, and dietary lipid absorption (259). Lymphatic pumping generates the force needed to drive fluid, proteins, and lipids toward the systemic circulation; meanwhile, the lymphatics transport antigens and lymphocytes from the tissue to the lymphatic nodes and, hence, are regarded as a vital part of the initiation and maintenance of immune responses (2, 5, 12, 25, 175, 176, 242). The deficient action of CRAC channels in the lymphatic system has been intensely studied in lymphocytes. The diminished I_{CRAC} caused by an Orai1 mutation, R91W, in SCID patients leads to significantly impaired T cell activation and NFAT-dependent gene expressions (90). Additionally, abolished expression of Orai1 proteins by Orai1 mutations, A88SfsX25, A103E, and L194P, also remarkably impaired the activation and proliferation of lymphocytes, including T cells and B cells, in patients with immunodeficiency (126). Consistent with the observations in human patients, Orai1 was intensely expressed in thymus, lymph nodes, and lymphocytes in wild-type C57BL/6 mice (146). Compared with the wild-type mice, Orai1 global knockout mice displayed significant reductions of I_{CRAC} in lymphocytes and showed perinatal lethality. After backcrossing to the outbred ICR mouse strain, the surviving Orai1-deficient mice displayed multiple defects in the lymphatic system, including splenomegaly,

lymphadenopathy, and decreased cytokine production by lymphocytes (146). Similar to the Orai1 defects, loss of functional STIM1, due to a mutation (E136X) causing a premature termination of STIM1 proteins, also led to lymphadenopathy and hepatosplenomegaly in human patients (129). Comparably, $CD4^+$ T cell-specific STIM1 and STIM2 double knockout mice showed notable splenomegaly, lymphadenopathy, leukocyte infiltration in the lungs and livers, and fewer T_{regs} in the spleen and lymph nodes (108). Taken together, these observations indicate CRAC channels have vital roles in lymphocyte activation and cytokine production; lacking functional CRAC channels may lead to severe lymphoid defects and immune deficiency.

However, the role of the CRAC channel in the lymphatic system, especially in LECs, is still largely unknown, despite the emerging functions of LECs in modulating the adaptive immune responses. It is well established that LECs recruit DCs, T-cells, and other immune cells, and modulate their trafficking/entry into the lymph nodes by producing a set of chemokines (e.g., CCL1, 2, 5, 7, 21 and CXCL1, 3, 5, 6, 8) (2, 260-263). In addition, LECs express multiple cell-cell adhesion molecules to facilitate leukocyte interaction and transmigration into the lymphatic vessels (9, 220). Intriguingly, LECs are also capable of presenting antigens and modulating T-cell functions directly via the major histocompatibility complex (MHC) class I and II on the cell surface (37, 264, 265). Furthermore, LECs can regulate T-cell homeostasis by producing IL-7, and influence T-cell activation by binding to DCs through intercellular adhesion molecule 1 (ICAM1) (266-269). Last but not least, LECs produce various cytokines, responding to environmental stimuli, that regulate the local inflammation and

immune responses dynamically (2, 37, 246, 263). Considering the role of LECs in the immune responses, it is possible that impaired CRAC channel activity in LECs may compromise the LEC functions responding to external stimuli and, therefore, contributing to the immunodeficiency in the human patients and genetically modified mouse models. In this dissertation, we present data that show CRAC channels are required for the Ca^{2+} signaling and downstream cytokine production in LECs, responding to FSS and histamine, emphasizing the importance of CRAC channels in the LEC-dependent regulation of inflammation and immune functions.

Lymphatic endothelium, the inner layer of the lymphatic vessel wall, is directly subjected to lymph flow and plays a critical role in regulating lymphatic functions based on the FSS and pressure (42, 43, 54, 56, 270). We have demonstrated the pattern and sources of FSS-induced Ca^{2+} dynamics in LECs and discovered that they are sensitive to a CRAC channel blocker, Synta66 (165). Others found that Orai1 mediated the laminar flow-dependent Ca^{2+} influx, LEC proliferation, and lymphatic spouting (166, 167). Nevertheless, the specific role of CRAC channels in the FSS-elicited Ca^{2+} signaling in LECs and the participating channel molecules have not been thoroughly studied. In this dissertation research, we determined that FSS evokes CRAC-mediated Ca^{2+} mobilization followed by ER Ca^{2+} store release in LECs, and the fundamental channel molecules behind this process are Orai1 and STIM1. We further ruled out the major involvement of Piezo proteins and TRPV4 channels, but found a marginal function of purinoceptors in this FSS-induced Ca^{2+} responses. We also found CRAC-dependent NFAT translocation and global transcriptional reprogramming after FSS treatment. In this transcriptional

regulation, we observed an anti-inflammatory effect of FSS due to the downregulation pro-inflammatory cytokines/chemokines and the upregulation anti-inflammatory cytokines. Utilizing qRT-PCR and ELISA, we confirmed that IL-8, a major pro-inflammatory cytokine produced by LECs, is significantly reduced by FSS in a CRAC-dependent manner.

In addition to mechanical forces, LECs are also exposed to many inflammatory factors and participate in modulating the local inflammation by producing and secreting cytokines to attract and interact with leukocytes (25, 44, 220, 271, 272). Histamine is a widely-studied inflammatory mediator involved in various immune responses (e.g., infections and allergies) (59). In BECs, histamine has an acute effect (within minutes) of disrupting the endothelial barrier function following Ca^{2+} mobilization and MLC phosphorylation (62, 67). At later stages (in hours), histamine induces the expression of IL-6 and IL-8 in a dose-dependent manner in HUVECs (71, 72). Our group previously reported that the CRAC channel was responsible for the histamine-induced Ca^{2+} entry, downstream NFAT translocation, and IL-8 expression in HUVECs (164). However, the effects of histamine in the lymphatic system have been largely overlooked. Recently, cAMP and ROCK were shown to inhibit histamine-induced LEC hyperpermeability (219). Another study found that histamine is involved in the flow-dependent lymphatic vessel relaxation (58). Despite the vital role of Ca^{2+} signaling in the histamine responses, the Ca^{2+} dynamics and conducting channels have not been studied in LECs upon histamine stimulation. In this dissertation, we described the Ca^{2+} mobilization triggered by different concentrations of histamine in LECs and determined the sensitivity of this

Ca^{2+} response to H_1R antagonists, PLC inhibitors, CRAC channel blockers, and extracellular Ca^{2+} sources. These results suggest that histamine binds to H_1R and activates PLC to release the ER Ca^{2+} stores, which evokes CRAC-mediated SOCE from the external environment into LECs. We further identified Orai1 and STIM1 to be the basic channel molecules for this Ca^{2+} entry, emphasizing the essential role of the CRAC channels in this process. In the downstream effects, the CRAC channel is required for histamine-induced VE-cadherin disruption, LEC hyperpermeability, and the production of IL-6 and IL-8. In summary, CRAC channels mediate histamine-evoked Ca^{2+} entry, barrier disruption, and cytokine production in LECs.

Unlike the blood circulation, the lymphatic system is blind-ended and does not have a heart to generate the force to drive lymph flow forward (2). Instead, the lymphatic vessels transport the lymph via the phasic and tonic contractions of the lymphangion and minimize the backflow with lymphatic valves (5, 10). The distinct features of force generation lead to completely different flow patterns in the bloodstream and the lymphatics (5, 10, 11, 41, 177). The flow is laminar and steady (>12 dyn/cm^2) in most regions of blood vessels, except for branching and curving areas where flow is lower and disturbed (± 4 dyn/cm^2) (273, 274). Many studies have discovered remarkably different responses to these two flow patterns in BECs: the disturbed flow induces a pro-inflammatory environment through apoptosis signal-regulating kinase 1 (ASK1) and c-Jun NH2-terminal kinase (JNK), while steady laminar flow prevents the inflammation and protects the BECs via KLF2 and nuclear factor erythroid 2-like 2 (Nrf2) (274). On the contrary, lymphatic flow is much more dynamic - spatially and temporally, and can

even be bi-directional near the valve (5, 11, 41, 177). Based on the data collected from rat mesenteric collecting lymphatics, the average FSS is approximately 0.4-0.6 dyn/cm^2, while the peak FSS can be 3-10 dyn/cm^2 (5). Given the unique flow pattern in the lymphatics, LECs are possibly more sensitive to low FSS and better adapted to disturbed flow, compared to BECs. To better characterize the FSS responses in LECs, we demonstrated that 4 dyn/cm^2 or lower FSS is sufficient to evoke significant CRAC-dependent Ca^{2+} dynamics in LECs and trigger downstream transcriptional regulation. Intriguingly, the FSS displays a "protective" effect by inducing the expression of anti-inflammatory cytokines as well as KLF2, 4, and 10, while downregulating the expression of pro-inflammatory cytokines in LECs. Furthermore, blockage of CRAC channels partially reverses this effect, which is also supported by our qRT-PCR and ELISA data of IL-8 production. In other words, these data support the idea that lymph flow helps to maintain the LECs at a resting status, while losing the FSS stimuli or key components of the mechanotransduction pathway (e.g., CRAC channel) triggers inflammatory responses in LECs. In lymphedema involving lymphatic obstruction or dysfunction, inflammation is commonly observed and primarily caused by the accumulation of macrophages and pro-inflammatory factors (23, 24, 244). Our data provide critical evidence that lacking flow/FSS stimuli increases the expression of pro-inflammatory cytokines and chemokines in LECs, and possibly contributes to the initial development of local inflammation. However, given that LECs are quite different from BECs in terms of participating in immune surveillance, whether this anti-inflammatory

effect of FSS in LECs is “protective”, as it is in BECs, remains to be elucidated in further investigations.

Histamine has been shown to lower blood pressure, dilate and transiently permeabilize blood capillaries, and induce interleukin expression in HUVECs (60, 73). Although the histamine-triggered hyperpermeability is a vital factor causing allergy and asthma, the molecular mechanism behind this process is still incompletely understood (69, 275, 276). Many studies reveal that the compromised barrier function after histamine stimulation results from disruption of intercellular junctions, including adherens and tight junctions (63-65, 68, 69, 277, 278). Ca^{2+} signaling, Rho family proteins, MLCK, and cAMP contribute to the formation of intercellular gaps, yet, the detailed signaling pathways are under debate (65, 68, 69, 249, 250, 278, 279). In the lymphatic system, the adhesive cell-to-cell junctions are specialized to meet the functions in different regions. The junctions are continuous and “zipper-like” in the collecting lymphatics, which are more similar to the blood vasculature, while the junctions are discontinuous and “bottom-like” in the initial lymphatics, which are more permeable to macromolecules and cells (9, 280). Breslin showed that inflammatory mediators, histamine and thrombin, disrupted lymphatic barrier function in a different manner compared with that in the blood endothelium (219). We provide evidence in this dissertation that Ca^{2+} entry via the CRAC channels is critical to the histamine-induced VE-cadherin disruption and barrier function of LECs. Specifically, we observed that histamine enhanced the permeability of the LEC monolayer using two different methods, the Transwell® assay with FITC-dextran and the TEER measurement. The Transwell®

assay evaluates the barrier function of cultured LECs to macromolecules (~40 kDa), which mimics the paracellular leakage of albumin and other proteins (239, 281). On the other hand, the TEER method measures the ionic conductance of the cell monolayer, which represents the integrity of intercellular adhesive junctions and the permeability to small electrolytes (282). Our data demonstrate that CRAC blockage completely prevents the macromolecule leakage caused by histamine in the Transwell® assay, while partially inhibiting the increased small electrolytes movement induced by histamine in TEER measurements. This result suggests that the CRAC channels play a dominant role in macromolecule permeability but only a partial role in small particle permeability in the LEC monolayer. The confocal images of VE-cadherin show that blocking CRAC channels prevents the majority of VE-cadherin disruption induced upon histamine stimulation, which again supports our permeability measurement data.

Over the past decade, the functional role of the lymphatic system in inflammatory diseases, adaptive immunity, and immune tolerance has become an emerging area of study (2, 22, 25, 37, 175, 259, 283). Especially, the immunomodulatory function of LECs is more accepted and focused, because LECs are closely involved in antigen presentation, leukocyte activation, as well as lymphocyte transportation (220, 283, 284). In this dissertation, we demonstrate that Ca^{2+} entry conducted by the CRAC channels is critical for LECs responding to both a mechanical stimulus (FSS) and an inflammatory mediator (histamine). The CRAC channels are required for mediating sustained Ca^{2+} signaling that triggers the downstream cellular functions (e.g., transcriptional reprogramming, intercellular junction modulation, and cytokine

production) in LECs. Most intriguingly, the CRAC channel contributes to the regulation of interleukin expression/secretion under both conditions (FSS and histamine stimuli), highlighting its crucial role in the immunomodulatory function of LECs.

4.2. Limitations of this study and future directions

In order to study the Ca^{2+} mobilization and cellular functions in LECs, we utilized three different batches of HDLECs that are isolated from juvenile human foreskin and commercially available at PromoCell. The lymphatic vessels in the skin include initial lymphatics and pre-collecting lymphatics and, therefore, the HDLEC line is a mixture of LECs from these different vessels. Since the data collected from different batches of HDLECs are stable and consistent in the early passages (passage 3-9), our results in this dissertation represent a reliable readout regarding the function of capillary and pre-collecting LECs responding to FSS and histamine. However, these conclusions should not be directly applied to the LECs from other sections of lymphatic vessels (e.g., the collecting lymphatic vessels and lymphatic ducts). The LECs from other regions of lymphatic vessels may present similar properties due to the similarity of these LECs, yet it would not be surprising if they display different features, considering the fact that the LECs in the initial lymphatics are quite unique in terms of functions and structures, and are not identical to the LECs in other regions of lymphatic vessels. To better study the cellular functions in LECs from different regions of lymphatic vessels, tissue-specific or vessel-specific LEC lines should be isolated and purified from healthy donors; and to

better understand the pathogenesis of lymphatic diseases, LEC lines are also needed from related patients at different ages and pathological stages.

As discussed above, lymph flow is extremely dynamic and varies from different regions of the body and in different parts of the lymphatic system (5, 10, 18, 38, 41, 177). The amplitude and direction of lymph flow can change dramatically or even be transiently opposite in the pumping collecting lymphatics (1, 5, 41). We used FSS to study the Ca^{2+} signaling and downstream pathways in LECs. The flow developed in the orbital shaker has a relatively low and disturbed FSS in the center, with a higher and more laminar FSS in the peripheral regions (285, 286). The FSS has some features that resemble the physiological lymphatic FSS, yet, it still cannot mimic lymph FSS in many aspects. A better way of studying lymph flow in cultured LECs is to record the flow pattern in the lymphatic vessel of interest *in vivo*, and then, mimic the flow in a computer-controlled perfusion system. In addition, the genetically-modified animal model expressing genetically encoded calcium indicators (e.g., GCaMPs) in LECs is also a promising option to study the Ca^{2+} signaling *in vivo* or *ex vivo* in future studies.

Taken together, the data in this dissertation emphasize the crucial role of CRAC channels in the Ca^{2+} signaling and downstream cell functions responding to FSS and histamine in LECs. Our results shed light on the cellular and molecular mechanisms behind the LEC-dependent regulation of lymphatic functions. Future investigations are still needed to further identify other participating factors in mechanotransduction and inflammatory responses in LECs. Moreover, the validation of these signaling pathways *in vivo* is also critical for the application of these findings.

5. REFERENCES

1. Swartz MA. The physiology of the lymphatic system. Advanced Drug Delivery Reviews. 2001;50(1):3-20.

2. Cueni LN, Detmar M. The lymphatic system in health and disease. Lymphatic Research and Biology. 2008;6(3-4):109-22.

3. Ikomi F, Hunt J, Hanna G, Schmid-Schonbein GW. Interstitial fluid, plasma protein, colloid, and leukocyte uptake into initial lymphatics. Journal of Applied Physiology. 1996;81(5):2060-7.

4. Gerli R, Solito R, Weber E, Agliano M. Specific adhesion molecules bind anchoring filaments and endothelial cells in human skin initial lymphatics. Lymphology. 2000;33(4):148-57.

5. Zawieja DC. Contractile physiology of lymphatics. Lymphatic Research and Biology. 2009;7(2):87-96.

6. Bazigou E, Wilson JT, Moore JE, Jr. Primary and secondary lymphatic valve development: molecular, functional and mechanical insights. Microvascular Research. 2014;96:38-45.

7. Skobe M, Detmar M, editors. Structure, function, and molecular control of the skin lymphatic system. Journal of Investigative Dermatology Symposium Proceedings; 2000: Elsevier.

8. Dixon JB. Lymphatic lipid transport: sewer or subway? Trends in Endocrinology & Metabolism. 2010;21(8):480-7.

9. Baluk P, Fuxe J, Hashizume H, Romano T, Lashnits E, Butz S, et al. Functionally specialized junctions between endothelial cells of lymphatic vessels. Journal of Experimental Medicine. 2007;204(10):2349-62.

10. Bridenbaugh EA, Gashev AA, Zawieja DC. Lymphatic muscle: a review of contractile function. Lymphatic Research and Biology. 2003;1(2):147-58.

11. von der Weid P-Y, Zawieja DC. Lymphatic smooth muscle: the motor unit of lymph drainage. The International Journal of Biochemistry & Cell Biology. 2004;36(7):1147-53.

12. Muthuchamy M, Gashev A, Boswell N, Dawson N, Zawieja D. Molecular and functional analyses of the contractile apparatus in lymphatic muscle. The FASEB Journal. 2003;17(8):920-2.

13. Quick CM, Venugopal AM, Gashev AA, Zawieja DC, Stewart RHJAJoP-R, Integrative, Physiology C. Intrinsic pump-conduit behavior of lymphangions. 2007;292(4):R1510-R8.

14. Sixt M, Kanazawa N, Selg M, Samson T, Roos G, Reinhardt DP, et al. The conduit system transports soluble antigens from the afferent lymph to resident dendritic cells in the T cell area of the lymph node. Immunity. 2005;22(1):19-29.

15. Junt T, Moseman EA, Iannacone M, Massberg S, Lang PA, Boes M, et al. Subcapsular sinus macrophages in lymph nodes clear lymph-borne viruses and present them to antiviral B cells. Nature. 2007;450(7166):110.

16. Kastenmüller W, Torabi-Parizi P, Subramanian N, Lämmermann T, Germain RN. A spatially-organized multicellular innate immune response in lymph nodes limits systemic pathogen spread. Cell. 2012;150(6):1235-48.

17. Lämmermann T, Bader BL, Monkley SJ, Worbs T, Wedlich-Söldner R, Hirsch K, et al. Rapid leukocyte migration by integrin-independent flowing and squeezing. Nature. 2008;453(7191):51.

18. Tal O, Lim HY, Gurevich I, Milo I, Shipony Z, Ng LG, et al. DC mobilization from the skin requires docking to immobilized CCL21 on lymphatic endothelium and intralymphatic crawling. Journal of Experimental Medicine. 2011;208(10):2141-53.

19. Debes GF, Arnold CN, Young AJ, Krautwald S, Lipp M, Hay JB, et al. Chemokine receptor CCR7 required for T lymphocyte exit from peripheral tissues. Nature Immunology. 2005;6(9):889.

20. Grigorova IL, Panteleev M, Cyster JG. Lymph node cortical sinus organization and relationship to lymphocyte egress dynamics and antigen exposure. Proceedings of the National Academy of Sciences. 2010:201009968.

21. Braun A, Worbs T, Moschovakis GL, Halle S, Hoffmann K, Bölter J, et al. Afferent lymph–derived T cells and DCs use different chemokine receptor CCR7–dependent routes for entry into the lymph node and intranodal migration. Nature Immunology. 2011;12(9):879.

22. Chakraborty S, Zawieja S, Wang W, Zawieja DC, Muthuchamy M. Lymphatic system: a vital link between metabolic syndrome and inflammation. Annals of the New York Academy of Sciences. 2010;1207:E94-E102.

23. Rockson SG. Lymphedema. The American Journal of Medicine. 2001;110(4):288-95.

24. Warren AG, Brorson H, Borud LJ, Slavin SA. Lymphedema: a comprehensive review. Annals of Plastic Surgery. 2007;59(4):464-72.

25. Alitalo K. The lymphatic vasculature in disease. Nature Medicine. 2011;17(11):1371-80.

26. Melrose WD. Lymphatic filariasis: new insights into an old disease. International Journal for Parasitology. 2002;32(8):947-60.

27. Vakoc BJ, Lanning RM, Tyrrell JA, Padera TP, Bartlett LA, Stylianopoulos T, et al. Three-dimensional microscopy of the tumor microenvironment in vivo using optical frequency domain imaging. Nature Medicine. 2009;15(10):1219.

28. Proulx ST, Luciani P, Derzsi S, Rinderknecht M, Mumprecht V, Leroux J-C, et al. Quantitative imaging of lymphatic function with liposomal indocyanine green. Cancer Research. 2010:0008-5472. CAN-10-0271.

29. Karkkainen MJ, Saaristo A, Jussila L, Karila KA, Lawrence EC, Pajusola K, et al. A model for gene therapy of human hereditary lymphedema. Proceedings of the National Academy of Sciences. 2001;98(22):12677-82.

30. Szuba A, Skobe M, Karkkainen MJ, Shin WS, Beynet DP, Rockson NB, et al. Therapeutic lymphangiogenesis with human recombinant VEGF-C. The FASEB Journal. 2002;16(14):1985-7.

31. Saaristo A, Veikkola T, Tammela T, Enholm B, Karkkainen MJ, Pajusola K, et al. Lymphangiogenic gene therapy with minimal blood vascular side effects. Journal of Experimental Medicine. 2002;196(6):719-30.

32. Tammela T, Saaristo A, Holopainen T, Lyytikkä J, Kotronen A, Pitkonen M, et al. Therapeutic differentiation and maturation of lymphatic vessels after lymph node dissection and transplantation. Nature Medicine. 2007;13(12):1458.

33. Visuri MT, Honkonen KM, Hartiala P, Tervala TV, Halonen PJ, Junkkari H, et al. VEGF-C and VEGF-C156S in the pro-lymphangiogenic growth factor therapy of lymphedema: a large animal study. Angiogenesis. 2015;18(3):313-26.

34. Buckley CD, Gilroy DW, Serhan CN, Stockinger B, Tak PP. The resolution of inflammation. Nature Reviews Immunology. 2013;13(1):59-66.

35. Kataru RP, Jung K, Jang C, Yang H, Schwendener RA, Baik JE, et al. Critical role of CD11b+ macrophages and VEGF in inflammatory lymphangiogenesis, antigen clearance, and inflammation resolution. Blood. 2009;113(22):5650-9.

36. Huggenberger R, Ullmann S, Proulx ST, Pytowski B, Alitalo K, Detmar M. Stimulation of lymphangiogenesis via VEGFR-3 inhibits chronic skin inflammation. Journal of Experimental Medicine. 2010;207(10):2255-69.

37. Alexander JS, Chaitanya GV, Grisham MB, Boktor M. Emerging roles of lymphatics in inflammatory bowel disease. Annals of the New York Academy of Sciences. 2010;1207 Suppl 1:E75-85.

38. von der Weid PY, Rehal S. Lymphatic pump function in the inflamed gut. Annals of the New York Academy of Sciences. 2010;1207(1).

39. von der Weid P-Y, Rehal S, Ferraz JG. Role of the lymphatic system in the pathogenesis of Crohn's disease. Current Opinion in Gastroenterology. 2011;27(4):335-41.

40. Quick CM, Venugopal AM, Gashev AA, Zawieja DC, Stewart RH. Intrinsic pump-conduit behavior of lymphangions. American Journal of Physiology-Regulatory, Integrative and Comparative Physiology. 2007;292(4):R1510-R8.

41. Gashev AA, Zawieja DC. Lymph transport and lymphatic system. Encyclopedia of Immunotoxicology. 2016:547-9.

42. Gashev AA. Lymphatic vessels: pressure ‐ and flow ‐ dependent regulatory reactions. Annals of the New York Academy of Sciences. 2008;1131(1):100-9.

43. Gashev AA. Inhibition of the active lymph pump by flow in rat mesenteric lymphatics and thoracic duct. The Journal of Physiology. 2002;540(3):1023-37.

44. Pepper MS, Skobe M. Lymphatic endothelium: morphological, molecular and functional properties. Journal of Cell Biology. 2003;163(2):209-13.

45. Palmer RM, Ashton D, Moncada S. Vascular endothelial cells synthesize nitric oxide from L-arginine. Nature. 1988;333(6174):664-6.

46. Moncada S, Higgs A. The L-arginine-nitric oxide pathway. New England Journal of Medicine. 1993;329(27):2002-12.

47. Förstermann U, Pollock JS, Schmidt H, Heller M, Murad F. Calmodulin-dependent endothelium-derived relaxing factor/nitric oxide synthase activity is present in the particulate and cytosolic fractions of bovine aortic endothelial cells. Proceedings of the National Academy of Sciences. 1991;88(5):1788-92.

48. Feelisch M. The biochemical pathways of nitric oxide formation from nitrovasodilators: appropriate choice of exogenous NO donors and aspects of preparation

and handling of aqueous NO solutions. Journal of Cardiovascular Pharmacology. 1991;17:S25-S33.

49. Radomski MW, Moncada S. The biological and pharmacological role of nitric oxide in platelet function. Mechanisms of Platelet Activation and Control: Springer; 1993. p. 251-64.

50. Garg UC, Hassid A. Nitric oxide-generating vasodilators and 8-bromo-cyclic guanosine monophosphate inhibit mitogenesis and proliferation of cultured rat vascular smooth muscle cells. The Journal of Clinical Investigation. 1989;83(5):1774-7.

51. Kubes P, Suzuki M, Granger D. Nitric oxide: an endogenous modulator of leukocyte adhesion. Proceedings of the National Academy of Sciences. 1991;88(11):4651-5.

52. Ferguson MK, DeFilippi VJ. Nitric oxide and endothelium-dependent relaxation in tracheobronchial lymph vessels. Microvascular Research. 1994;47(3):308-17.

53. Bohlen HG, Wang W, Gashev A, Gasheva O, Zawieja D. Phasic contractions of rat mesenteric lymphatics increase basal and phasic nitric oxide generation in vivo. American Journal of Physiology-Heart and Circulatory Physiology. 2009;297(4):H1319-H28.

54. Gasheva OY, Zawieja DC, Gashev AA. Contraction-initiated NO-dependent lymphatic relaxation: a self-regulatory mechanism in rat thoracic duct. The Journal of Physiology. 2006;575(Pt 3):821-32.

55. Tsunemoto H, Ikomi F, Ohhashi T. Flow-mediated release of nitric oxide from lymphatic endothelial cells of pressurized canine thoracic duct. The Japanese Journal of Physiology. 2003;53(3):157-63.

56. Bohlen HG, Gasheva OY, Zawieja DC. Nitric oxide formation by lymphatic bulb and valves is a major regulatory component of lymphatic pumping. American Journal of Physiology-Heart and Circulatory Physiology. 2011;301(5):H1897-906.

57. Fox JL, von Der Weid PY. Effects of histamine on the contractile and electrical activity in isolated lymphatic vessels of the guinea pig mesentery. British Journal of Pharmacology. 2002;136(8):1210-8.

58. Nizamutdinova IT, Maejima D, Nagai T, Bridenbaugh E, Thangaswamy S, Chatterjee V, et al. Involvement of histamine in endothelium-dependent relaxation of mesenteric lymphatic vessels. Microcirculation. 2014;21(7):640-8.

59. Akdis CA, Blaser K. Histamine in the immune regulation of allergic inflammation. Journal of Allergy and Clinical Immunology. 2003;112(1):15-22.

60. MacGlashan D. Histamine. Journal of Allergy and Clinical Immunology. 2003;112(4):S53-S9.

61. Ashina K, Tsubosaka Y, Nakamura T, Omori K, Kobayashi K, Hori M, et al. Histamine Induces Vascular Hyperpermeability by Increasing Blood Flow and Endothelial Barrier Disruption In Vivo. PLoS One. 2015;10(7):e0132367.

62. Rotrosen D, Gallin JI. Histamine type I receptor occupancy increases endothelial cytosolic calcium, reduces F-actin, and promotes albumin diffusion across cultured endothelial monolayers. Journal of Cell Biology. 1986;103(6):2379-87.

63. Dejana E, Orsenigo F, Lampugnani MG. The role of adherens junctions and VE-cadherin in the control of vascular permeability. Journal of Cell Science. 2008;121(Pt 13):2115-22.

64. Gardner TW, Lesher T, Sonny K, Cuong V, Barber AJ, Brennan WA. Histamine reduces ZO-1 tight-junction protein expression in cultured retinal microvascular endothelial cells. Biochemical Journal. 1996;320(3):717-21.

65. Guo M, Breslin JW, Wu MH, Gottardi CJ, Yuan SY. VE-cadherin and beta-catenin binding dynamics during histamine-induced endothelial hyperpermeability. American Journal of Physiology-Cell Physiology. 2008;294(4):C977-84.

66. Baldwin AL, Thurston G. Changes in endothelial actin cytoskeleton in venules with time after histamine treatment. American Journal of Physiology-Heart and Circulatory Physiology. 1995;269(5):H1528-H37.

67. Amerongen GPvN, Draijer R, Vermeer MA, van Hinsbergh VW. Transient and prolonged increase in endothelial permeability induced by histamine and thrombin: role of protein kinases, calcium, and rho A. Circulation Research. 1998;83(11):1115-23.

68. Hirase T, Kawashima S, Wong EY, Ueyama T, Rikitake Y, Tsukita S, et al. Regulation of tight junction permeability and occludin phosphorylation by Rhoa-p160 ROCK-dependent and -independent mechanisms. Journal of Biological Chemistry. 2001;276(13):10423-31.

69. Mikelis CM, Simaan M, Ando K, Fukuhara S, Sakurai A, Amornphimoltham P, et al. RhoA and ROCK mediate histamine-induced vascular leakage and anaphylactic shock. Nature Communications. 2015;6:6725.

70. Lantoine F, Iouzalen L, Devynck M-A, Millanvoye-Van Brussel E, David-Dufilho M. Nitric oxide production in human endothelial cells stimulated by histamine requires Ca^{2+} influx. Biochemical Journal. 1998;330(2):695-9.

71. Delneste Y, Lassalle P, Jeannin P, Joseph M, Tonnel A, Gosset P. Histamine induces IL‐6 production by human endothelial cells. Clinical & Experimental Immunology. 1994;98(2):344-9.

72. Jeannin P, Delneste Y, Gosset P, Molet S, Lassalle P, Hamid Q, et al. Histamine induces interleukin-8 secretion by endothelial cells. Blood. 1994;84(7):2229-33.

73. Parsons ME, Ganellin CR. Histamine and its receptors. British Journal of Pharmacology. 2006;147 Suppl 1:S127-35.

74. Dodd AN, Kudla J, Sanders D. The language of calcium signaling. Annual Review of Plant Biology. 2010;61:593-620.

75. Bootman MD. Calcium signaling. Cold Spring Harbor Perspectives in Biology. 2012;4(7):a011171.

76. Putney JW. Pharmacology of store-operated calcium channels. Molecular Interventions. 2010;10(4):209.

77. Prakriya M, Lewis RS. Store-Operated Calcium Channels. Physiological Reviews. 2015;95(4):1383-436.

78. Parekh AB, Putney Jr JW. Store-operated calcium channels. Physiological Reviews. 2005;85(2):757-810.

79. Feske S. CRAC channelopathies. Pflügers Archiv. 2010;460(2):417-35.

80. Hoth M, Penner R. Depletion of intracellular calcium stores activates a calcium current in mast cells. Nature. 1992;355(6358):353.

81. Hoth M. Calcium and barium permeation through calcium release-activated calcium (CRAC) channels. Pflügers Archiv. 1995;430(3):315-22.

82. Zweifach A, Lewis RS. Mitogen-regulated Ca^{2+} current of T lymphocytes is activated by depletion of intracellular Ca^{2+} stores. Proceedings of the National Academy of Sciences. 1993;90(13):6295-9.

83. Cahalan MD, Zhang SL, Yeromin AV, Ohlsen K, Roos J, Stauderman KA. Molecular basis of the CRAC channel. Cell Calcium. 2007;42(2):133-44.

84. Liou J, Kim ML, Do Heo W, Jones JT, Myers JW, Ferrell Jr JE, et al. STIM is a Ca^{2+} sensor essential for Ca^{2+}-store-depletion-triggered Ca^{2+} influx. Current Biology. 2005;15(13):1235-41.

85. Roos J, DiGregorio PJ, Yeromin AV, Ohlsen K, Lioudyno M, Zhang S, et al. STIM1, an essential and conserved component of store-operated Ca^{2+} channel function. Journal of Cell Biology. 2005;169(3):435-45.

86. Zhang SL, Yu Y, Roos J, Kozak JA, Deerinck TJ, Ellisman MH, et al. STIM1 is a Ca^{2+} sensor that activates CRAC channels and migrates from the Ca^{2+} store to the plasma membrane. Nature. 2005;437(7060):902.

87. Prakriya M, Feske S, Gwack Y, Srikanth S, Rao A, Hogan PG. Orai1 is an essential pore subunit of the CRAC channel. Nature. 2006;443(7108):230-3.

88. Vig M, Peinelt C, Beck A, Koomoa D, Rabah D, Koblan-Huberson M, et al. CRACM1 is a plasma membrane protein essential for store-operated Ca^{2+} entry. Science. 2006;312(5777):1220-3.

89. Zhang SL, Yeromin AV, Zhang XH-F, Yu Y, Safrina O, Penna A, et al. Genome-wide RNAi screen of Ca^{2+} influx identifies genes that regulate Ca^{2+} release-activated Ca^{2+} channel activity. Proceedings of the National Academy of Sciences. 2006;103(24):9357-62.

90. Feske S, Gwack Y, Prakriya M, Srikanth S, Puppel SH, Tanasa B, et al. A mutation in Orai1 causes immune deficiency by abrogating CRAC channel function. Nature. 2006;441(7090):179-85.

91. Vig M, Beck A, Billingsley JM, Lis A, Parvez S, Peinelt C, et al. CRACM1 multimers form the ion-selective pore of the CRAC channel. Current Biology. 2006;16(20):2073-9.

92. Yeromin AV, Zhang SL, Jiang W, Yu Y, Safrina O, Cahalan MD. Molecular identification of the CRAC channel by altered ion selectivity in a mutant of Orai. Nature. 2006;443(7108):226-9.

93. Hou X, Pedi L, Diver MM, Long SB. Crystal structure of the calcium release–activated calcium channel Orai. Science. 2012:1228757.

94. Hou X, Burstein SR, Long SB. Structures reveal opening of the store-operated calcium channel Orai. Elife. 2018;7:e36758.

95. Yen M, Lokteva LA, Lewis RS. Functional analysis of Orai1 concatemers supports a hexameric stoichiometry for the CRAC channel. Biophysical Journal. 2016;111(9):1897-907.

96. Cai X, Zhou Y, Nwokonko RM, Loktionova NA, Wang X, Xin P, et al. The Orai1 store-operated calcium channel functions as a hexamer. Journal of Biological Chemistry. 2016:jbc. M116. 758813.

97. Williams RT, Manji SS, Parker NJ, Hancock MS, van Stekelenburg L, Jean-Pierre E, et al. Identification and characterization of the STIM (stromal interaction molecule) gene family: coding for a novel class of transmembrane proteins. Biochemical Journal. 2001;357(3):673-85.

98. Cahalan MD. STIMulating store-operated Ca 2+ entry. Nature Cell Biology. 2009;11(6):669.

99. Liou J, Fivaz M, Inoue T, Meyer T. Live-cell imaging reveals sequential oligomerization and local plasma membrane targeting of stromal interaction molecule 1 after Ca^{2+} store depletion. Proceedings of the National Academy of Sciences. 2007;104(22):9301-6.

100. Luik RM, Wang B, Prakriya M, Wu MM, Lewis RS. Oligomerization of STIM1 couples ER calcium depletion to CRAC channel activation. Nature. 2008;454(7203):538-42.

101. Luik RM, Wu MM, Buchanan J, Lewis RS. The elementary unit of store-operated Ca^{2+} entry: local activation of CRAC channels by STIM1 at ER-plasma membrane junctions. Journal of Cell Biology. 2006;174(6):815-25.

102. Wu MM, Buchanan J, Luik RM, Lewis RS. Ca^{2+} store depletion causes STIM1 to accumulate in ER regions closely associated with the plasma membrane. Journal of Cell Biology. 2006;174(6):803-13.

103. Gwack Y, Srikanth S, Feske S, Cruz-Guilloty F, Oh-hora M, Neems DS, et al. Biochemical and functional characterization of Orai proteins. Journal of Biological Chemistry. 2007;282(22):16232-43.

104. Lis A, Peinelt C, Beck A, Parvez S, Monteilh-Zoller M, Fleig A, et al. CRACM1, CRACM2, and CRACM3 are store-operated Ca^{2+} channels with distinct functional properties. Current Biology. 2007;17(9):794-800.

105. DeHaven WI, Smyth JT, Boyles RR, Putney JW. Calcium inhibition and calcium potentiation of Orai1, Orai2, and Orai3 calcium release-activated calcium channels. Journal of Biological Chemistry. 2007;282(24):17548-56.

106. Gross SA, Wissenbach U, Philipp SE, Freichel M, Cavalié A, Flockerzi V. Murine ORAI2 splice variants form functional CRAC channels. Journal of Biological Chemistry. 2007.

107. Brandman O, Liou J, Park WS, Meyer T. STIM2 is a feedback regulator that stabilizes basal cytosolic and endoplasmic reticulum Ca^{2+} levels. Cell. 2007;131(7):1327-39.

108. Oh-Hora M, Yamashita M, Hogan PG, Sharma S, Lamperti E, Chung W, et al. Dual functions for the endoplasmic reticulum calcium sensors STIM1 and STIM2 in T cell activation and tolerance. Nature Immunology. 2008;9(4):432-43.

109. Putney JW. Pharmacology of capacitative calcium entry. Molecular Interventions. 2001;1(2):84.

110. Bird GS, DeHaven WI, Smyth JT, Putney Jr JW. Methods for studying store-operated calcium entry. Methods. 2008;46(3):204-12.

111. Ma H-T, Patterson RL, Birnbaumer L, Mikoshiba K, Gill DL. Requirement of the inositol trisphosphate receptor for activation of store-operated Ca^{2+} channels. Science. 2000;287(5458):1647-51.

112. Mercer JC, DeHaven WI, Smyth JT, Wedel B, Boyles RR, Bird GS, et al. Large store-operated calcium selective currents due to co-expression of Orai1 or Orai2 with the intracellular calcium sensor, Stim1. Journal of Biological Chemistry. 2006;281(34):24979-90.

113. DeHaven WI, Smyth JT, Boyles RR, Bird GS, Putney JW. Complex actions of 2-aminoethyldiphenyl borate on store-operated calcium entry. Journal of Biological Chemistry. 2008;283(28):19265-73.

114. Tran Q-K, Watanabe H, Le H-Y, Pan L, Seto M, Takeuchi K, et al. Myosin light chain kinase regulates capacitative Ca^{2+} entry in human monocytes/macrophages. Arteriosclerosis, Thrombosis, and Vascular Biology. 2001;21(4):509-15.

115. Smyth JT, DeHaven WI, Bird GS, Putney JW. Ca^{2+}-store-dependent and-independent reversal of Stim1 localization and function. Journal of Cell Science. 2008;121(6):762-72.

116. Sweeney ZK, Minatti A, Button DC, Patrick S. Small‐molecule inhibitors of store‐operated calcium entry. ChemMedChem. 2009;4(5):706-18.

117. Schindl R, Bergsmann J, Frischauf I, Derler I, Fahrner M, Muik M, et al. 2-aminoethoxydiphenyl borate alters selectivity of Orai3 channels by increasing their pore size. Journal of Biological Chemistry. 2008.

118. Zhang SL, Kozak JA, Jiang W, Yeromin AV, Chen J, Yu Y, et al. Store-dependent and-independent modes regulating CRAC channel activity of human Orai1 and Orai3. Journal of Biological Chemistry. 2008.

119. Kawasaki T, Lange I, Feske S. A minimal regulatory domain in the C terminus of STIM1 binds to and activates ORAI1 CRAC channels. Biochemical and Biophysical Research Communications. 2009;385(1):49-54.

120. Muik M, Fahrner M, Derler I, Schindl R, Bergsmann J, Frischauf I, et al. A cytosolic homomerization and a modulatory domain within STIM1 C-terminus determine coupling to ORAI1 channels. Journal of Biological Chemistry. 2009.

121. Park CY, Hoover PJ, Mullins FM, Bachhawat P, Covington ED, Raunser S, et al. STIM1 clusters and activates CRAC channels via direct binding of a cytosolic domain to Orai1. Cell. 2009;136(5):876-90.

122. Yuan JP, Zeng W, Dorwart MR, Choi Y-J, Worley PF, Muallem S. SOAR and the polybasic STIM1 domains gate and regulate Orai channels. Nature Cell Biology. 2009;11(3):337.

123. Feske S, Giltnane J, Dolmetsch R, Staudt LM, Rao A. Gene regulation mediated by calcium signals in T lymphocytes. Nature Immunology. 2001;2(4):316.

124. Feske S, Müller JM, Graf D, Kroczek RA, Dräger R, Niemeyer C, et al. Severe combined immunodeficiency due to defective binding of the nuclear factor of activated T cells in T lymphocytes of two male siblings. European Journal of Immunology. 1996;26(9):2119-26.

125. Feske S, Prakriya M, Rao A, Lewis RS. A severe defect in CRAC Ca^{2+} channel activation and altered K+ channel gating in T cells from immunodeficient patients. Journal of Experimental Medicine. 2005;202(5):651-62.

126. McCarl CA, Picard C, Khalil S, Kawasaki T, Rother J, Papolos A, et al. ORAI1 deficiency and lack of store-operated Ca^{2+} entry cause immunodeficiency, myopathy, and ectodermal dysplasia. The Journal of Allergy and Clinical Immunology. 2009;124(6):1311-8 e7.

127. Partiseti M, Le Deist F, Hivroz C, Fischer A, Korn H, Choquet D. The calcium current activated by T cell receptor and store depletion in human lymphocytes is absent in a primary immunodeficiency. Journal of Biological Chemistry. 1994;269(51):32327-35.

128. Le Deist F, Hivroz C, Partiseti M, Thomas C, Buc HA, Oleastro M, et al. A primary T-cell immunodeficiency associated with defective transmembrane calcium influx. Blood. 1995;85(4):1053-62.

129. Picard C, McCarl C-A, Papolos A, Khalil S, Lüthy K, Hivroz C, et al. STIM1 mutation associated with a syndrome of immunodeficiency and autoimmunity. New England Journal of Medicine. 2009;360(19):1971-80.

130. Bohm J, Chevessier F, Maues De Paula A, Koch C, Attarian S, Feger C, et al. Constitutive activation of the calcium sensor STIM1 causes tubular-aggregate myopathy. American Journal of Human Genetics. 2013;92(2):271-8.

131. Misceo D, Holmgren A, Louch WE, Holme PA, Mizobuchi M, Morales RJ, et al. A Dominant STIM 1 Mutation Causes S tormorken Syndrome. Human Mutation. 2014;35(5):556-64.

132. Morin G, Bruechle NO, Singh AR, Knopp C, Jedraszak G, Elbracht M, et al. Gain‐of‐function mutation in STIM1 (P. R304W) is associated with Stormorken syndrome. Human Mutation. 2014;35(10):1221-32.

133. Nesin V, Wiley G, Kousi M, Ong E-C, Lehmann T, Nicholl DJ, et al. Activating mutations in STIM1 and ORAI1 cause overlapping syndromes of tubular myopathy and congenital miosis. Proceedings of the National Academy of Sciences. 2014:201312520.

134. Böhm J, Chevessier F, Koch C, Peche GA, Mora M, Morandi L, et al. Clinical, histological and genetic characterisation of patients with tubular aggregate myopathy caused by mutations in STIM1. Journal of Medical Genetics. 2014;51(12):824-33.

135. Markello T, Chen D, Kwan JY, Horkayne-Szakaly I, Morrison A, Simakova O, et al. York platelet syndrome is a CRAC channelopathy due to gain-of-function mutations in STIM1. Molecular Genetics and Metabolism. 2015;114(3):474-82.

136. Noury J-B, Böhm J, Peche GA, Guyant-Marechal L, Bedat-Millet A-L, Chiche L, et al. Tubular aggregate myopathy with features of Stormorken disease due to a new STIM1 mutation. Neuromuscular Disorders. 2017;27(1):78-82.

137. Walter MC, Rossius M, Zitzelsberger M, Vorgerd M, Müller-Felber W, Ertl-Wagner B, et al. 50 years to diagnosis: Autosomal dominant tubular aggregate myopathy caused by a novel STIM1 mutation. Neuromuscular Disorders. 2015;25(7):577-84.

138. Hedberg C, Niceta M, Fattori F, Lindvall B, Ciolfi A, D'Amico A, et al. Childhood onset tubular aggregate myopathy associated with de novo STIM1 mutations. Journal of Neurology. 2014;261(5):870-6.

139. Harris E, Burki U, Marini-Bettolo C, Neri M, Scotton C, Hudson J, et al. Complex phenotypes associated with STIM1 mutations in both coiled coil and EF-hand domains. Neuromuscular Disorders. 2017;27(9):861-72.

140. Fahrner M, Stadlbauer M, Muik M, Rathner P, Stathopulos P, Ikura M, et al. A dual mechanism promotes switching of the Stormorken STIM1 R304W mutant into the activated state. Nature Communications. 2018;9(1):825.

141. Endo Y, Noguchi S, Hara Y, Hayashi YK, Motomura K, Miyatake S, et al. Dominant mutations in ORAI1 cause tubular aggregate myopathy with hypocalcemia via constitutive activation of store-operated Ca(2)(+) channels. Human Molecular Genetics. 2015;24(3):637-48.

142. Böhm J, Bulla M, Urquhart JE, Malfatti E, Williams SG, O'sullivan J, et al. ORAI1 mutations with distinct channel gating defects in tubular aggregate myopathy. Human Mutation. 2017;38(4):426-38.

143. Garibaldi M, Fattori F, Riva B, Labasse C, Brochier G, Ottaviani P, et al. A novel gain‐of‐function mutation in ORAI1 causes late‐onset tubular aggregate myopathy and congenital miosis. Clinical Genetics. 2017;91(5):780-6.

144. Bohm J, Laporte J. Gain-of-function mutations in STIM1 and ORAI1 causing tubular aggregate myopathy and Stormorken syndrome. Cell Calcium. 2018;76:1-9.

145. Braun A, Varga-Szabo D, Kleinschnitz C, Pleines I, Bender M, Austinat M, et al. Orai1 (CRACM1) is the platelet SOC channel and essential for pathological thrombus formation. Blood. 2009;113(9):2056-63.

146. Gwack Y, Srikanth S, Oh-Hora M, Hogan PG, Lamperti ED, Yamashita M, et al. Hair loss and defective T- and B-cell function in mice lacking ORAI1. Molecular and Cellular Biology. 2008;28(17):5209-22.

147. Vig M, DeHaven WI, Bird GS, Billingsley JM, Wang H, Rao PE, et al. Defective mast cell effector functions in mice lacking the CRACM1 pore subunit of store-operated calcium release–activated calcium channels. Nature Immunology. 2008;9(1):89.

148. Beyersdorf N, Braun A, Vögtle T, Varga-Szabo D, Galdos RR, Kissler S, et al. STIM1-independent T cell development and effector function in vivo. The Journal of Immunology. 2009;182(6):3390-7.

149. Stiber J, Hawkins A, Zhang ZS, Wang S, Burch J, Graham V, et al. STIM1 signalling controls store-operated calcium entry required for development and contractile function in skeletal muscle. Nature Cell Biology. 2008;10(6):688-97.

150. Lu W, Wang J, Peng G, Shimoda LA, Sylvester J. Knockdown of stromal interaction molecule 1 attenuates store-operated Ca^{2+} entry and Ca^{2+} responses to acute hypoxia in pulmonary arterial smooth muscle. American Journal of Physiology-Lung Cellular and Molecular Physiology. 2009;297(1):L17-L25.

151. Potier M, Gonzalez JC, Motiani RK, Abdullaev IF, Bisaillon JM, Singer HA, et al. Evidence for STIM1- and Orai1-dependent store-operated calcium influx through ICRAC in vascular smooth muscle cells: role in proliferation and migration. The FASEB Journal. 2009;23(8):2425-37.

152. Abdullaev IF, Bisaillon JM, Potier M, Gonzalez JC, Motiani RK, Trebak M. Stim1 and Orai1 mediate CRAC currents and store-operated calcium entry important for endothelial cell proliferation. Circulation Research. 2008;103(11):1289-99.

153. Abdullaev IF, Bisaillon JM, Potier M, Gonzalez JC, Motiani RK, Trebak M. Stim1 and Orai1 Mediate CRAC Currents and Store-Operated Calcium Entry Necessary for Endothelial Cell Proliferation. Biophysical Journal. 2009;96(3):670a.

154. Guibert C, Ducret T, Savineau J-P. Voltage-independent calcium influx in smooth muscle. Progress in Biophysics and Molecular Biology. 2008;98(1):10-23.

155. Giachini FR, Chiao C-W, Carneiro FS, Lima VV, Carneiro ZN, Dorrance AM, et al. Increased activation of stromal interaction molecule-1/Orai-1 in aorta from hypertensive rats: a novel insight into vascular dysfunction. Journal of Hypertension. 2009;53(2):409-16.

156. Domínguez-Rodríguez A, Díaz I, Rodríguez-Moyano M, Calderón-Sánchez E, Rosado JA, Ordóñez A, et al. Urotensin-II signaling mechanism in rat coronary artery: role of STIM1 and Orai1-dependent store operated calcium influx in vasoconstriction. Arteriosclerosis, Thrombosis, and Vascular Biology. 2012;32(5):1325-32.

157. Li J, McKeown L, Ojelabi O, Stacey M, Foster R, O'regan D, et al. Nanomolar potency and selectivity of a Ca^{2+} release-activated Ca^{2+} channel inhibitor against store - operated Ca^{2+} entry and migration of vascular smooth muscle cells. British Journal of Pharmacology. 2011;164(2):382-93.

158. Beech DJ. Orai1 calcium channels in the vasculature. Pflügers Archiv. 2012;463(5):635-47.

159. Guo R-w, Yang L-x, Li M-q, Pan X-h, Liu B, Deng Y-l. Stim1-and Orai1-mediated store-operated calcium entry is critical for angiotensin II-induced vascular smooth muscle cell proliferation. Cardiovascular Research. 2011;93(2):360-70.

160. Li J, Sukumar P, Milligan CJ, Kumar B, Ma Z-Y, Munsch CM, et al. Interactions, functions, and independence of plasma membrane STIM1 and TRPC1 in vascular smooth muscle cells. Circulation Research. 2008;103(8):e97-e104.

161. Li J, Cubbon RM, Wilson LA, Amer MS, McKeown L, Hou B, et al. Orai1 and CRAC channel dependence of VEGF-activated Ca^{2+} entry and endothelial tube formation. Circulation Research. 2011;108(10):1190-8.

162. Zhang W, Halligan KE, Zhang X, Bisaillon JM, Gonzalez-Cobos JC, Motiani RK, et al. Orai1-mediated I (CRAC) is essential for neointima formation after vascular injury. Circulation Research. 2011;109(5):534-42.

163. Aubart FC, Sassi Y, Coulombe A, Mougenot N, Vrignaud C, Leprince P, et al. RNA interference targeting STIM1 suppresses vascular smooth muscle cell proliferation and neointima formation in the rat. Molecular Therapy. 2009;17(3):455-62.

164. Zhou MH, Zheng H, Si H, Jin Y, Peng JM, He L, et al. Stromal interaction molecule 1 (STIM1) and Orai1 mediate histamine-evoked calcium entry and nuclear factor of activated T-cells (NFAT) signaling in human umbilical vein endothelial cells. Journal of Biological Chemistry. 2014;289(42):29446-56.

165. Jafarnejad M, Cromer WE, Kaunas RR, Zhang SL, Zawieja DC, Moore JE, Jr. Measurement of shear stress-mediated intracellular calcium dynamics in human dermal lymphatic endothelial cells. American Journal of Physiology-Heart and Circulatory Physiology. 2015;308(7):H697-706.

166. Choi D, Park E, Jung E, Seong YJ, Hong M, Lee S, et al. ORAI1 activates proliferation of lymphatic endothelial cells in response to laminar flow through Krüppel-like factors 2 and 4. Circulation Research. 2017;120(9):1426-39.

167. Choi D, Park E, Jung E, Seong YJ, Yoo J, Lee E, et al. Laminar flow downregulates Notch activity to promote lymphatic sprouting. The Journal of Clinical Investigation. 2017;127(4):1225-40.

168. Chatzizisis YS, Coskun AU, Jonas M, Edelman ER, Feldman CL, Stone PH. Role of endothelial shear stress in the natural history of coronary atherosclerosis and vascular remodeling: molecular, cellular, and vascular behavior. Journal of the American College of Cardiology. 2007;49(25):2379-93.

169. Resnick N, Yahav H, Shay-Salit A, Shushy M, Schubert S, Zilberman LCM, et al. Fluid shear stress and the vascular endothelium: for better and for worse. Progress in Biophysics and Molecular Biology. 2003;81(3):177-99.

170. Davies PF. Flow-mediated endothelial mechanotransduction. Physiological Reviews. 1995;75(3):519-60.

171. Harrison DG, Widder J, Grumbach I, Chen W, Weber M, Searles C. Endothelial mechanotransduction, nitric oxide and vascular inflammation. Journal of Internal Medicine. 2006;259(4):351-63.

172. Nizamutdinova IT, Maejima D, Nagai T, Bridenbaugh E, Thangaswamy S, Chatterjee V, et al. Involvement of histamine in endothelium‐dependent relaxation of mesenteric lymphatic vessels. Microcirculation. 2014;21(7):640-8.

173. Malek AM, Izumo S. Mechanism of endothelial cell shape change and cytoskeletal remodeling in response to fluid shear stress. Journal of Cell Science. 1996;109(4):713-26.

174. Zarins CK, Giddens DP, Bharadvaj B, Sottiurai VS, Mabon RF, Glagov S. Carotid bifurcation atherosclerosis. Quantitative correlation of plaque localization with flow velocity profiles and wall shear stress. Circulation Research. 1983;53(4):502-14.

175. Ferris RL, Lotze MT, Leong SP, Hoon DS, Morton DL. Lymphatics, lymph nodes and the immune system: barriers and gateways for cancer spread. Clinical & Experimental Metastasis. 2012;29(7):729-36.

176. Olszewski W. Lymphatics, lymph and lymphoid cells: an integrated immune system. European Surgical Research. 1986;18(3-4):264-70.

177. Dixon JB, Greiner ST, Gashev AA, Cote GL, Moore JE, Zawieja DC. Lymph flow, shear stress, and lymphocyte velocity in rat mesenteric prenodal lymphatics. Microcirculation. 2006;13(7):597-610.

178. Benoit JN, Zawieja DC, Goodman AH, Granger HJ. Characterization of intact mesenteric lymphatic pump and its responsiveness to acute edemagenic stress. American Journal of Physiology-Heart and Circulatory Physiology. 1989;257(6):H2059-H69.

179. Moccia F, Berra-Romani R, Tanzi F. Update on vascular endothelial Ca^{2+} signalling: A tale of ion channels, pumps and transporters. World Journal of Biological Chemistry. 2012;3(7):127.

180. Dragoni S, Laforenza U, Bonetti E, Lodola F, Bottino C, Berra-Romani R, et al. Vascular endothelial growth factor stimulates endothelial colony forming cells proliferation and tubulogenesis by inducing oscillations in intracellular Ca^{2+} concentration. Stem Cells. 2011;29(11):1898-907.

181. Kuchan M, Frangos J. Role of calcium and calmodulin in flow-induced nitric oxide production in endothelial cells. American Journal of Physiology-Cell Physiology. 1994;266(3):C628-C36.

182. Busse R, Mülsch A. Calcium-dependent nitric oxide synthesis in endothelial cytosol is mediated by calmodulin. FEBS Letters. 1990;265(1-2):133-6.

183. Tiruppathi C, Minshall RD, Paria BC, Vogel SM, Malik AB. Role of Ca^{2+} signaling in the regulation of endothelial permeability. Vascular Pharmacology. 2002;39(4-5):173-85.

184. Sandoval R, Malik AB, Naqvi T, Mehta D, Tiruppathi C. Requirement for Ca^{2+} signaling in the mechanism of thrombin-induced increase in endothelial permeability. American Journal of Physiology-Lung Cellular and Molecular Physiology. 2001;280(2):L239-L47.

185. Shen J, Luscinskas FW, Connolly A, Dewey Jr CF, Gimbrone Jr M. Fluid shear stress modulates cytosolic free calcium in vascular endothelial cells. American Journal of Physiology-Cell Physiology. 1992;262(2):C384-C90.

186. Parekh AB. Store-operated CRAC channels: function in health and disease. Nature Reviews Drug Discovery. 2010;9(5):399-410.

187. Lacruz RS, Feske S. Diseases caused by mutations in ORAI1 and STIM1. Annals of the New York Academy of Sciences. 2015;1356:45-79.

188. Feske S, Wulff H, Skolnik EY. Ion channels in innate and adaptive immunity. Annual Review of Immunology. 2015;33:291-353.

189. Shim AH, Tirado-Lee L, Prakriya M. Structural and functional mechanisms of CRAC channel regulation. Journal of Molecular Biology. 2015;427(1):77-93.

190. Zheng H, Zhou M-H, Hu C, Kuo E, Peng X, Hu J, et al. Differential roles of the C and N termini of Orai1 protein in interacting with stromal interaction molecule 1 (STIM1) for Ca^{2+} release-activated Ca^{2+} (CRAC) channel activation. Journal of Biological Chemistry. 2013;288(16):11263-72.

191. Lioudyno MI, Kozak JA, Penna A, Safrina O, Zhang SL, Sen D, et al. Orai1 and STIM1 move to the immunological synapse and are up-regulated during T cell activation. Proceedings of the National Academy of Sciences. 2008;105(6):2011-6.

192. Kim D, Pertea G, Trapnell C, Pimentel H, Kelley R, Salzberg SL. TopHat2: accurate alignment of transcriptomes in the presence of insertions, deletions and gene fusions. Genome Biology. 2013;14(4):R36.

193. Langmead B, Salzberg SL. Fast gapped-read alignment with Bowtie 2. Nature Methods. 2012;9(4):357.

194. Liao Y, Smyth GK, Shi W. featureCounts: an efficient general purpose program for assigning sequence reads to genomic features. Bioinformatics. 2013;30(7):923-30.

195. Robinson MD, McCarthy DJ, Smyth GK. edgeR: a Bioconductor package for differential expression analysis of digital gene expression data. Bioinformatics. 2010;26(1):139-40.

196. Huang DW, Sherman BT, Lempicki RA. Systematic and integrative analysis of large gene lists using DAVID bioinformatics resources. Nature Protocols. 2008;4(1):44.

197. Huang DW, Sherman BT, Lempicki RA. Bioinformatics enrichment tools: paths toward the comprehensive functional analysis of large gene lists. Nucleic Acids Research. 2008;37(1):1-13.

198. Tzima E, Irani-Tehrani M, Kiosses WB, Dejana E. A mechanosensory complex that mediates the endothelial cell response to fluid shear stress. Nature. 2005;437(7057):426.

199. Yamamoto K, Korenaga R, Kamiya A, Ando J. Fluid shear stress activates Ca^{2+} influx into human endothelial cells via P2X4 purinoceptors. Circulation Research. 2000;87(5):385-91.

200. Hierck BP, Van der Heiden K, Alkemade FE, Van de Pas S, Van Thienen JV, Groenendijk BC, et al. Primary cilia sensitize endothelial cells for fluid shear stress. Developmental Dynamics. 2008;237(3):725-35.

201. Pahakis MY, Kosky JR, Dull RO, Tarbell JM. The role of endothelial glycocalyx components in mechanotransduction of fluid shear stress. Biochemical Biophysical Research Communications. 2007;355(1):228-33.

202. Ando J, Komatsuda T, Kamiya A. Cytoplasmic calcium response to fluid shear stress in cultured vascular endothelial cells. In Vitro Cellular Developmental Biology. 1988;24(9):871-7.

203. Coste B, Mathur J, Schmidt M, Earley TJ, Ranade S, Petrus MJ, et al. Piezo1 and Piezo2 are essential components of distinct mechanically activated cation channels. Science. 2010;330(6000):55-60.

204. Li J, Hou B, Tumova S, Muraki K, Bruns A, Ludlow MJ, et al. Piezo1 integration of vascular architecture with physiological force. Nature. 2014;515(7526):279.

205. Nonomura K, Lukacs V, Sweet DT, Goddard LM, Kanie A, Whitwam T, et al. Mechanically activated ion channel PIEZO1 is required for lymphatic valve formation. Proceedings of the National Academy of Sciences. 2018;115(50):12817-22.

206. Ranade SS, Qiu Z, Woo S-H, Hur SS, Murthy SE, Cahalan SM, et al. Piezo1, a mechanically activated ion channel, is required for vascular development in mice. Proceedings of the National Academy of Sciences. 2014;111(28):10347-52.

207. Ranade SS, Woo S-H, Dubin AE, Moshourab RA, Wetzel C, Petrus M, et al. Piezo2 is the major transducer of mechanical forces for touch sensation in mice. Nature. 2014;516(7529):121.

208. Lukacs V, Mathur J, Mao R, Bayrak-Toydemir P, Procter M, Cahalan SM, et al. Impaired PIEZO1 function in patients with a novel autosomal recessive congenital lymphatic dysplasia. Nature Communications. 2015;6:8329.

209. Hartmannsgruber V, Heyken W-T, Kacik M, Kaistha A, Grgic I, Harteneck C, et al. Arterial response to shear stress critically depends on endothelial TRPV4 expression. PloS one. 2007;2(9):e827.

210. Mendoza SA, Fang J, Gutterman DD, Wilcox DA, Bubolz AH, Li R, et al. TRPV4-mediated endothelial Ca^{2+} influx and vasodilation in response to shear stress. American Journal of Physiology-Heart and Circulatory Physiology. 2009.

211. Harrington LS, Mitchell JA. Novel role for P2X receptor activation in endothelium-dependent vasodilation. British Journal of Pharmacology. 2004;143(5):611-7.

212. Sathanoori R, Rosi F, Gu B, Wiley J, Müller C, Olde B, et al. Shear stress modulates endothelial KLF2 through activation of P2X4. Purinergic Signalling. 2015;11(1):139-53.

213. Sathanoori R, Bryl-Gorecka P, Müller CE, Erb L, Weisman GA, Olde B, et al. P2Y 2 receptor modulates shear stress-induced cell alignment and actin stress fibers in human umbilical vein endothelial cells. Cellular and Molecular Life Sciences. 2017;74(4):731-46.

214. Seeger H, Bonani M, Segerer S. The role of lymphatics in renal inflammation. Nephrol Dial Transplant. 2012;27(7):2634-41.

215. Vetrano S, Borroni EM, Sarukhan A, Savino B, Bonecchi R, Correale C, et al. The lymphatic system controls intestinal inflammation and inflammation-associated colon cancer through the chemokine decoy receptor D6. Gut. 2010;59(2):197-206.

216. Breslin JW, Gaudreault N, Watson KD, Reynoso R, Yuan SY, Wu MH. Vascular endothelial growth factor-C stimulates the lymphatic pump by a VEGF receptor-3-dependent mechanism. American Journal of Physiology-Heart and Circulatory Physiology. 2007;293(1):H709-18.

217. Hong YK, Harvey N, Noh YH, Schacht V, Hirakawa S, Detmar M, et al. Prox1 is a master control gene in the program specifying lymphatic endothelial cell fate. Developmental Dynamics. 2002;225(3):351-7.

218. Podgrabinska S, Braun P, Velasco P, Kloos B, Pepper MS, Jackson DG, et al. Molecular characterization of lymphatic endothelial cells. Proceedings of the National Academy of Sciences. 2002;99(25):16069-74.

219. Breslin JW. ROCK and cAMP promote lymphatic endothelial cell barrier integrity and modulate histamine and thrombin-induced barrier dysfunction. Lymphatic Research and Biology. 2011;9(1):3-11.

220. Johnson LA, Clasper S, Holt AP, Lalor PF, Baban D, Jackson DG. An inflammation-induced mechanism for leukocyte transmigration across lymphatic vessel endothelium. Journal of Experimental Medicine. 2006;203(12):2763-77.

221. Ahmmed GU, Malik AB. Functional role of TRPC channels in the regulation of endothelial permeability. Pflügers Archiv. 2005;451(1):131-42.

222. Clapham DE. Calcium signaling. Cell. 2007;131(6):1047-58.

223. Zhang SL, Yeromin AV, Hu J, Amcheslavsky A, Zheng H, Cahalan MD. Mutations in Orai1 transmembrane segment 1 cause STIM1-independent activation of Orai1 channels at glycine 98 and channel closure at arginine 91. Proceedings of the National Academy of Sciences. 2011;108(43):17838-43.

224. Loew ER, MacMILLAN R, Kaiser ME. The anti-histamine properties of Benadryl, β-dimethylaminoethyl benzhydryl ether hydrochloride. Journal of Pharmacology Experimental Therapeutics. 1946;86(3):229-38.

225. Simpson K, Jarvis B. Fexofenadine. Drugs. 2000;59(2):301-21.

226. Patterson RL, van Rossum DB, Nikolaidis N, Gill DL, Snyder SH. Phospholipase C-gamma: diverse roles in receptor-mediated calcium signaling. Trends in Biochemical Sciences. 2005;30(12):688-97.

227. Bleasdale JE, Fisher SK. Use of U-73122 as an inhibitor of phospholipase C-dependent processes. Neuroprotocols. 1993;3(2):125-33.

228. Jin W, Lo T-M, Loh HH, Thayer SA. U73122 inhibits phospholipase C-dependent calcium mobilization in neuronal cells. Brain Research. 1994;642(1-2):237-43.

229. Smallridge RC, Kiang JG, Gist ID, Fein HG, Galloway RJ. U-73122, an aminosteroid phospholipase C antagonist, noncompetitively inhibits thyrotropin-releasing hormone effects in GH3 rat pituitary cells. Endocrinology. 1992;131(4):1883-8.

230. Tatrai A, Suk KL, Stern PH. U-73122, a phospholipase C antagonist, inhibits effects of endothelin-1 and parathyroid hormone on signal transduction in UMR-106 osteoblastic cells. Biochimica et Biophysica Acta -Molecular Cell Research. 1994;1224(3):575-82.

231. Wang J. U-73122, an aminosteroid phospholipase C inhibitor, may also block Ca 2+ influx through phospholipase C-independent mechanism in neutrophil activation. Naunyn-Schmiedeberg's Archives of Pharmacology. 1996;353(6):599-605.

232. Smyth JT, Hwang SY, Tomita T, DeHaven WI, Mercer JC, Putney JW. Activation and regulation of store-operated calcium entry. Journal of Cellular and Molecular Medicine. 2010;14(10):2337-49.

233. Zitt C, Strauss B, Schwarz EC, Spaeth N, Rast G, Hatzelmann A, et al. Potent inhibition of Ca^{2+} release-activated Ca^{2+} channels and T-lymphocyte activation by the pyrazole derivative BTP2. Journal of Biological Chemistry. 2004;279(13):12427-37.

234. Chung SC, McDonald TV, Gardner P. Inhibition by SK&F 96365 of Ca^{2+} current, IL‐2 production and activation in T lymphocytes. British Journal of Pharmacology. 1994;113(3):861-8.

235. Lytton J, Westlin M, Hanley MR. Thapsigargin inhibits the sarcoplasmic or endoplasmic reticulum Ca-ATPase family of calcium pumps. Journal of Biological Chemistry. 1991;266(26):17067-71.

236. Prakriya M. Store-operated Orai channels: structure and function. Current Topics in Membranes. 2013;71:1-32.

237. Moy AB, Winter M, Kamath A, Blackwell K, Reyes G, Giaever I, et al. Histamine alters endothelial barrier function at cell-cell and cell-matrix sites. American Journal of Physiology-Lung Cellular and Molecular Physiology. 2000;278(5):L888-L98.

238. Esser S, Lampugnani MG, Corada M, Dejana E, Risau W. Vascular endothelial growth factor induces VE-cadherin tyrosine phosphorylation in endothelial cells. Journal of Cell Science. 1998;111(13):1853-65.

239. Hordijk PL, Anthony E, Mul F, Rientsma R, Oomen L, Roos D. Vascular-endothelial-cadherin modulates endothelial monolayer permeability. Journal of Cell Science. 1999;112(12):1915-23.

240. Wójciak-Stothard B, Potempa S, Eichholtz T, Ridley AJ. 9Rgr; and Rac but not Cdc42 regulate endothelial cell permeability. Journal of Cell Science. 2001;114(7):1343-55.

241. Dewi BE, Takasaki T, Kurane I. In vitro assessment of human endothelial cell permeability: effects of inflammatory cytokines and dengue virus infection. Journal of Virological Methods. 2004;121(2):171-80.

242. Girard JP, Moussion C, Forster R. HEVs, lymphatics and homeostatic immune cell trafficking in lymph nodes. Nature Reviews Immunology. 2012;12(11):762-73.

243. Pullinger BD, Florey H. Proliferation of lymphatics in inflammation. The Journal of Pathology Bacteriology. 1937;45(1):157-70.

244. Rockson SG. The lymphatics and the inflammatory response: lessons learned from human lymphedema. Lymphatic Research and Biology. 2013;11(3):117-20.

245. Saharinen P, Tammela T, Karkkainen MJ, Alitalo K. Lymphatic vasculature: development, molecular regulation and role in tumor metastasis and inflammation. Trends in Immunology. 2004;25(7):387-95.

246. Wilting J, Becker J, Buttler K, Weich H. Lymphatics and inflammation. Current Medicinal Chemistry. 2009;16(34):4581-92.

247. Fanger CM, Hoth M, Crabtree GR, Lewis RS. Characterization of T cell mutants with defects in capacitative calcium entry: genetic evidence for the physiological roles of CRAC channels. Journal of Cell Biology. 1995;131(3):655-67.

248. Vig M, DeHaven WI, Bird GS, Billingsley JM, Wang H, Rao PE, et al. A major defect in mast cell effector functions in CRACM1-/-mice. Nature Immunology. 2008;9(1):89.

249. Gavard J. Breaking the VE-cadherin bonds. FEBS Letters. 2009;583(1):1-6.

250. Sandoval R, Malik AB, Minshall RD, Kouklis P, Ellis CA, Tiruppathi C. Ca^{2+} signalling and PKCα activate increased endothelial permeability by disassembly of VE—cadherin junctions. The Journal of Physiology. 2001;533(2):433-45.

251. Romano M, Sironi M, Toniatti C, Polentarutti N, Fruscella P, Ghezzi P, et al. Role of IL-6 and its soluble receptor in induction of chemokines and leukocyte recruitment. Immunity. 1997;6(3):315-25.

252. Kaplanski G, Marin V, Montero-Julian F, Mantovani A, Farnarier C. IL-6: a regulator of the transition from neutrophil to monocyte recruitment during inflammation. Trends in Immunology. 2003;24(1):25-9.

253. Hebert C, Luscinskas F, Kiely J, Luis E, Darbonne W, Bennett G, et al. Endothelial and leukocyte forms of IL-8. Conversion by thrombin and interactions with neutrophils. The Journal of Immunology. 1990;145(9):3033-40.

254. Baggiolini M, Walz A, Kunkel S. Neutrophil-activating peptide-1/interleukin 8, a novel cytokine that activates neutrophils. The Journal of Clinical Investigation. 1989;84(4):1045-9.

255. Huber AR, Kunkel SL, Todd RF, Weiss SJ. Regulation of transendothelial neutrophil migration by endogenous interleukin-8. Science. 1991;254(5028):99-102.

256. Mierke CT, Ballmaier M, Werner U, Manns MP, Welte K, Bischoff SC. Human endothelial cells regulate survival and proliferation of human mast cells. Journal of Experimental Medicine. 2000;192(6):801-12.

257. Ashman LK. The biology of stem cell factor and its receptor C-kit. The International Journal of Biochemistry & Cell Biology. 1999;31(10):1037-51.

258. Reber L, Da Silva CA, Frossard N. Stem cell factor and its receptor c-Kit as targets for inflammatory diseases. European Journal of Pharmacology. 2006;533(1-3):327-40.

259. Mortimer PS, Rockson SG. New developments in clinical aspects of lymphatic disease. The Journal of Clinical Investigation. 2014;124(3):915-21.

260. Johnson LA, Jackson DG. Cell traffic and the lymphatic endothelium. Annals of the New York Academy of Sciences. 2008;1131(1):119-33.

261. Randolph GJ, Angeli V, Swartz MA. Dendritic-cell trafficking to lymph nodes through lymphatic vessels. Nature Reviews Immunology. 2005;5(8):617.

262. Cyster JG. Chemokines and cell migration in secondary lymphoid organs. Science. 1999;286(5447):2098-102.

263. Mancardi S, Vecile E, Dusetti N, Calvo E, Stanta G, Burrone OR, et al. Evidence of CXC, CC and C chemokine production by lymphatic endothelial cells. Immunology. 2003;108(4):523-30.

264. Cohen JN, Guidi CJ, Tewalt EF, Qiao H, Rouhani SJ, Ruddell A, et al. Lymph node–resident lymphatic endothelial cells mediate peripheral tolerance via Aire-independent direct antigen presentation. Journal of Experimental Medicine. 2010;207(4):681-8.

265. Tewalt EF, Cohen JN, Rouhani SJ, Guidi CJ, Qiao H, Fahl SP, et al. Lymphatic endothelial cells induce tolerance via PD-L1 and lack of costimulation leading to high-level PD-1 expression on CD8 T cells. Blood. 2012;120(24):4772-82.

266. Miller CN, Hartigan-O'Connor DJ, Lee MS, Laidlaw G, Cornelissen IP, Matloubian M, et al. IL-7 production in murine lymphatic endothelial cells and induction in the setting of peripheral lymphopenia. International Immunology. 2013;25(8):471-83.

267. Link A, Vogt TK, Favre S, Britschgi MR, Acha-Orbea H, Hinz B, et al. Fibroblastic reticular cells in lymph nodes regulate the homeostasis of naive T cells. Nature Immunology. 2007;8(11):1255.

268. Podgrabinska S, Kamalu O, Mayer L, Shimaoka M, Snoeck H, Randolph GJ, et al. Inflamed lymphatic endothelium suppresses dendritic cell maturation and function via Mac-1/ICAM-1-dependent mechanism. The Journal of Immunology. 2009;183(3):1767-79.

269. Nörder M, Gutierrez MG, Zicari S, Cervi E, Caruso A, Guzmán CA. Lymph node-derived lymphatic endothelial cells express functional costimulatory molecules and impair dendritic cell-induced allogenic T-cell proliferation. The FASEB Journal. 2012;26(7):2835-46.

270. McHale N, Roddie I. The effect of transmural pressure on pumping activity in isolated bovine lymphatic vessels. The Journal of Physiology. 1976;261(2):255.

271. Vigl B, Aebischer D, Nitschké M, Iolyeva M, Röthlin T, Antsiferova O, et al. Tissue inflammation modulates gene expression of lymphatic endothelial cells and dendritic cell migration in a stimulus-dependent manner. Blood. 2011:blood-2010-12-326447.

272. Muller WA. Leukocyte–endothelial-cell interactions in leukocyte transmigration and the inflammatory response. Trends in Immunology. 2003;24(6):326-33.

273. Malek AM, Alper SL, Izumo S. Hemodynamic shear stress and its role in atherosclerosis. The Journal of the American Medical Association. 1999;282(21):2035-42.

274. Nigro P, Abe J-i, Berk BC. Flow shear stress and atherosclerosis: a matter of site specificity. Antioxidants & Redox Signaling. 2011;15(5):1405-14.

275. White MV. The role of histamine in allergic diseases. Journal of Allergy and Clinical Immunology. 1990;86(4):599-605.

276. Benard A, Desreumeaux P, Huglo D, Hoorelbeke A, Tonnel A-B, Wallaert B. Increased intestinal permeability in bronchial asthma. Journal of Allergy and Clinical Immunology. 1996;97(6):1173-8.

277. Mehta D, Malik AB. Signaling mechanisms regulating endothelial permeability. Physiological Reviews. 2006;86(1):279-367.

278. Orlova VV, Economopoulou M, Lupu F, Santoso S, Chavakis T. Junctional adhesion molecule-C regulates vascular endothelial permeability by modulating VE-cadherin-mediated cell-cell contacts. Journal of Experimental Medicine. 2006;203(12):2703-14.

279. Turowski P, Martinelli R, Crawford R, Wateridge D, Papageorgiou AP, Lampugnani MG, et al. Phosphorylation of vascular endothelial cadherin controls lymphocyte emigration. Journal of Cell Science. 2008;121(Pt 1):29-37.

280. Dejana E, Orsenigo F, Molendini C, Baluk P, McDonald DM. Organization and signaling of endothelial cell-to-cell junctions in various regions of the blood and lymphatic vascular trees. Cell and Tissue Research. 2009;335(1):17-25.

281. Hoffmann A, Bredno J, Wendland M, Derugin N, Ohara P, Wintermark M. High and low molecular weight fluorescein isothiocyanate (FITC)–dextrans to assess blood-brain barrier disruption: Technical considerations. Translational Stroke Research. 2011;2(1):106-11.

282. Srinivasan B, Kolli AR, Esch MB, Abaci HE, Shuler ML, Hickman JJ. TEER measurement techniques for in vitro barrier model systems. Journal of Laboratory Automation. 2015;20(2):107-26.

283. Liao S, von der Weid PY. Lymphatic system: an active pathway for immune protection. Seminars in Cell and Developmental Biology. 2015;38:83-9.

284. Card CM, Shann SY, Swartz MA. Emerging roles of lymphatic endothelium in regulating adaptive immunity. The Journal of Clinical Investigation. 2014;124(3):943-52.

285. Dardik A, Chen L, Frattini J, Asada H, Aziz F, Kudo FA, et al. Differential effects of orbital and laminar shear stress on endothelial cells. Journal of Vascular Surgery. 2005;41(5):869-80.

286. Kim H, Yang KH, Cho H, Gwak G, Park SC, Kim JI, et al. Different effects of orbital shear stress on vascular endothelial cells: comparison with the results of in vivo study with rats. Vascular Specialist International. 2015;31(2):33.